TYRAMINERGIC G PROTEIN-COUPLED RECEPTORS MODULATE LOCOMOTION AND NAVIGATIONAL BEHAVIOR IN *C. ELEGANS*

A Dissertation Presented by

JAMIE LYNN DONNELLY

Submitted to the Faculty of the
University of Massachusetts Graduate School of Biomedical Sciences, Worcester
in partial fulfillment of the requirements for the degree of

DOCTOR OF PHILOSOPHY

August 4, 2011

Biomedical Sciences

Program in Neuroscience

TYRAMINERGIC G PROTEIN-COUPLED RECEPTORS MODULATE LOCOMOTION AND NAVIGATIONAL BEHAVIOR IN *C. ELEGANS*

A Dissertation Presented by

JAMIE LYNN DONNELLY

The signatures of the Dissertation Defense Committee signifies completion and approval as to style and content of the Dissertation

_____
Mark Alkema, Thesis Advisor

_____
Michael Francis, Member of Committee

_____
Claire Benard, Member of Committee

_____
Hong Sheng Li, Member of Committee

_____
Daniel Chase, Member of Committee

The signature of the Chair of the Committee signifies that the written dissertation meets the requirements of the Dissertation Committee

_____
Marc Freeman, Chair of Committee

The signature of the Dean of the Graduate School of Biomedical Sciences signifies that the student has met all graduation requirements of the school.

_____
Anthony Carruthers, Ph.D.
Dean of the Graduate School of Biomedical Sciences

Program in
Neuroscience
August 4, 2011

Dedicated to my husband James.

ACKNOWLEDGENTS

Returning to school after a few years of working corporate jobs turned out to be a highly rewarding decision. I remember arriving in Massachusetts after my 3500 mile road trip from California thinking, “what am I doing here?”. I knew I wanted a challenge and to be part of cutting edge science, but as to what exactly I was going to do over the next half decade, I didn’t know. The UMass umbrella program was a great place to be, since my love of biology was very broad. But before I made a six year commitment, I needed some refinement and guidance. Luckily, I met my future mentor, Mark Alkema, during the first week on campus. Mark helped me focus my attention on the program in neuroscience, pointing out that it encompassed everything I loved: genetics, molecular biology, and cell biology. He also nurtured my very excited and green attitude into a more critical, scientific mind. Coming from a microbiology background, his patience and love of teaching enabled me to grow as a scientist. He opened a door to the microscopic wonder that is *C. elegans* behavioral research.

In addition to showing me the ways of worm neuroscience, Mark also provided a fantastic assemblage of people to work with. The Alkema Lab is comprised of great individuals, who all contribute to an environment open to scientific communication and the not-so-scientific conversations of the latest pop-culture or newest restaurant review. Chris Clark was my west coast connection,

worm tracker fixer, and most importantly, babysitter. The juxtaposition that is Sean Maguire will stay in my memory always: vegetarian-Bad Religion-lover. Sean could always come up with a cool idea for an experiment or a new vegan concoction to try in his Vitamix. Yung-Chi Huang added a quiet touch of quick wit, humor, and provided fantastic Taiwanese food products. And of course, there is Jenn Pirri: my confidant and partner-in-crime. Without Jenn and our coffee sessions, I wouldn't have been able to vent my personal and academic woes, get invaluable scientific advice, celebrate small victories, or share the latest gossip.

In addition to the Alkema Lab, my colleagues at UMass Medical School gave this experience a personal touch. The "poker crew" provided much needed relaxing times, even for parents of infants and toddlers. John Moore and Nicole Alton-Moore were always there for a fun dinner party or night out, and some much needed conversation about life outside of science. And of course, Linzy Hendrickson gave me the ability to persevere, and continue to live in Worcester when I really didn't want to. From the first night I met Linzy, back in 2006, I knew we would be life-long friends. She was there for me at my wedding, during both of my children's first years of life, and now when we are both moving on. Although we will no longer share an area code, our fun times will not come to an end.

The support of my family was critical to my success. My mother and father always gave me the utmost confidence that I could follow my academic

heart anywhere. My siblings, and now in-law siblings, can always be counted on to listen to my excitement over my latest work. And above all, I give my thanks to my husband James, who left the beautiful Central Coast of California to follow me and our future. He's given me an amazing daughter, a wonderful son, and a whole bunch of patience during these last six years. I could not have made it to the finish line without the love of my life and my best friend.

ABSTRACT

An animal's ability to navigate through its natural environment is critical to its survival. Navigation can be slow and methodical such as an annual migration, or purely reactive such as an escape response. How sensory input is translated into a fast behavioral output to execute goal oriented locomotion remains elusive. In this dissertation, I aimed to investigate escape response behavior in the nematode *C. elegans*. It has been shown that the biogenic amine tyramine is essential for the escape response. A tyramine-gated chloride channel, LGC-55, has been revealed to modulate suppression of head oscillations and reversal behavior in response to touch. Here, I discovered key modulators of the tyraminergic signaling pathway through forward and reverse genetic screens using exogenous tyramine drug plates. *ser-2*, a tyramine activated G protein-coupled receptor mutant, was partially resistant to the paralytic effects of exogenous tyramine on body movements, indicating a role in locomotion behavior. Further analysis revealed that *ser-2* is asymmetrically expressed in the VD GABAergic motor neurons, and that SER-2 inhibits neurotransmitter release along the ventral nerve cord. Although overall locomotion was normal in *ser-2* mutants, they failed to execute omega turns by fully contracting the ventral musculature. Omega turns allow the animal to reverse and completely change directions away from a predator during the escape response. Furthermore, my studies developed an assay to investigate instantaneous velocity changes during

the escape response using machine based vision. We sought to determine how an animal accelerates in response to a mechanical stimulus, and subsequently decelerates to a basal locomotion rate. Mutant analysis using this assay revealed roles for both dopamine and tyramine signaling. During my doctoral work, I have further established the importance for tyramine in the nematode, as I have demonstrated two additional roles for tyramine in modulating escape response behavior in *C. elegans.*

TABLE OF CONTENTS

LIST OF TABLES

LIST OF FIGURES

LIST OF FIGURES (CONTINUED)

LIST OF MOVIES

LIST OF ABBREVIATIONS

Ach	acetylcholine
BBB	blood brain barrier
cAMP	cyclic adenosine monophosphate
CPG	central pattern generator
ChR2	channelrhodopsin-2
EMS	ethyl methanesulfonate
GABA	gamma-aminobutyric acid
GFP	green fluorescent protein
GPCR	G protein-coupled receptor
IPN	interpeduncular nucleus
IPSC	inhibitory post synaptic current
NGM	nematode growth media
NMJ	neuromuscular junction
NpHR	halorhodopsin
PCR	polymerase chain reaction
SNP	single nucleotide polymorphism
SWIP	swim induced paralysis
TAAR	trace amine receptor
UTR	untranslated region
VNC	ventral nerve cord

CHAPTER I

INTRODUCTION

On the simplest of levels, this dissertation aims to explore how sensory input is translated into a behavioral output. For centuries, mankind has asked the question of how we behave the way that we do. How we sense light, feel cold, and smell food are all intriguing biological processes, as well has how we react to these inputs as we squint our eyes, search for shelter, and salivate. With great advances in science, we have utilized the simple nervous systems of as well as the more complex nervous systems of mammals to begin to elucidate how sensory input is received, and how behavior is generated. Decades ago, the first simple anatomic studies answered the foremost questions behind the anatomy and physiology of behavior. Today, we are mapping molecular pathways and precise circuits. My work aims to further investigate how a behavior such as locomotion is produced and altered by the sensory system in the nematode, *C. elegans*.

An animal's primary goal is to survive and reproduce. To do so, food and water must be consumed, mates must be found, and predators must be evaded.

Diverse sensory input and locomotion are required for the animal to reach his survival goal. The field of neuroethology seeks to understand how biological functions are generated by natural behavior. Simple and complex behavioral paradigms can be tested in the laboratory setting which attempt to recapture elements of the wild. Although the environment is artificial, much can be learned as to how the nematode may react to predators in a native state. My research seeks to illuminate new pathways for the modulation of locomotion in context of the nematode escape response, and to investigate the behavioral role of tyraminergic G protein-coupled receptors.

This introduction aims to layout what is known about escape and navigational locomotion behavior, as well as how the use of a powerful model organism, *C. elegans*, can enable deep understanding of behavioral responses. Most importantly, I will describe the neuronal and muscular anatomy responsible for generating locomotion in the nematode, in addition to the molecules which convey the necessary signals. And finally, since my research investigates a neurotransmitter (tyramine) which is conserved in mammals, I will describe what is known about tyramine in a more complex nervous system.

A. Navigation and escape behavior

The innate ability of an animal to sense its environment, and in response, modulate its course of locomotion, is an evolutionary advantage. Locomotion

enables acquisition of food, detection of suitable mates, and escape from predators. Movement can be simply reactive, or a complex cognitive process.

1. Navigational behavior tactics in the wild and in the laboratory.

Navigation describes how one's position and direction of movement are determined and controlled from one place to another. While random movement may enable an organism to eventually get to their desired location, navigation to that location is much more efficient. Methods of navigation amongst animals vary widely, as their sensory input and locomotory output govern this behavioral ability. Highly complex mammals, as well as fruit flies and other invertebrates, can integrate visual, olfactory, and mechanical sensory inputs to determine their current and desired locations. The mechanism of navigation may utilize innate responses or learned experiences. There are three main forms of navigation: beacon, landmark, and path trajectory. Some animals may utilize all three, and others may favor one or two methods.

Beacon (or taxon) navigation is the simplest means of navigation. Just as a lighthouse attracts a sailor to shore, an animal may simply follow a single cue to their desired location. For example, insects can navigate using phototaxis, which is seen commonly as a moth approaches a candle flame or a campfire. It is believed that phototaxis allows the moth to determine the direction of the moon for navigation, as it is the brightest point in the night sky. Phototactic behavior

has been shown to be dependent on the age of the larva and adult, as well as the time of night (Gerson and Kelsey, 1997; Castrejon and Rojas, 2010). Olfactory beacon navigation is also often seen in nature. Sharks can track the scent of blood for over a mile to find an injured fish as an easy meal. The mechanisms of this simple navigational behavior are quite complex, as differences in concentration and bilateral timing of odor sensation may enable acute tracking of the prey (Johnson and Teeter, 1985; Gardiner and Atema, 2010). Locomotion along a gradient of sensory input is an important way for an animal to increase its ability to find food, a mate, and a safe place to be.

Using multiple visual (or other sensory) cues to learn where to find a goal location has been termed landmark, or piloting navigation (O'Keefe and Nadal, 1978). Since gray whale pods stay near the shore while they migrate, it is hypothesized that they employ landmark navigation as they migrate up and down the North American coast in the Pacific Ocean. Quite simply, the whale keeps the continent in view to the left when traveling south, and to the right when traveling north. To delve deeper into the mechanisms of piloting, laboratory studies have been done using many behavioral paradigms. For example, the Morris water maze has been developed to show that visual cues can enable a swimming rat to find a hidden platform and learn where to find it in the future (Morris, 1981). These studies determined minimal cue requirements as well as cognitive function and necessary cortical regions to efficiently navigate to complete the tested task (Morris et al., 1982; Brandeis et al., 1989).

The third type of navigation is path integration, also known as dead reckoning. By far the most intriguing and least understood form of navigation, it is described as an animal's awareness of its starting location, and the ability to track its own movement cues (velocity and direction) over its time in locomotion (Etienne and Jeffery, 2004). The trajectory can be determined using different cues. Optic flow has been shown to be employed by honeybees to determine flying velocity as they navigate through wind and enclosed spaces (Srinivasan et al., 1996). Magnetic fields of the earth are also used as cues for the mole rat, as the animal navigates subterranean spaces (Kimchi et al., 2004). As landmark navigation has its down-sides since natural landmarks can be changed as the day or season progresses, path integration becomes helpful in a novel environment.

The cortical and subcortical limbic regions of the mammalian brain are thought to be essential for landmark and dead reckoning navigation, as spatially responsive neurons have been identified in this region. Specifically, the hippocampus has been well studied for its role in learning and has been described as the cognitive map. Subsets of neurons, coined place cells, are active when the animal is in a specific area of its environment(O'Keefe and Drostrovsky, 1971; O'Keefe and Nadel, 1978). Upon surgical or drug induced hippocampal lesions, animals fail to learn visual cues to guide them to the destination goals (Jarrard, 1978; Morris, 1982; Sutherland et al. 1983). Spatial learning in the hippocampus may require long term potentiation (LTP), and thus

involve NMDA receptors and glutamatergic signaling (reviewed in Nakazawa et al., 2004). Additional studies have found that the interpeduncular nucleus (IPN) is important for some navigational tasks, as rats with lesions in the IPN are deficient in landmark and path trajectory navigation, but not beacon navigation (Clark and Taube, 2009).

2. Navigational studies in *C. elegans.*

Although anatomical studies have been done in vertebrates to study navigation, the cellular and molecular pathways which regulate navigational behavior have not been elucidated. In contrast, the nematode has been used to study the cellular and molecular underpinnings of navigational behavior, as beacon navigation has been observed using thermotaxis, chemotaxis and aerotaxis behavioral assays (Ward, 1973; Hedgecock and Russell, 1975; Dusenbery, 1980; Gray et al., 2004). *C. elegans* locomotion during chemotaxis has been described as the pirouette model as they navigate toward a stimulus (Pierce-Shimomura et al., 1999). This has been characterized by long forward runs with intermittent periods of reversals and high angled turns, termed pirouettes or omega turns. A second navigational device employed by *C. elegans* is the use of gradual turning during a long forward run, termed the weathervane strategy, which has been observed during salt chemotaxis (Iino and Yoshida, 2009). Periods of turning increases and decreases based on the

conditions, and changes in body bend depth and curvature may enable the animal to reach the desired destination more efficiently.

The locomotion behavior of the worm changes depending on the absence or presence of food. On a food plate, an animal typically is engaged in forward locomotion, with periods of short reversals and rare omega turns. When an animal is transferred to a plate without food, the velocity of the animal is 10-fold faster, periods of turning increase, and reversals are longer (Hills et al., 2004; Wakabayashi et al. 2004; Gray et al., 2005). This change in behavior is hypothesized to aid the animal to navigate to a food lawn, by attempting to pick up a cue which would lead back to favorable conditions. This behavioral strategy changes once again, after approximately 40 minutes in the absence of food, as the animal initiates long forward runs, possibly "giving up" on the current location, in search of an outlying food source (Wakabayashi et al., 2004; Gray et al., 2005). Laser ablation studies, as well as developmental mutant analysis, have determined which amphid sensory neurons are an integral part of the food sensing circuit, and which neurons aid in modulating the change between environmental states. Similarly, downstream interneurons and motor neurons were ablated to determine the circuit for the navigational output. *C. elegans* display a ventral bias in navigational behavior, as omega turns predominantly occur is initiated with a deep ventral head swing, modulated by the RIV neurons, which makes synapses only with the ventral (and not the dorsal) neck muscles (Gray et al., 2005). By carefully characterizing these behavioral states, and the

circuit which modulates the navigation, the ability to investigate the molecular control of navigation is now promising.

3. Escape responses of vertebrates and invertebrates.

Ethological and neurophysiological studies of predator-prey relationships have provided key insights into purely reactive behaviors of organisms. Escape responses are an urgent navigational behavior, as sensory input is integrated into an immediate locomotory output. Central pattern generator networks (CPGs) have been described from the sensory level to motor programs that enable goal-directed movement (reviewed in Grillner, S., 2003; 2006; Grillner et al., 2008). Sequential activation of neuronal and muscular circuits define CPGs (Brown, T.G., 1911), and are often required for vertebrate escape responses. For example, in the goldfish c-start, activation of the Mauthner cell modulates the deep full spinal and muscular body bend away from a stimulus, engaging in a predictable behavior as the fish quickly swims away (Korn et al., 1978). Similarly, invertebrates also utilize CPGs to employ an escape response. The caridoid reaction, or tail flip, is an escape response used by many crustaceans including the lobster, crayfish, and shrimp (Wiersma, 1946; Krasne, 1969; Edwards et al., 1999). Neuronal mechanisms and physiologic requirements have been studied to further our understanding of how the animal quickly generates the swift contraction of the tail muscle. Observations of the physiology of prey

escape responses have been well described in natural environments, but utilizing model organisms such as *Drosophila* and *C. elegans* in the laboratory may shed new light on the genetic and molecular control of these essential behaviors.

As *C. elegans* moves across the agar plate, forward locomotion is accompanied by head oscillations (Croll and Smith, 1978). These quick nose movements are thought to be a way for the animal to sense its environment, as the anterior tip of the animal contains the dendrites of many sensory neurons (Ward et al., 1975; Ware et al., 1975). Light touch of the animal induces an escape response. If the touch is applied on the posterior portion of the animal, the result is accelerated forward locomotion, while still moving the nose from side to side. If the animal is touched on the nose, forward locomotion ceases, and a reversal is initiated (Chalfie et al., 1985). Head oscillations also continue during the reversal. Interestingly, when the animal is gently touched on the anterior region (near the pharynx), a backward movement is initiated, but exploratory head oscillations terminate for the length of the reversal (Alkema et al, 2005). After long reversals, the animal often makes an omega turn to change directions (Croll, 1975), and then upon reinitiation of forward locomotion, head oscillations recommence (Figure 1-1). By analyzing this simple circuit, the escape response of *C. elegans* has been completely described.

Why has *C. elegans* developed an escape response? Nematodes are prey for many organisms including other predacious nematodes, mites, and

nematophagous fungi (Barron, 1977). Many nematophagous fungi use constricting rings as trapping devices which are able to catch nematodes that come in contact, most likely utilizing the worm as a source of nitrogen. These rings are made up of three cells which extend from the fungal hyphae, and upon stimulation, the rings swell and close the trap strangling the nematode (Thorn and Barron, 1984). After trapping its prey, the fungus invades the body of the nematode with hyphae and devours the animal using proteases (Barron, 1977). The observation that head oscillations are consistent in *C. elegans* locomotion throughout spontaneous forward and backward locomotion, but are suppressed during the anterior escape response leads to the hypothesis that this behavior is part of a specific escape response to evade nematophagous fungi. From the time of stimulating the trap, the closure of the trap is delayed for approximately 5 seconds (Sean Maguire and Mark Alkema, personal communication). By suppressing head oscillations during a reversal, this may allow for a quicker, more efficient reversal after anterior touch, leading to a better chance of escape from the fungal ring. The amazing genetic and molecular tools that are available for *C. elegans* research provides a novel aspect to study coevolution of predator-prey relationships.

B. Locomotion in *C. elegans*

C. elegans locomotion is characterized as a sinusoidal wave which can be propagated in a forward and reverse manner. Over the past three decades, the anatomy and molecular components that drive this modest behavior have been analyzed in great detail. After my six years of watching the nematode glide across the microscope field, I have come to agree with Mahlon Hoagland, that "simplicity is indeed often the sign of truth and a criterion of beauty".

1. Anatomy and wiring of the locomotory nervous system.

C. elegans is used as a model system to explore locomotion behavior not only due to the beautifully simple genetics, availability of mutants, and plethora of molecular techniques, but also the extremely well defined nervous system and musculature. In the adult hermaphrodite, the nervous system is relatively robust, having 302 neurons and 56 glial cells, which together account for over a third of all somatic cells (White et al., 1986). Heroic work from the "godfathers" of *C. elegans* research defined the cell lineage from embryo to adult, as well as the complete wiring diagram including all chemical and electrical synapses (Sulston and Horvitz, 1977; Sulston et al., 1983; White et al., 1986). Using their work, we know the nervous system is laid out with the majority of the cell somas in head and tail ganglia, with most neurons sending processes into the primitive brain, termed the nerve ring. Between the head and the tail ganglia resides the ventral

nerve cord (VNC), which is similar to a spinal cord as it is composed of motor neurons stretching the length of the nematode's body, making synaptic connections with the body wall muscles (White et al., 1986). The ongoing investigation of how the development, function, and regulation of the head, tail, and ventral nerve cord neurons involved in *C. elegans* locomotion, demonstrates the complexity of genetics and circuitry in a "simple" behavior.

The locomotory circuit of *C. elegans* is comprised of command neurons in the head and tail ganglia that are responsible for directionality of the wave propagation, and the motor neurons located in the ventral nerve cord that are responsible for contracting and relaxing body wall muscles to generate movement. PVC and AVB command neurons activate forward locomotion, and AVA and AVD command neurons activate backward locomotion. These command neurons can be activated and inhibited via connections to upstream sensory neurons, which relay input from the external environment including odors, osmotic change, thermal gradients, and mechanical stress. Subsequently, the command neurons electrically and chemically synapse on the cholinergic motor neurons (DA, DB, VA, and VB) leading to a contraction of body wall muscles. Cholinergic motor neurons in turn modulate the relaxation of body wall muscles by activating the GABAergic neurons (VD and DD) which may lead to the characteristic sinusoidal wave pattern (Figure 1-1) (White et al., 1976; 1986; Chalfie and White, 1988; McIntire et al., 2003) . It is believed that these

neurons are sufficient to control locomotion, with other neurons enabling modulation of the nematode's movement.

In addition to the nervous system required for *C. elegans* locomotion, muscles that connect the nervous system to the hypodermis and cuticle are required to contract and relax to exert enough force for movement. Of the two primary muscle types in the nematode, non-striated and obliquely striated, the obliquely striated compose the 95 body wall muscles. These muscles are organized into 3 distinct regions, where 16 are head muscles, which are innervated by head motor neurons, 16 are neck muscles, innervated by both head motor neurons and the ventral nerve cord, leaving 63 body wall muscles that make connections solely with the ventral nerve cord. Body wall muscles are grouped into four rows which extend down the length of the animal, making connections with the nearest motor neuron. These connections are not stereotypical connections found in most other animals where the neuron sends a process to the muscle. In *C. elegans*, muscle arms are formed, which are a simple branched extension from the muscle to the motor neurons, composing the neuromuscular junction (NMJ) (Sulston and Horvitz, 1977; Sulston et al., 1983; White et al., 1986; Dixon and Roy, 2005).

2. Circuitry and receptors for mechanosensation.

As the nematode navigates through its native soil environment, mechanical stresses exerted on the animal are translated by mechanosensory neurons into a behavioral output. In the laboratory environment, the mechanosensory circuit and receptors have been well defined. There are 30 putative neurons in the hermaphrodite which are hypothesized to sense external forces, six of which can sense gentle touch. These touch sensory neurons (ALMR, ALML, AVM, PLMR, PLML, PVM) and the circuit which governs this sensory input have been carefully defined by Chalfie and colleagues (Chalfie et al., 1985). Light anterior touch is sensed by the ALM and AVM mechanosensory neurons, which send processes from the anterior body region into the nerve ring. The PLM and PVM mechanosensory neurons sense posterior touch, with processes extending from the tail up through the ventral nerve cord. In turn, these neurons synapse with the forward and backward command neurons (AVB and AVA, respectively), which dictate the direction of locomotion (Chalfie et al., 1985; Kaplan and Horvitz, 1993). Head oscillations are coupled into this circuit via the RIM motor neurons, which innervates the radial symmetric neck muscles that responsible for the exploratory movements (White et al., 1986) (Figure 1-2).

Touch sensation signals are transduced using transient receptor potential (TRP) channels. Gentle touch is sensed by a DEG/ENaC ion channel complex known as the MEC-4 complex in *C. elegans*. This complex is composed of four

channel proteins: two degenerins, MEC-4 and MEC-10, a stomatin-like protein, MEC-2, and a paraoxonase-like protein, MEC-6 (Chelur et al., 2002; Goodman et al., 2002; Goodman and Schwartz, 2003). Expression of these channel proteins is seen in a punctate pattern along mechanosensory processes. Calcium transient analysis, mechanoreceptor potentials, and mechanoreceptor currents have been tested during mechanical stresses to verify the necessity of this circuit and channel complex in touch sensation (Suzuki et al., 2003; O'Hagan et al., 2005).

3. Neurotransmitters involved in *C. elegans* locomotion.

Nematodes utilize neurotransmitters conserved across phyla of invertebrates and vertebrates to modulate behavior. These include classical neurotransmitters such as glutamate, acetylcholine, GABA, biogenic amines, and neuropeptides (Mellanby, 1955; del Castillo et al., 1963; Sulston et al., 1975; Horvitz et al., 1982; Johnson and Stretton, 1987; Guestella et al., 1991; Li et al., 1999; Sanyal et al., 2004, Alkema et al., 2005). The complete genome, fluorescent reporters, RNAi, mutant analysis, electrophysiology, and laser ablation experiments have all been used to explore how each signaling molecule contributes to behaviors in the worm.

Acetylcholine acts as the main excitatory neurotransmitter at the NMJ, and GABA acts as the primary inhibitory neurotransmitter. Animals which are

deficient in cholinergic signaling (*unc-17* mutants) are highly uncoordinated and fail to generate a sinusoidal wave (Alfonso et al., 1993). GABA deficient mutants (*unc-25* and *unc-47*) also have locomotion defects, where the wave is generated with disjointed movement at a slower velocity (McIntire et al., 1997; Jin et al., 1999). This mutant analysis along with the ventral nerve cord wiring and connectivity diagram suggests that acetylcholine and GABA control the sinusoidal wave pattern. Acetylcholine is released from DA and DB neurons onto dorsal body wall muscles, and from the VA and VB neurons onto ventral body wall muscles. Contralateral excitement of GABAergic VD and DD neurons leads to the relaxation of the laterally opposite side to the contracted muscles (Figure 1-2) (White et al., 1986; Schuske et al, 2004). Although propagation of the wave is well described, it is still unclear where the wave originates, whether it is in the head or the tail.

Although glutamate acts as the major excitatory neurotransmitter at the *Drosophila* NMJ (Bate and Broadie, 1995), glutamate receptors are not present on the body wall muscles post synaptic to the VNC in *C. elegans* (Richmond and Jorgensen, 1999). Instead, glutamate mediates the translation of sensory input to a motor output in the nematode. Spontaneous reversals, nose touch backing responses, foraging, and avoidance of volatile and hypoosmotic stimuli are locomotion behaviors in which glutamate has been shown to play a necessary role (Hart et al., 1995; Maricq et al., 1995; Hart et al., 1999; Zheng et al., 1999; Mellem et al., 2002; Hills et al., 2004).

The *C. elegans* proteome includes over 250 neuropeptides encoded by 113 genes (Li and Kim, 2008). The impact of these signaling peptides has been gradually revealed as key regulatory agents in many aspects of development and behavior. With extensive expression in the nervous system, it is not surprising that neuropeptides are an integral part of locomotion behavior. Neuropeptides have been shown to be expressed in the ventral nerve cord (Nathoo et al., 2001), and four neuropeptide mutants are aldicarb resistant, indicating a role in acetylcholine modulation (Sieburth et al., 2005). As neuropeptide signaling is further studied in *C. elegans*, it is highly likely to reveal increasingly important roles in motor output.

Four biogenic amines are expressed in the worm: dopamine, serotonin, octopamine, and tyramine (Sulston et al., 1975; Horvitz et al., 1982; Alkema et al., 2005). Biogenic amine signaling modulates many nematode behaviors such as egg laying, pharyngeal pumping, defecation, mating, and locomotion. Analysis of mutants deficient in each of the biogenic amines, as well as administration of exogenous biogenic amines to wild-type animals have enabled discovery of many aspects of locomotion behavioral control in the animal (Horvitz et al., 1982; Schafer and Kenyon, 1995; Sawin et al., 2000; Chase et al., 2004; Alkema et al., 2005) .

Dopamine affects locomotion behavior by modulating how locomotion patterns change in response to external stimuli. There are eight neurons that

synthesize dopamine in the hermaphrodite (Sulston et al., 1975), all of which form synapses with motor neurons (White et al., 1986) Three dopaminergic G-protein coupled receptor are expressed in the ventral nerve cord. Exogenous dopamine inhibits locomotion in wild-type animals, but the dopamine receptor mutant, *dop-3* is resistant to the paralytic effects, indicating a role for dopamine in modulating locomotion (Chase et al., 2004). *cat-2* mutants (dopamine deficient mutants) fail to slow when encountering a food lawn (Sawin et al., 2000), and are defective in area restricted search (Hills et al., 2004), which is an important foraging behavior. Dopamine also modulates *C. elegans* learning, as it helps the animal adapt based on previous experiences. Habituation responses are altered in dopamine deficient mutants, as *cat-2* mutants habituate faster than wild-type to a plate tapping stimulus (Sanyal et al., 2004). Additionally, dopamine plays a role in swim induced paralysis (SWIP). SWIP assays show that wild-type worms will remain swimming in a drop of liquid for a 20 minute period. Animals mutant for the dopamine reuptake transporter (*dat-1*), which have a chronically elevated level of dopamine at the synapse, fail to remain swimming, and become paralyzed after 5 minutes (McDonald et al., 2007). Studies in mammalian systems also have determined that dopamine plays a major role in regulating locomotion, as depletion of dopamine leads to the debilitating movement neuropathy of Parkinson's disease (Davie, C.A., 2008).

In addition to dopamine, serotonin also plays a major role in relaying the state of the food environment to the animal, thus affecting locomotion. When a

starved animal comes in contact with a food source, it will come to an almost complete stop in locomotion in order to feed. Serotonin deficient animals are defective in this “enhanced-slowing response”, and application of exogenous serotonin masks the mutant phenotype (Sawin et al., 2000). Additionally, serotonin is synthesized in VC4 and VC5 in the ventral nerve cord (Duerr et al., 1999), yet these neurons are thought to be primarily part of the egg laying apparatus (Bany et al., 2003).

Octopamine and tyramine are often considered the invertebrate counterparts to mammalian norepinephrine and epinephrine, respectively. Previously, tyramine was only thought of as a precursor to octopamine in the biosynthetic pathway (Figure 1-3), but upon further analysis in *C. elegans*, it has been shown that tyramine and octopamine can modulate distinct behaviors. Both octopamine and tyramine are found in low levels, determined by HPLC, in the animal, which may be due to expression in only a few cells. Octopamine is synthesized in the RIC interneurons and the gonadal sheath, whereas tyramine is synthesized in the RIM interneurons and the UV1 cells (as well as the octopaminergic cells) (Alkema et al., 2005). Upon analysis of octopamine deficient mutants (*tbh-1* mutants), defects in locomotion are not apparent, but may play the antagonistic role to serotonin (Horvitz et al., 1982; Rogers et al., 2001; Niacaris and Avery, 2003). Recently, the role that tyramine plays in modulating *C. elegans* locomotion has become increasingly apparent.

4. Tyramine modulates distinct behaviors in *C. elegans*.

The importance of octopamine in modulating invertebrate behavior has long been established, as it has been implicated in biological roles such as firefly light emission and learning in fruit flies (Nathanson, 1979; Schwaerzel et al., 2003). Until recently, the role of tyramine in invertebrate physiology and behavior was unclear.

C. elegans provides a unique system in order to investigate the role of tyramine in animal behavior, as it is released from only one set of neurons in the nerve ring (in addition to octopaminergic neurons). Laser ablation of tyraminergic neurons, as well as analysis of tyramine deficient mutants, has led to the discovery of behavioral defects that are independent of octopamine deficient mutants, revealing a role for tyramine beyond its function as an intermediate in the biosynthetic pathway. Specifically, *tdc-1* mutants are hyperactive in egg laying, have reversal defects, and fail to suppress head oscillations in response to touch (Alkema et al., 2005). In wild-type animals, a gentle anterior touch will induce a long reversal while the animal suppresses its normal head swings used for foraging (Chalfie et al., 1985; Alkema et al., 2005). In *tdc-1* mutants, the length of the reversal is shorter, and the head swings continue through the backward locomotion (Alkema et al., 2005). These behavioral defects implicate a possible role for tyramine in modulating the escape response.

5. Tyraminergic receptors.

Although distinct tyraminergic neurons have not been identified in insects or other invertebrates besides *C. elegans*, tyramine receptors have been found in other species. G-protein coupled receptors that are activated by tyramine have been characterized in honeybees, cockroaches, locusts, fruit flies, tobacco hornworms, and silk moths, but it has yet to be determined if tyramine is acting as the endogenous ligand in these organisms (Saudou et al., 1990; Blenau et al., 2000; Ohta et al., 2003; Rotte et al., 2009). In addition to the *C. elegans* discrete tyraminergic neurons, tyramine receptors have been identified, enabling a deeper understanding into the molecular pathways of tyramine signaling.

Currently, there are four known tyramine activated receptors in *C. elegans*: LGC-55, SER-2, TYRA-2, and TYRA-3. LGC-55 is a tyramine-gated chloride channel (Pirri et al., 2009), and SER-2, TYRA-2, and TYRA-3 are GPCRs (Rex and Komuniecki, 2002; Rex et al., 2005; Wragg et al., 2007). This battery of tyramine receptors is somewhat similar for the organization of other biogenic amine receptors in the worm genome, as serotonin and dopamine also have a dedicated ion channel in addition to multiple GPCRs (Olde and McCombie, 1997; Hamdan et al., 1999; Ranganathan et al., 2000; Suo et al., 2002; Hobson et al., 2003; Suo et al., 2003; Ringstad et al., 2009). This may have a functional role, as the ion channel is fast-acting, and can modulate quick

sensory inputs, where GPCRs may modulate behaviors which do not have a strict time requirement.

The ligand-gated cation channel, LGC-55, has been shown to be activated by tyramine in heterologous system, as well as during *in vivo* experiments with tyramine application in an intact animal. Mutant analysis has shown that LGC-55 regulates specific behaviors in the *C. elegans* escape response. Upon gentle anterior touch, *lgc-55* mutants fail to suppress head oscillations similar to *tdc-1* mutants. Also, LGC-55 modulates the length of the reversal during the escape response, since *lgc-55* mutants make shorter reversals. Expression of this chloride channel correlates with the observed behavior as expression in the head muscles is sufficient for suppression of head oscillations, and expression in the AVB (forward command neuron) modulates the longer reversal (Pirri et al., 2009). The post-synaptic location of LGC-55 receptors to the RIM tyraminergic neuron indicates that LGC-55 is a primary target for tyraminergic signaling, and that tyramine is acting as a genuine neurotransmitter in *C. elegans*.

Upon *in vitro* pharmacological characterization using COS-7 cells, SER-2, TYRA-2, and TYRA-3 display a high affinity for tyramine (Rex and Komuniecki, 2002; Rex et al., 2005; Wragg et al., 2007), suggesting that these GPCRs may act as tyraminergic receptors in the worm. Sequence analysis has been conducted in order to predict the coupling of these receptors to the three possible G protein pathways in *C. elegans*: G_q, $G_{i/o}$, and G_s (Wragg et al., 2007).

Previously, it has been shown that octopaminergic receptors couple to the G_s pathways to elevate cAMP, and tyraminergic receptors couple to the $G_{i/o}$ pathway to decrease cAMP levels, yet now there is evidence that tyraminergic GPCRs may have variation in their signal transduction pathways. SER-2 and TYRA-2 are suggested to be $G_{i/o}$ (GOA-1) coupled (Rex and Komuniecki, 2002; Rex et al., 2005), as pharmacological induced decreases in cellular cAMP levels were seen in heterologous systems, but interestingly, TYRA-3 is thought to be G_q coupled by both sequence homology and the lack of a decrease in cellular cAMP levels (Wragg et al., 2007). This array of receptors provides the potential to study how a single biogenic amine can modulate behavior by diverse molecular mechanisms.

Although the gene structure, expression patterns, and *in vitro* pharmacological activity have been analyzed for each of the putative tyraminergic GPCRs, the physiological role for each of the receptors is unknown. Deletion alleles are available for all three genes, yet in each case, the mutant's morphology and overall behavior on normal food plates are grossly normal. *ser-2* mutants have been reported to display a minor defect in serotonin induced pharyngeal pumping (Rex et al., 2004), but have normal sensory and locomotory behaviors (Tsalik, et al., 2003). *tyra-3* mutants are defective in the tyramine induced inhibition of the serotonin dependent dilute octanol response (Wragg et al., 2007), and recently it has been shown that *tyra-3* modulates leaving behavior from food lawns (Bendesky et al., 2011). The expansive expression pattern of

these tyraminergic GPCRs suggests possible roles in modulation of locomotion and reproduction, yet the impact on these behaviors has yet to be determined.

C. Tyramine: receptors and disease in mammals

By furthering our knowledge of how tyramine signals in invertebrates, we may soon be able to understand how tyramine may affect the mammalian nervous system. Currently, research has found consequences of tyramine signaling changes, as symptoms and disease occurs when tyramine levels increase and decrease in humans. It is unclear what the physiological role of tyramine is in mammals, but the answer is slowly being elucidated.

1. Tyramine is present in mammalian nervous systems and food products.

Unlike classical biogenic amines such as serotonin and dopamine, the role of trace amines in modulation of mammalian behavior remains unclear. Trace amines, such as tyramine, octopamine, tryptamine, and β-phenylethyamine, are heterologously expressed and present in one hundred fold less concentrations than serotonin and dopamine in the mammalian brain (Boulton and Majer, 1971; Boulton and Baker, 1975). With such low levels and broad expression, it is predicted that trace amines may be neuromodulators of other neuroactive molecules in addition to the possible role as neurotransmitters in their own right.

Tyramine may be synthesized in the mammalian brain similarly to invertebrates, and it is unknown if it is being released from synaptic, or if it passes transiently through axons. However, it is known that tyramine can affect the mammalian nervous system through ingestion. Many edible plants such as avocados, raspberries, and spinach contain tyramine, as well as most fermented foods such as wine, aged cheese, and pickled herring (McCabe et al., 1986; Brown and Bryant, 1988). Consumed tyramine cannot cross the blood brain barrier (BBB), so it is thought that tyramine from food could be responsible for sympathetic nervous system induced changes in blood pressure and heart rate. Patients taking monoamine oxidase inhibitors (MAOIs) are advised to avoid diets high in tyramine, since MAOIs breakdown tyramine, resulting in a hypertensive crisis (Jansen et al., 2003).

Migraines have been reported after high intake of tyramine (Youdim et al., 1971), but it is still unclear if tyramine is a causative agent for the onset of severe headaches. Red wine and chocolate have long been regarded as triggers for migraines, and since both foods contain tyramine, it seems a likely candidate. The hypothesis that migraines are caused by biochemical irregularities has been stated since the 1980's, and recent evidence of dopamine and trace amine (including tyramine) fluctuations migraine pathology has been established. In patients with migraine and cluster headaches, there was a marked increase in circulating dopamine, octopamine, synephrine, and tyramine in the hypothalamus, amygdala, and dopaminergic systems (Grazzi et al, 2007;

D'Andrea et al., 2007). The receptors which are activated by trace amines, and may play a role in migraine etiology are currently under investigation.

2. Trace amine receptors (TAARs) in mammals.

In 2001, Borowsky and colleagues identified a class of mammalian GPCRs which were activated by trace amines (Borowsky et al., 2001; Bunzow et al., 2001). This discovery renewed interest in trace amines as modulators of the nervous system, and as potential drug targets for numerous neuropathies. The trace amine receptors (TAARs) were characterized *in vitro* to determine which trace amine bound to the receptor with the highest affinity. Interestingly, TAAR-1 (Human TA1) was most robustly activated by tyramine and β-phenylethylamie. *In situ* hybridization studies and RT-PCR detected TA1 in many tissues including the stomach, kidneys, amygdala, hypothalamus, and the cerebellum. The expression profile of TA1 and the other trace amine receptors is currently being investigated, with interesting results of wide expression across organ systems and brain regions (Borowsky et al., 2001).

Exploration of mouse and rat TAARs has revealed many possible modulatory roles for trace amines in the central and sympathetic nervous systems. For example, *in vitro* studies have shown that there is a reciprocal expression regulation between the dopamine transporter (DAT) and TAAR1 in mice (Xie and Miller, 2007; Lindemann et al., 2008). Additionally, due to the

expression of TAAR1 in the monoaminergic systems like the dorsal raphe nucleus and ventral tegmental area, it is hypothesized that trace amines may modulate the release of other neurotransmitters via the TAARs in these specialized regions (Borowsky et al., 2001). Further *in vitro* tests have shown a role for tyramine modulation of dopaminergic, glutamatergic, and GABAergic activity through TAAR1 (Revel et al., 2011). However, *Taar1* null mice have no apparent phenotype in most behavioral and neurological tests.

The endogenous role of TAARs has yet to be fully elucidated. Although the sequence homology between invertebrate tyramine receptors and mammalian TAARs is quite weak, we may be able to shed light on possible physiologic roles of trace amine signaling by investigating tyramine signaling in *C. elegans*. Specifically, by delineating how tyramine transmits a signal through GPCRs, and how cellular activity is modulated.

3. Tyramine signaling dysfunction correlates to numerous neuropathies.

Although trace amines, such as tyramine, are usually viewed as sympathomimetic in action, the presence of tyramine in the human brain suggests a role in the central nervous system. Deregulation of trace amines in the mammalian brain has been implicated in numerous disorders such as Parkinson's disease, attention deficit disorder, depression, and schizophrenia (Davis and Boulton, 1994; Branchek and Blackburn, 2003; Burchett and Hicks,

2006). Researchers are now attempting to tease apart the role of specific biogenic amines and their role in the etiology of these diseases.

Studies in humans have shown that trace amine level changes can be associated with neurological disorders. Patients with decreases in tyramine and octopamine have a higher occurrence of depression (Sandler et al., 1979). Other clinical studies have compared urinary and blood trace amine levels in patients with depression and ADHD (Davis and Boulton, 1994; Kusaga et al., 2002) to find altered levels compared to control groups. Further characterization of what these changes in trace amine levels are affecting will further the field of neuropharamacology and provide new drug targets for treatment of these disorders.

Current data which indicates a role for tyramine in human neuropathies has been mostly correlative, and thus incomplete on the possible mechanism of tyramine in modulating neuronal activity. My studies aim to use *C. elegans* to begin to answer how a trace amine can signal in the nervous system, how deficits in signaling can affect other neurotransmitters, and finally, how these deficits can affect behavior. By further elucidating these mechanisms, we may be able determine how invertebrates use tyramine to modulate behavior, and begin to hypothesize how a trace amine could change neuronal activity in the human brain.

Figure 1-1

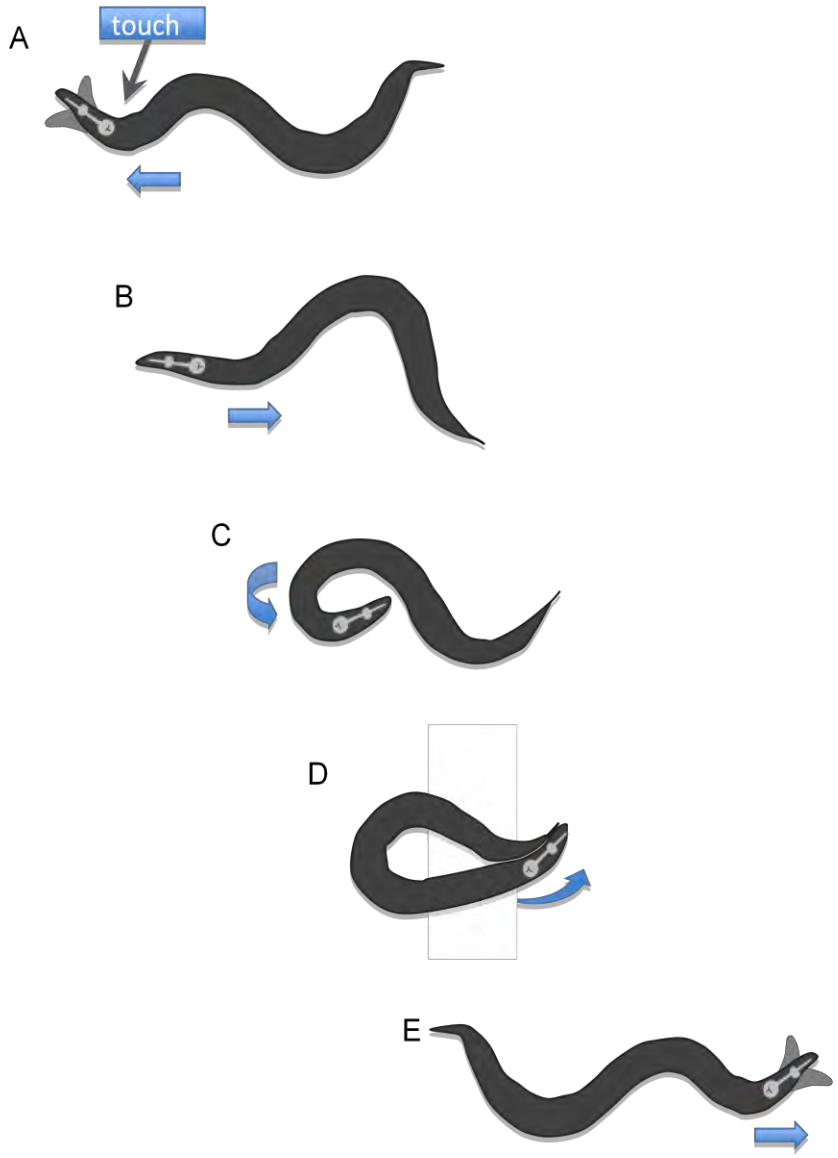

***C. elegans* escape behavior in response to gentle anterior touch.**

(A)The animal moves forward with exploratory head oscillations. (B) Upon anterior touch, the animal reverses while suppressing head oscillations. (C) After longer reversals, of 3 or more body bends, a deep ventral bend is initiated. (D) An omega turn is executed as the head of the worm slides down the length of the body. (E) Forward locomotion is reinitiated with head oscillations.

Figure 1-2

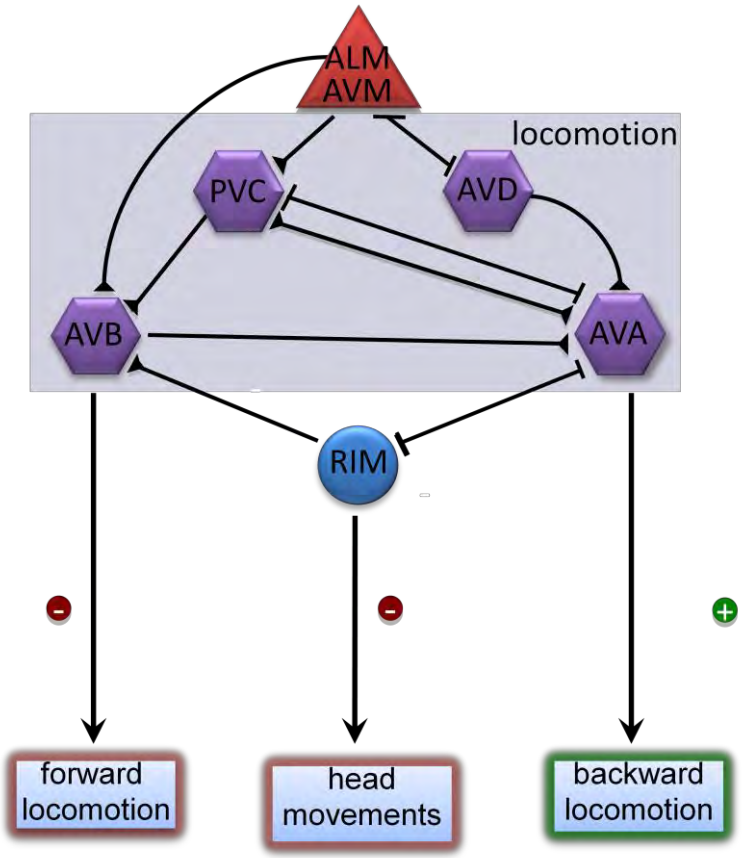

***C. elegans* senses and reacts to gentle anterior touch through a defined circuit.**

The ALM and AVM mechanosensory neurons synapse with command neurons to inhibit forward locomotion, and activate backward locomotion. A gap junction from the AVA activates tyramine release from the RIM interneuron, suppressing head oscillations.

Figure 1-3

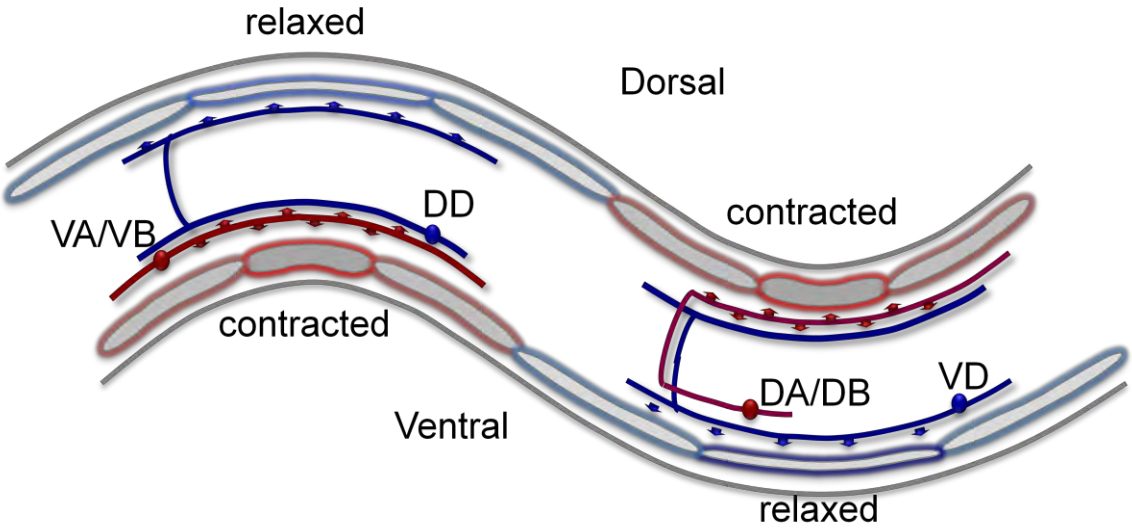

Cholinergic and GABAergic neurons comprise the ventral nerve cord.

VA and VB cholinergic neurons form NMJs with the ventral body wall muscles, while DA and DB cholinergic neurons form NMJs with the dorsal body wall muscles. DD and VD GABAergic neurons relax the dorsal and ventral muscles, respectively, and receive synaptic input from contralateral cholinergic neurons. This excitatory and inhibitory neuronal configuration is hypothesized to propagate the sinusoidal wave that *C. elegans* uses in locomotion behavior.

Figure 1-4

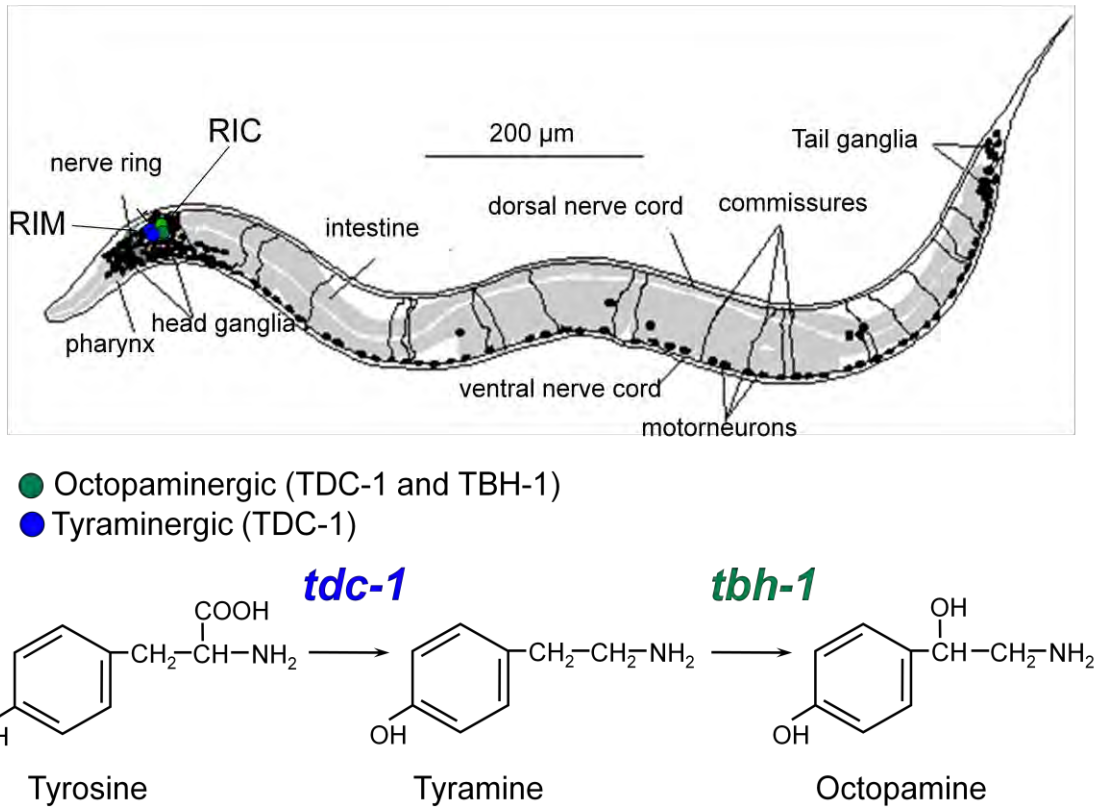

The RIM neurons are distinctly tyraminergic.

Tyrosine decarboxylase (TDC-1) converts tyrosine to tyramine. Tyramine β-hydroxylase converts tyramine to octopamine. The RIM motor neurons do not express *tbh-1* indicating that tyramine is the end product in those neurons. The RIC interneurons express both *tdc-1* and *tbh-1*, resulting in the production of octopamine.

CHAPTER II

Forward and Reverse Genetic Screens to Identify Tyraminergic Receptors and Signaling Pathways

This chapter is comprised of work that I commenced during my first rotation in the Alkema lab, as well as the continuation of identifying mutations from screens throughout the duration of my thesis work. The dose response of wild-type animals on exogenous tyramine, as well as the isolation of *lgc-55* mutants from an EMS screen, were my contributions to the 2009 publication in *Neuron*, "A Tyramine-Gated Chloride Channel Coordinates Distinct Motor Programs of a *Caenorhabditis elegans* Escape Response". The text and figures were written and constructed by myself, with editorial and content feedback from Jennifer Pirri and Christopher Clark.

A. Introduction

Biogenic amines control animal behavior and modulate neuronal activity in vertebrates and invertebrates. Trace amines, which are a subclass of biogenic amines, are present in concentrations one hundred fold less in mammalian brain tissue and are heterogeneously expressed (Boulton and Majer, 1971; Boulton and Baker, 1975). Not much is known about the role of trace amines, including tyramine, in the human brain, but deregulation of trace amines in mammals have been implicated in many neurological disorders including Parkinson's disease, obsessive compulsive disorder, attention deficit disorder, and migraine headaches (Davis and Boulton, 1994; Branchek and Blackburn, 2003; Burchett and Hicks, 2006; Grazzi et al, 2007; D'Andrea et al., 2007). Most studies have been done using post-mortem tissues or urine samples from patients with these disorders, leading to an obvious limitation in discovering the genetic and molecular pathways of trace amine signal transduction.

C. elegans uses four biogenic amines as for neuronal signaling in their simple, yet elegant nervous system: serotonin, dopamine, octopamine, and tyramine (Sulston et al., 1975; Horvitz et al., 1982; Alkema et al., 2005). The biosynthetic pathway of tyrosine conversion into octopamine suggests that tyramine is merely an intermediate precursor, but recently, tyramine has been shown to act as a genuine neurotransmitter in the nematode. The RIM interneurons are thought to be discretely tyraminergic, expressing a tyrosine

decarboxylase, *tdc-1*, the biosynthetic enzyme which converts tyrosine to tyramine. The RIC interneurons also express *tdc-1*, but coexpression of a tyrosine beta-hydroxylase, *tbh-1*, indicates that tyramine is converted to octopamine before vesicular release. In addition to understanding the biosynthetic pathway, tyramine deficient mutants have specific behavioral defects such as an increase in reversals, slight decrease in locomotion rate, and an increase in egg laying rate (Alkema et al., 2005).

Using the powerful genetics and molecular tools of *C. elegans* we sought to identify how tyramine modulates behavior in the animal. Firstly, we conducted a forward genetic screen to take an unbiased approach to uncover signaling components. Secondly, we did a reverse genetic screen by using mutants of known receptor and signaling genes to examine defined signaling pathways. These two experiments uncovered tyraminergic receptors and signaling pathways, in addition to revealing roles for tyramine receptors in modulation of locomotion and egg laying behavior.

B. Results

1. A forward genetic screen on exogenous tyramine drug plates.

To understand how tyramine could modulate behavior in *C. elegans*, we developed a pharmacological assay to apply tyramine to the animal. Previous

work with dopamine and serotonin has been done (Horvitz et al., 1982; Schafer and Kenyon, 1995; Sawin et al., 2000; Chase et al., 2004), showing that biogenic amines can cross the cuticle of the nematode and affect behavior. Similar to these studies, agar plates with varying concentrations of tyramine hydrochloride were made to assess the effect of exogenous tyramine on the animal. Well-fed animals were transferred to the drug plates and behavior was assessed. While low concentrations of exogenous tyramine slowed the locomotion rate, 30 mM exogenous tyramine rendered the animal immobilized within 5 minutes (Figure 2-1, Movie 2-1).

Using this pharmacological assay, we conducted a genetic screen to find post-synaptic signaling pathways. Adult animals were mutagenized with EMS, allowed to recover, and then transferred to large NGM plates for serial egg lays over the next 12 hours. In the F2 generation, plates of worms were screened on 30 mM exogenous tyramine to find mutants which were resistant to the paralytic effects. Isolates were then allowed to self-reproduce, and retested for resistance to exogenous tyramine. Three independent EMS screens were conducted, where 20,000 haploid genomes were screened, and 24 mutant alleles were isolated. Of these isolates, seven tyramine resistant mutants have been mapped to genes (Table 2-1).

Two of the tyramine resistant isolates (*zf11* and *zf53*) were highly resistant to the paralytic effects of exogenous tyramine on head movements. Although the

body of the animal paralyzed similarly to wild-type, the head of the animals continued to move for the 20 minute assay (Pirri et al., 2009). *zf11* and *zf53* were mapped to the right arm of chromosome IV by single nucleotide polymorphism mapping and classical mapping methods. Sequence analysis found point mutations in the *lgc-55* gene. *zf11* was found to be a mutation in the splice acceptor site of exon 9, resulting in a frame shift which leads to a truncated protein, while *zf53* was a point mutation which changed the first cysteine codon of the Cys-loop to a tyrosine. The Cys-loop motif forms disulfide bonds between subunits which are required for receptor assembly and gating of the ion channel. The tyramine resistant phenotype of our isolated mutants was recapitulated by an available deletion allele of *lgc-55* (*tm2913*). LGC-55 was further characterized to be a tyramine-gated chloride channel expressed in head neurons, neck muscles, and the reproductive system (Pirri et al, 2009).

In addition to the two alleles of *lgc-55*, another mutant isolate, *zf109*, was highly resistant to head immobilization, with a partial resistance to body immobilization on exogenous tyramine. On food plates, the animal appeared uncoordinated and disjointed in forward locomotion. I mapped this mutation to chromosome X, where it was determined to be an allele of *unc-9*, an innexin protein. Innexins are transmembrane channel proteins that form invertebrate gap junctions. UNC-9 and UNC-7 make up the *C. elegans* gap junctions which are required for electrical synapse signaling.

Four isolates from the exogenous tyramine screen were highly resistant to the paralytic effects exogenous tyramine on body movements. Three of the four isolates also displayed increased velocity and body bending depths in the absence of drug, as well as a constitutive egg laying phenotype. *zf47* was mapped to the center of chromosome one by SNP mapping, and sequence analysis confirmed a mutation in the *goa-1* gene, which encodes the G alpha o/i homolog protein. *zf97* and *zf98* were SNP mapped to the left arm of chromosome X. Sequence analysis confirmed two independent mutations of a diacylglycerol kinase, *dgk-1*. Isolating alleles of *goa-1* and *dgk-1* in a screen for tyramine resistant mutants indicated that tyraminergic signaling is acting through a G protein-coupled receptor through the GOA-1 pathway.

The fourth isolate which showed full body resistance to exogenous tyramine, *zf51*, was first mapped using SNP mapping and classical mapping methods. These results were unclear due to linkage on both chromosome IV and X. We then employed the power of deep sequencing to get a sequence read of all mutations in the genome. After analyzing the SNP mapping and deep sequencing results, we concluded the tyramine resistance phenotype could be a compound effect of multiple mutations. Firstly, a mutation in the *ptr*-5 gene was analyzed, since the mutation caused an early stop in a cuticle development gene located on chromosome X. If the animal failed to molt, the result could cause a difference in drug penetration. Analysis of a deletion mutant of *ptr*-5 on exogenous tyramine showed a weak tyramine resistance phenotype not similar

to *zf51* mutants (data not shown). By comparing our SNP mapping and deep sequencing results, a mutation in a protein tyrosine kinase, *y116a8c.24* on the right arm of chromosome IV, was also a likely candidate. Mutant alleles were not readily available, and little is known about the expression or function of this kinase, therefore we sought to further characterize this gene.

2. Y116A8C.24: An uncharacterized protein tyrosine kinase is resistant to exogenous tyramine.

Protein kinases are one of the largest and most important protein families in the nematode, encoded by 438 genes that possibly phosphorylate up to 30% of the *C. elegans* genome (Plowman et al., 1999). *y116a8c.24* encodes an uncharacterized protein tyrosine kinase that has a SH2 motif and an ATP binding motif. On exogenous tyramine, *zf51* mutants are only 30 % immobilized at 10 minutes, while wild-type is 100% immobilized (Figure 2-2). On food plates in the absence of drug, *zf51* mutants display mostly wild-type behavior. To test if *zf51* is an allele of *y116a8c.24*, a PCR product was amplified from whole worm lysate including 2kb of the promoter, the predicted genomic sequence, and 500 bp of the 3' UTR. The PCR product was injected into *zf51* mutants with a coelomocyte GFP marker. Three transgenic lines partially restored sensitivity to exogenous tyramine (Figure 2-2), indicating that *zf51* may be an allele of *y116a8c.24* .

3. A reverse genetic screen for tyramine signaling mutants.

Our second approach to identify tyraminergic signaling components was to take a candidate gene approach. In addition to the tyramine-gated chloride channel, LGC-55, there are three known tyraminergic G-protein coupled receptors: TYRA-2, TYRA-3, and SER-2 (Rex and Komuniecki, 2002; Rex et al., 2005; Wragg et al., 2007). Deletion mutants of each of the receptors were tested on 30 mM exogenous tyramine. Although *tyra-2* and *tyra-3* mutants were 100% immobilized after 10 minutes, *ser-2* mutants were partially resistant to exogenous tyramine (Figure 2-3A) for body movements, unlike the head movement resistance shown by *lgc-55* mutants (Pirri et al., 2009). Interestingly, *ser-2* mutants begin to paralyze similar to wild-type within the first five minutes of the assay, but then begin to move on the drug plate for the remainder of the 20 minute assay. Our data indicates that *ser-2* may act to modulate body locomotion, where *lgc-55* is playing a separate role to inhibit head movements in the presence of exogenous tyramine.

. The GOA-1 pathway has been shown to modulate locomotion and egg laying through the inhibition of the EGL-30 pathway (Mendel et al., 1995; Segelat et al., 1995; Lackner et al., 1999; Miller et al., 1999). Since our forward genetic screen on exogenous tyramine identified alleles of G protein signaling components, known mutants from the GOA-1 pathway were tested on exogenous tyramine. *goa-1, gpb-2, dgk-1,* and *egl-16* mutants were all resistant

to immobilization. Furthermore, a gain of function mutation in *egl-30*, the $G_{\alpha q}$ homolog, was also highly resistant to immobilization (Figure 2-3A). These results indicate that G-protein coupled receptor, SER-2, may be working through the GOA-1 pathway to inhibit body locomotion on exogenous tyramine.

Wild-type animals fully immobilize on exogenous tyramine between 4-7 minutes. Upon closer examination, *tyra-3* mutants immobilized faster than wild-type, showing 100% paralysis by 3 minutes on 30 mM tyramine, indicating a hypersensitivity phenotype (Figure 2-3B). To further investigate the dynamics of *tyra-3* immobilization, 10 mM exogenous tyramine assays were conducted. Whereas wild-type animals remained partially resistant to low levels of exogenous tyramine, *tyra-3* mutants were fully immobilized (Figure 2-3C), confirming *tyra-3* as hypersensitive to exogenous tyramine.

4. Multiple mutant analysis of tyramine receptors.

Double mutant strains were made for all tyramine receptor combinations. The most mobile strain on 30 mM exogenous tyramine was *lgc-55*;*ser-2* mutants. When *tyra-3* mutants were crossed into either *lgc-55* or *ser-2* mutants, the percent of immobilized animals increased. The most immobilized strain, for head and body movements, were *tyra-3 tyra-2* double mutants, indicating that SER-2 and LGC-55 are the key receptors for modulating locomotion on exogenous tyramine (Figure 2-4A).

To further uncover the role of LGC-55, SER-2, and TYRA-3 in exogenous tyramine assays, triple mutant strains were constructed. In each strain, only one receptor was left in the wild-type form, allowing for analysis of how exogenous tyramine interacts on each receptor alone. In *lgc-55;tyra-2 ser-2* triple mutants, the population of animals on tyramine continue to move for the entirety of the assay, indicating that TYRA-3 may act to bind tyramine and induce locomotion. In *lgc-55;tyra-2 tyra-3* triple mutants, the animals are completely immobilized at 10 minutes, showing that SER-2 inhibits locomotion on exogenous tyramine. When all three of the G protein-coupled receptors are mutant in the *tyra-3 tyra-2 ser-2* triple mutant, the population is partially immobilized showing an intermediate phenotype between *ser-2* and *tyra-3* mutants, but the head movements remains completely relaxed and immobilized (data not shown) due to the wild-type allele of *lgc-55*. Quadruple mutants, *lgc-55;tyra-3 tyra-2 ser-2*, are resistant to exogenous tyramine, but less than the *lgc-55;tyra-2 ser-2* strain (Figure 2-4B). Since immobilization still occurs in some quadruple mutants, this indicates that either there are one or more tyramine receptors left to be identified, or the concentration of tyramine is high enough to bind to other biogenic amine receptors in the nematode which are not activated by tyramine at endogenous levels.

5. *tyra-3* is expressed in head neurons, spermatheca, distal tip cells, and tail neurons.

Not much is known about the endogenous function of TYRA-3. Previous research on TYRA-3 has reported a partial expression pattern of the gene, and has described TYRA-3 as a modulator of leaving behavior on food (Wragg et al., 2007; Bendensky et al., 2011). Bendensky and colleagues reported that *tyra-3* was expressed in sensory neurons including the ASK, ADL, BAG, and OLQ sensory neurons (Bendensky et al., 2011). To further identify the expression pattern of *tyra-3* and characterize the possible role of TYRA-3 in tyraminergic signaling, an mCherry transcriptional reporter was constructed that contained 2kb of the upstream promoter, and the first exon and intron. From analysis of the expression pattern, we hoped to determine which neurons were important for the *tyra-3* mutant phenotype on exogenous tyramine, and to identify additional roles for TYRA-3 in modulating *C. elegans* behavior.

Similar to previous reports, the transgene was broadly expressed in head neurons, the spermatheca, distal tips cells, and tail neurons. We sought to identify the head neurons by using multiple coexpression GFP reporters. Dopaminergic coexpression was analyzed using a *pdat-1*::GFP. *tyra-3*::mCherry was coexpressed in the four CEP neurons, but not the ADE neurons or the PDE neurons posterior to the vulva (Figure 2-5A). To determine if the *tyra-3* hypersensitivity phenotype was due to modulation of dopaminergic neurons, a

full length *tyra-3* cDNA was injected under the control of the *dat-1* promoter to see if the hypersensitivity phenotype could be rescued. Three independent lines were tested on 10 mM exogenous tyramine, but the hypersensitivity phenotype remained (Figure 2-5B), indicating that expression in the CEP neurons is not responsible for the exogenous tyramine hypersensitivity phenotype.

Additional coexpression and positional analysis was done, which identified *tyra-3* expression in the PVQ tail neurons and the SDQL neuron (data not shown). A cholinergic reporter, *punc-17*::GFP, coexpresses with *tyra-3*::mCherry in two additional unidentified neurons (data not shown). Coexpression with the vesicular glutamate transporter GFP reporter, *peat-4*::GFP, was seen in many neurons. By combining my expression analysis with published results (Bendensky et al., 2011), *tyra-3* is coexpressed in the OLQ, ASK, AIN,and LAU glutamatergic neurons (Figure 2-6), indicating a possible modulatory role where *tyra-3* would increase glutamate signaling through the G_q pathway upon activation by tyramine.

C. Materials and Methods

1. Exogenous tyramine assays.

All strains were grown on nematode growth media (NGM) agar plates with *E. coli* (OP50) provided as a food source. Behavioral assays were conducted

with young adult animals (24 hours post L4) at 22°C. Tyramine drug plates were made by autoclaving 1.7% agar in water, cooling the solution to 55°C, and adding variable concentrations of tyramine hydrochloride (Sigma), and glacial acetic acid to a final concentration of 2 mM as a preservative.

Animals were placed on drug plates from food plates with minimal bacterial transfer. The percentage of immobilized animals was scored every minute for a 20 minute assay. An animal was deemed immobilized if it lacked sustained body locomotion for a five second interval. Body locomotion was defined as forward or backward locomotion regardless of velocity.

2. Genetic screen and mapping.

The wild-type strain (Bristol N2) was mutagenized with 50 mM ethyl methanesulfonate (EMS) (Brenner, 1974). Young adults of the F2 generation were tested on 40 mM exogenous tyramine drug plates and assessed for immobilization. Animals that were resistant to paralysis were picked as isolates and progeny were retested on 30 mM exogenous tyramine to decrease false positive isolates. Mutants were backcrossed twice into the wild-type background and mapped to chromosomal locations.

Classical and single nucleotide polymorphism mapping (SNP mapping) were employed to identify alleles of *lgc-55*, *goa-1*, *dgk-1*, and *unc-9*. Tyramine

mutants were crossed into triple mutant strains, MT3751(*dpy-5*(I);*rol-6*(II);*unc-32*(III)) and MT464(*unc-5*(IV);*dpy-11*(V);*lon-2*(X)) to identify the chromosomal locale of the mutation in classical mapping experiments. SNP mapping was done following the Jorgensen Lab protocol using the CB4856 Hawaiian strain (Davis et al., 2005). Deep sequencing of *zf51* was done by preparing a concentrated genomic DNA sample using Qiagen's Puregene Kit. 5µg of DNA was sent to the Hobert Lab for deep sequencing.

3. Cloning and cell identification of *tyra-3.*

A *ptyra-3*::mCherry construct was made by inserting a PCR product that includes 2kb upstream of the *tyra-3* start site, as well as the first intron into the pPD95.75 mCherry plasmid. Transgenic lines were obtained by microinjection of plasmid DNA into a *lin-15(n765ts)* mutant background with a *lin-15* rescuing plasmid as a coinjection marker. Integration of the extrachromosomal array was done using x-ray radiation.

Cell identification was done using *ptyra*-3::mCherry overlays with Nomarski images and with coexpression of cell-specific GFP markers. GFP strains used for identification crosses were: *punc-17*::GFP, *peat-4*::GFP(*adIs1240*), *pdat-1*::GFP, and *psra-6*::GFP(*oyIS14*). Coexpression was determined using confocal microscopy (Zeiss) and imaging software (Image J).

Dopaminergic *tyra-3* expression was cloned by inserting the 400 bp *dat-1* promoter in front of a *tyra-3* cDNA. The *pdat-1*::TYRA-3 plasmid (20 ng/µl) was injected into *tyra-3 lin-15* double mutants with a *lin-15* rescuing plasmid (50 ng/µl). Independent extrachromosomal lines were assayed on 10 mM tyramine drug plates for rescue of the tyramine hypersensitivity phenotype.

4. *y116a8c.24* PCR rescue.

Primers were designed to amplify the 2 kb *y116a8c.24* genomic DNA, 2 kb of promoter, and 500 bp of the 3' UTR (GGAACACCTCATGCTTGTCTG, CTCTCGCACAGAGCTGAAATT). This 4.5 kb PCR product was gel isolated and injected (20 ng/µl) into *zf51* mutants with a coelomocyte GFP coinjection marker (pPD98.97 at 50 ng/µl). Three stable transgenic lines were isolated and tested on 30 mM exogenous tyramine to determine if expression of *y116a8c.24* rescued the tyramine resistance phenotype of *zf51* mutants.

D. Discussion

Our two genetic approaches to discover tyramine signaling components revealed receptors and downstream transduction pathways which affect locomotion on exogenous tyramine. The unbiased forward genetic screen resulted in the isolation of many mutants, including seven alleles representing five different genes. Although gene candidate studies are biased, our reverse

screen discovered different roles for three of the four tyramine receptors in modulation of *C. elegans* locomotion behavior.

LGC-55 modulates head movement on exogenous tyramine, as the body is paralyzed in *lgc-55* mutants, but the neck and head still maintain locomotion. SER-2 inhibits body locomotion on exogenous tyramine, as *ser-2* mutants remain capable of slow locomotion while wild-type animals are completely immobilized. Interestingly, *tyra-3* mutants were hypersensitive to exogenous tyramine, indicating that TYRA-3 activates locomotion in the presence of tyramine. Through detailed double, triple, and quadruple mutant analysis, we have confirmed distinct behavioral phenotypes for each receptor mutant. Interestingly, although two alleles of *lgc*-55 were isolated from the forward genetic screen, we have yet to isolate a mutant of *ser-2*. The phenotype of the *ser-2* deletion alleles is quite robust, but possibly EMS point mutations have yet to produce a null allele.

Previous *in vitro* work suggests that SER-2 is coupled to the GOA-1 pathway, and TYRA-3 is coupled to the EGL-30 pathway, indicating a possible role for two tyraminergic GPCRs to function in inhibitory and excitatory signal transduction pathways. This hypothesis could explain our opposing pharmacological phenotypes seen between the two mutants. Our analysis of *goa-1* mutants genetically supports the prediction of SER-2 coupling, but we

have yet to confirm which G protein pathway is utilized by TYRA-3 using our pharmacological assay.

In addition to the pharmacological assessment of tyramine receptor mutants, behavioral studies can be conducted to detect the endogenous role of each tyramine receptor. Further expression analysis of the receptors needs to be done to help guide behavioral investigations. In Chapter Three of this dissertation, the expression of *ser-2* and the behavior of *ser-2* mutants are explored in detail, but *tyra-3* behavioral analysis has yet to yield significant results.

In addition to a tyramine receptor and GPCR signaling mutants, an innexin, UNC-9 was identified. The discovery of the involvement of *unc-9* regulating locomotion on tyramine drug plates is perplexing, as we assumed post-synaptic activation of tyramine receptors and the immediate downstream signaling cascade would be sufficient to inhibit locomotion. Gap junctions may be necessary to transduce the signal provided by tyramine receptors to downstream neurons in the locomotion circuit. Another possibility of how UNC-9 may modulate locomotion on drug plates is that of an unidentified role for the innexin. It has been shown that *unc-9* mutants are resistant to GABA and ivermectin, an anthelmintic (Boswell et al., 1990). Further experiments are critical to detect correct neuronal circuitry, excitability, and receptor localization.

Lastly, an allele of a protein tyrosine kinase, *y116a8c.24*, was isolated from the exogenous tyramine screen. Specificity to the effects of tyramine can be analyzed by conducting exogenous drug assays using other biogenic amines to determine if *zf51* mutants are also resistant to immobilization. Future analysis of deletion mutants and identifying the expression pattern will shed light on the role that this kinase plays in modulating locomotion in *C. elegans*.

Only a small percentage of the isolated mutants from EMS screen were mapped to chromosome locations and subsequently identified as alleles of specific genes. This was due to the surprisingly difficult mapping on exogenous tyramine drug plates. We found that during SNP mapping, the Hawaiian strain was less sensitive to exogenous tyramine, resulting in picking false positive mutants during the crosses. With heterogeneous mixtures of Bristol and Hawaiian *C. elegans* DNA, the single nucleotide polymorphisms did not project a clear location for the mutation. Only the mutants which had a strong phenotype on exogenous tyramine were successfully mapped to completion, leaving a freezer full of interesting, partially resistant, tyramine signaling mutants. Hopefully in the future, more careful, detailed analysis will be conducted to identify these genes, which may elucidate additional tyramine signaling pathways.

Figure 2-1

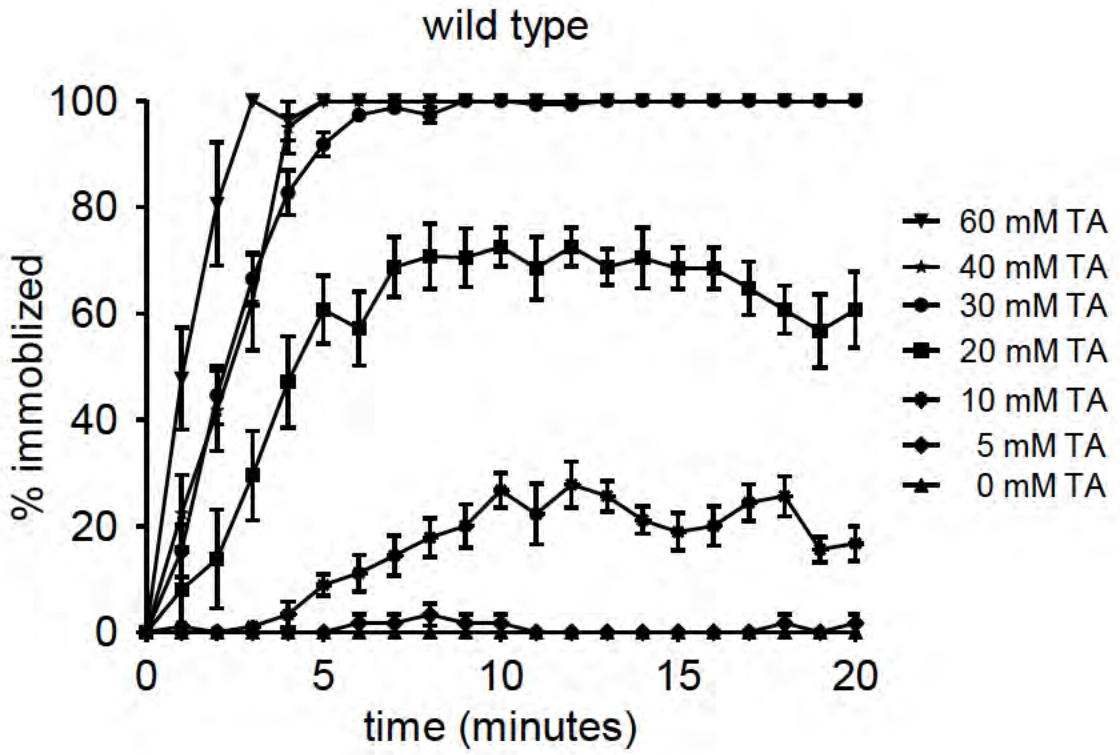

Exogenous tyramine inhibits wild-type locomotion in a dose dependent manner.

Agar plates with dissolved tyramine hydrochloride were prepared at varying concentrations. On plates containing 30 mM exogenous tyramine, animals are 100% immobilized by 5 minutes. Error bars represent S.E.M.

Table 2-1

allele	gene	known function
zf11	*lgc-55*	tyramine-gated chloride channel
zf47	*goa-1*	heterotrimeric G protein alpha subunit
zf51	*y116a8c.24* *ptr-5*	tyrosine protein kinase SSD protein
zf53	*lgc-55*	tyramine-gated chloride channel
zf97	*dgk-1*	diacylglycerol kinase
zf98	*dgk-1*	diacylglycerol kinase
zf109	*unc-9*	innexin

Isolates from tyramine resistance EMS screen.

Seven alleles were mapped to chromosomal locations by SNP or classical mapping methods, and confirmed by sequence analysis.

Figure 2-2

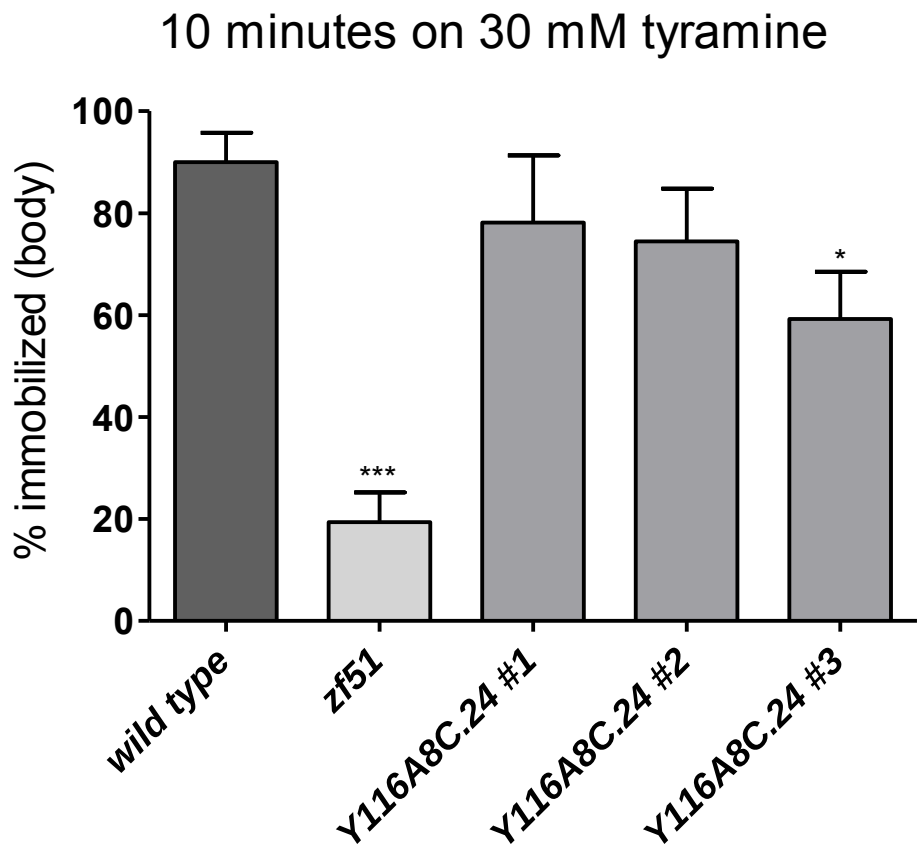

***zf51* is an allele of *y116a8c.24*, a protein tyrosine kinase.**

zf51 mutants are resistant to the paralytic effects of exogenous tyramine. Three independent transgenic lines, where a full genomic PCR product of *y116a8c.24* was injected, show restoration of wild-type paralysis on 30 mM exogenous tyramine. Error bars depict S.E.M. Statistical difference relative to wild-type; Student's t test *p<0.05, ***p<0.001.

Figure 2-3

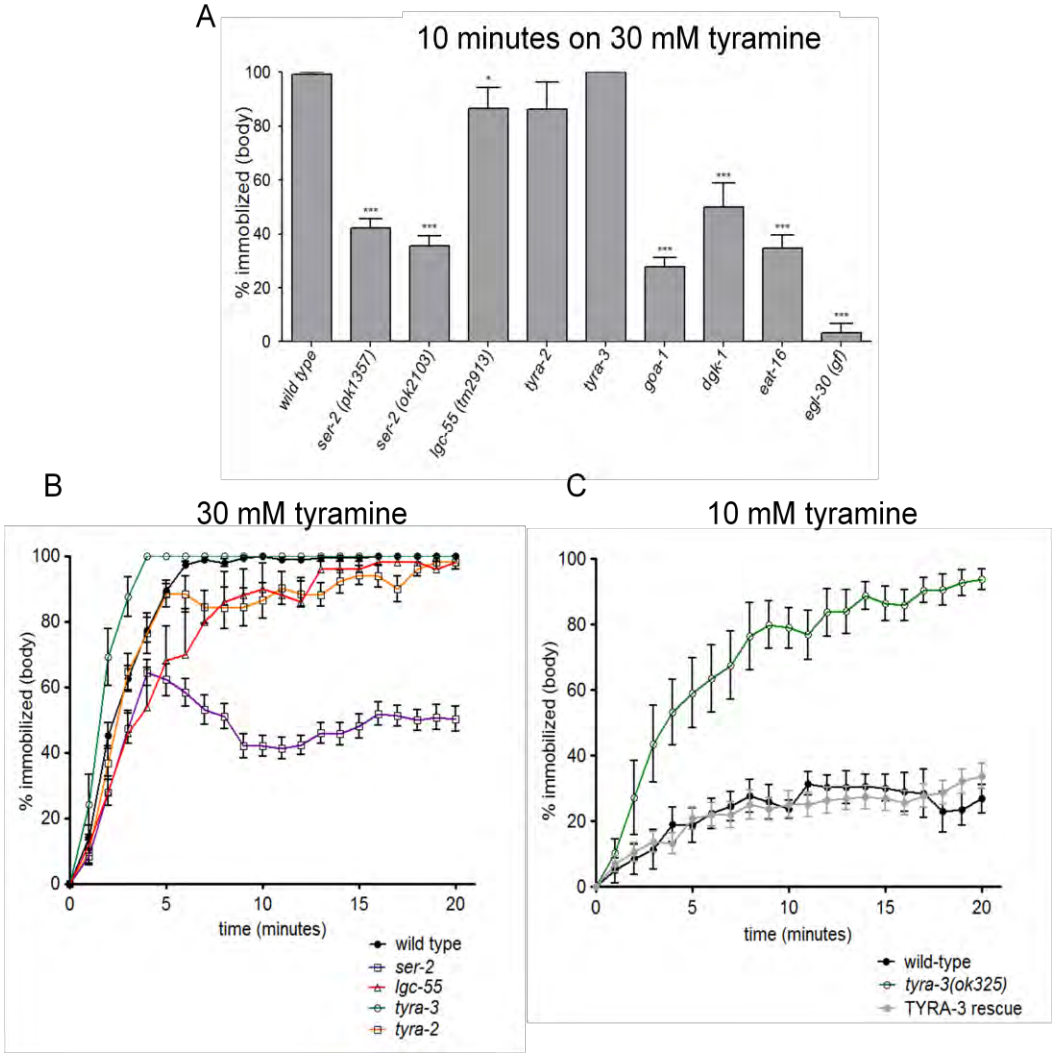

Tyramine receptor and G protein signaling mutants on exogenous tyramine. (A) After 10 minutes on 30 mM exogenous tyramine, *ser-2* mutants and GOA-1 pathway signaling mutants are resistant to exogenous tyramine. (B) Time course tyramine assays show that *ser-2* mutants are resistant to 30 mM tyramine, and *tyra-3* mutants are hypersensitive to exogenous tyramine. (C) Hypersensitivity phenotype of *tyra-3* mutants on exogenous tyramine is more apparent at 10 mM concentration. Error bars depict S.E.M. Statistical difference relative to wild-type; Student's t test *p<0.05, ***p<0.001.

Figure 2-4

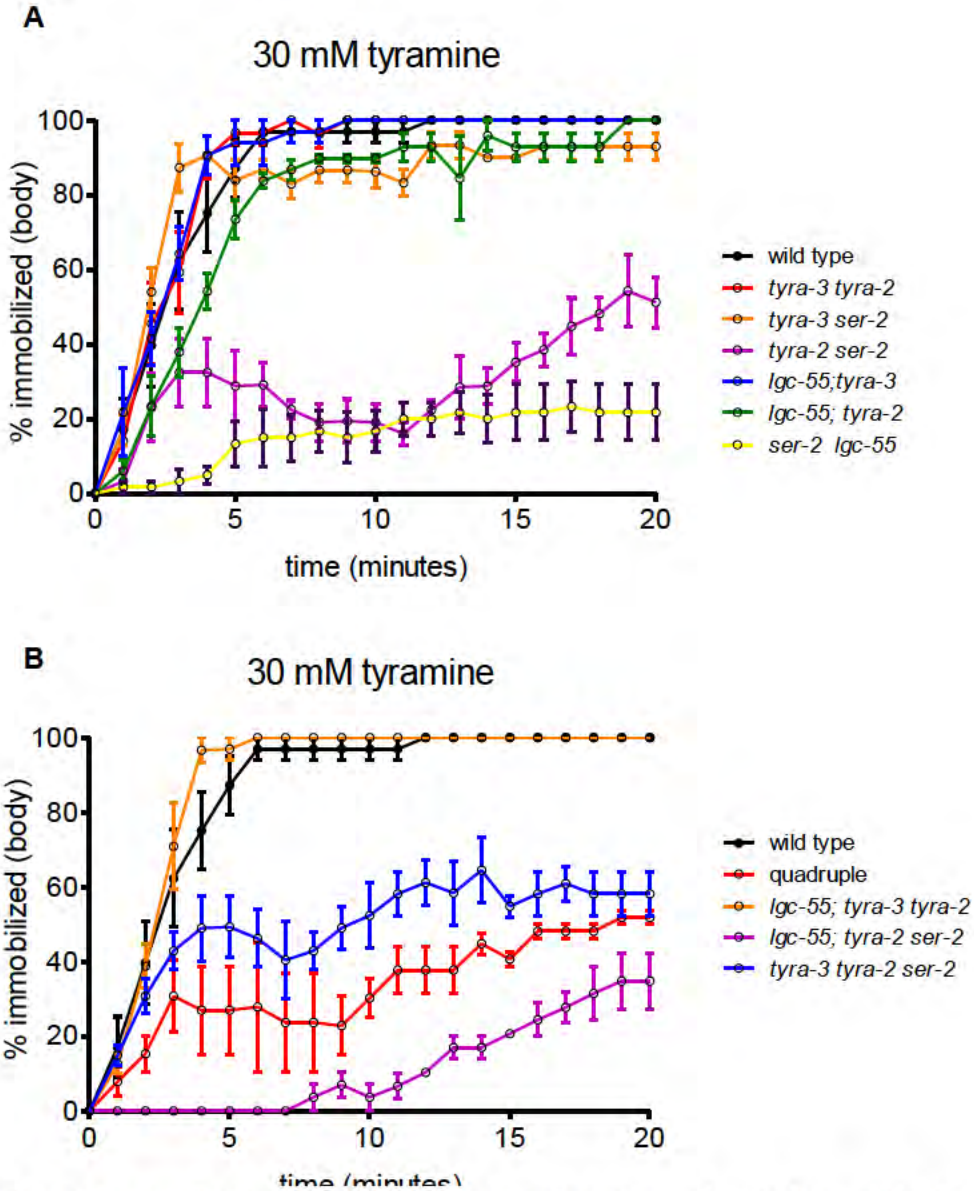

Receptor mutant combinations on exogenous tyramine. (A) Double tyramine activated receptor mutants were tested on 30 mM exogenous tyramine. *ser-2* mutant combinations were the most resistant to body immobilization. (B) Triple and quadruple tyramine receptor mutants confer the role of *ser-2* in inhibiting locomotion on tyramine drug plates, and *tyra-3* activating locomotion on tyramine drug plates. Error bars depict S.E.M.

Figure 2-5

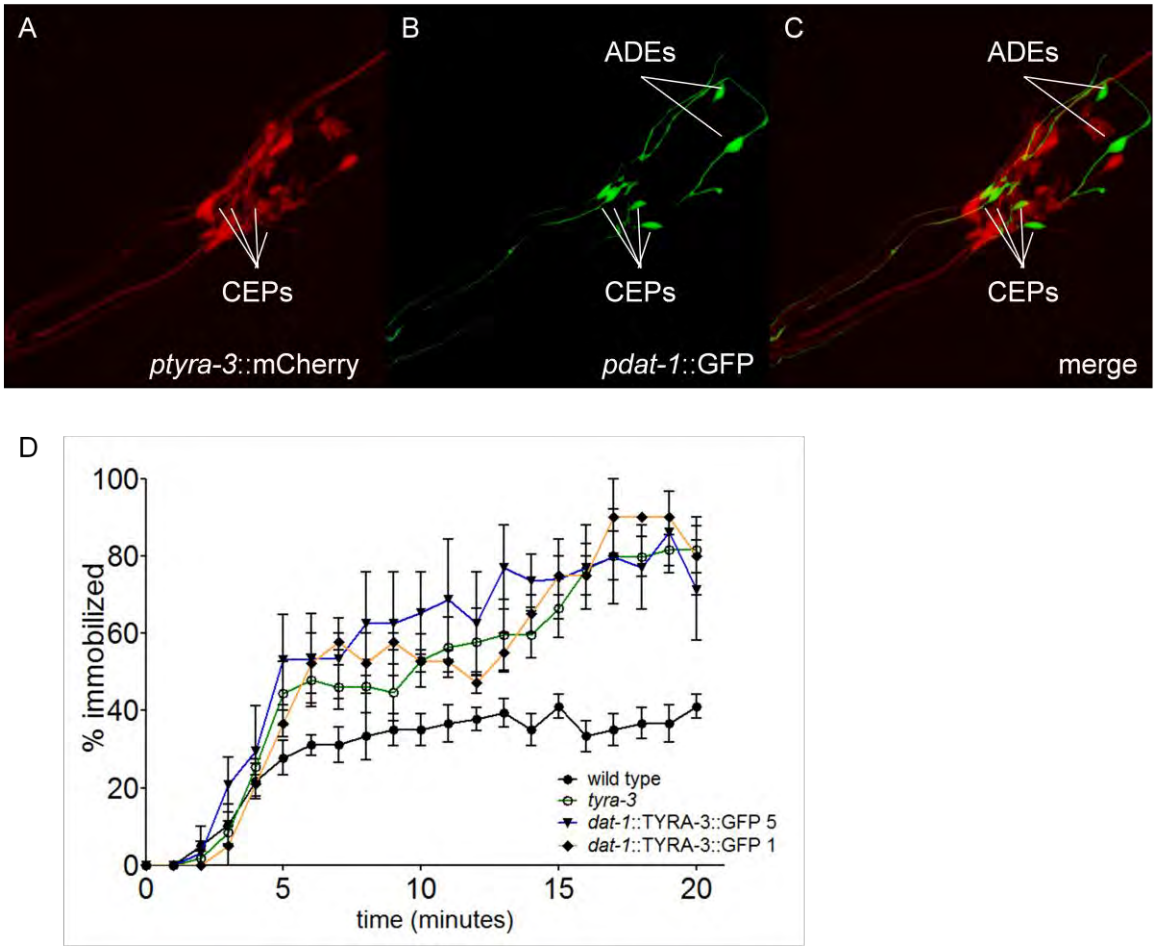

***tyra-3* is expressed in dopaminergic neurons.**

(A) A *tyra-3* mCherry transcriptional reporter is expressed in many head neurons. (B) *pdat-1*::GFP is expressed in 6 dopaminergic neurons in the head, and two in the body. (C) Merged image shows coexpression in CEP neurons, but not the ADE neurons. (D) Cell-specific expression of *tyra-3* cDNA in dopaminergic neurons, under the *dat-1* promoter, does not rescue *tyra-3* mutant hypersensitivity to exogenous tyramine (10 mM). Error bars depict S.E.M.

Figure 2-6

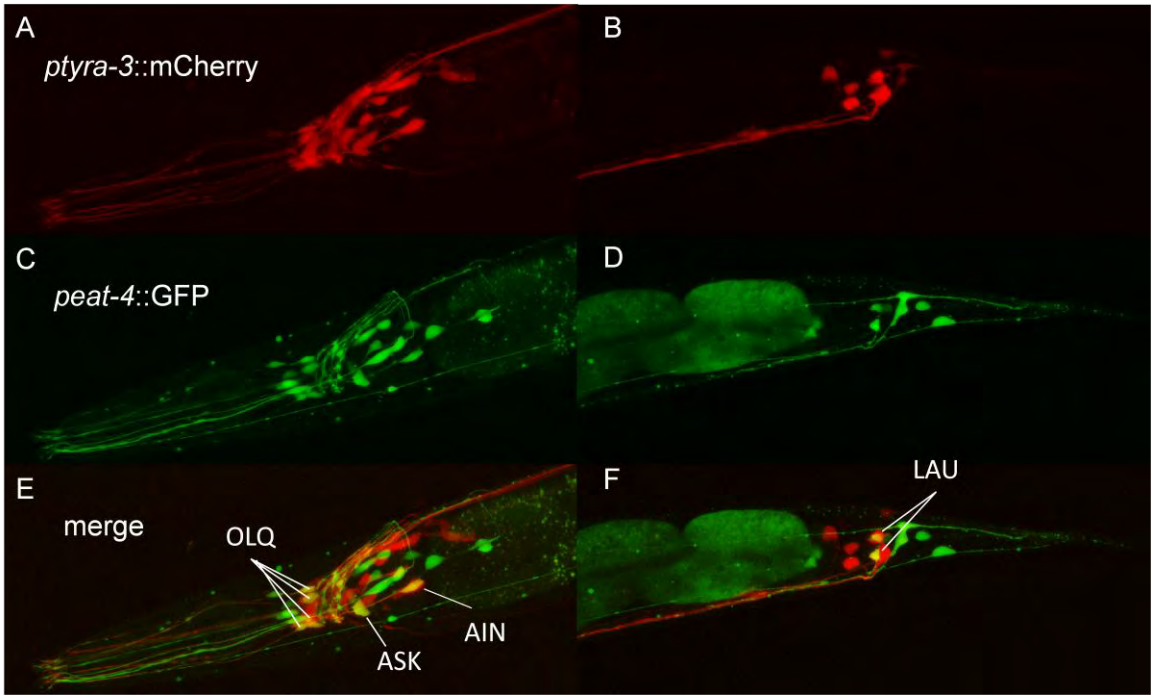

***tyra-3* is expressed in glutamatergic neurons.**

(A-B) *ptyra-3*::mCherry is expressed in head and tail neurons (C-D) *peat-4*::GFP (vesicular glutamate transporter reporter) is expressed in identified head and tail neurons. (E-F) *ptyra-3*::mCherry is coexpressed with the glutamate reporter *peat-4*::GFP. Coexpression is seen in OLQ, ASK, and LUA neurons.

Movie 2-1

Wild-type animals on 30 mM tyramine.

A population of wild-type animals were transferred to a 30 mM exogenous tyramine plate in a drop of water. Water is removed with a Kimwipe after transfer. Over the next five minutes, the animals go through a period of long reversals and straightening of the head. By five minutes, the population of animals were immobilized. Movie is shown at five times normal speed.

CHAPTER III

Biogenic Amine Receptors Control Navigation in *C. elegans*

This chapter represents the majority of my dissertation work, identifying a role for SER-2 in *C. elegans* behavior. The final version of "Biogenic amine receptors control navigation in *C. elegans*" will be submitted to *Neuron* in Fall of 2011. The strain building, tyramine assays, aldicarb assays, DD channelrhodopsin bending index, and omega turning behavior experiments were conducted by me. The VD and DD ablation experiments were done by Christopher Clark, the electrophysiology was done by Marian Haburcak and Michael Francis, head movement analysis was done by Jennifer Pirri, and the worm imaging of DD activation and inhibition was done by Andrew Leifer. The text was written by Mark Alkema and me, with feedback from Christopher Clark and Jennifer Pirri.

A. Introduction

Escape responses are important mechanisms for survival spanning phyla from microscopic organisms through complex mammals. These responses vary in their intricacy, yet all require sensory input, signal integration, and locomotory behavioral output to allow for evasion of predators. Animals have adapted to efficiently orchestrate a series of movements to best distance themselves from various aversive sensory inputs including visual, odor, and mechanical stimulation. The nematode *C. elegans* displays a unique behavioral paradigm in response to touch. Upon gentle anterior touch, the nematode discontinues forward locomotion, suppresses head movements, reverses the sinusoidal wave, and often executes an omega turn to change directions.

Animal behavior is modulated by biogenic amines. In *C. elegans*, tyramine has been shown to function as a neurotransmitter that coordinates distinct motor programs in escape behavior (Alkema et al., 2005). Upon gentle anterior mechanical stimulation, a single pair of tyraminergic RIM motor neurons release tyramine through the activation of the ALM and AVM mechanosensory neurons (Chalfie et al, 1985). We have previously shown that the biogenic amine tyramine acts through a fast acting ligand-gated ion channel, LGC-55 (Pirri et al, 2009). Here, we have uncovered another layer of complexity to how this amine further coordinates the escape response through a metabotropic, slow acting G protein-coupled receptor (GPCR).

Amine activated GPCRs can act as highly sensitive modulators of animal behavior. A class of GPCRs that are activated by trace amines, like tyramine, has been identified in the mammalian brain. The defining member of this trace-amine associated receptor family, TAAR-1, is broadly expressed in the mouse brain and has a high affinity for tyramine, yet its endogenous role remains elusive (Borowsky et al., 2001). *C. elegans* also has three known GPCRs that bind tyramine: TYRA-2, TYRA-3, and SER-2 (Rex et al., 2002; Rex et al., 2005; Wragg et al., 2007). Phylogenic comparisons and *in vitro* cAMP assays suggest SER-2 is $G\alpha_o$ (GOA-1) coupled (Rex et al., 2002). Furthermore, the neuronal and muscle expression pattern of *ser-2::gfp* reporters (Tsalik et al., 2003) suggest a possible role in nematode locomotion, egg laying and feeding, however *ser-2* mutants display grossly normal behavior.

Our analysis reveals a new role for SER-2 in *C. elegans* escape response behavior. After tyramine release quickly suppresses head oscillations and enables a long reversal, mediated by LGC-55, we propose that SER-2 is asymmetrically positioned in the ventral nerve cord to modulate the execution of an efficient omega turn, leading to a smooth “get-away”. Our model suggests that tyramine orchestrates this fixed action pattern through postsynaptic fast acting channels, and slow acting metabotropic GPCRs. The sequence of the nematode’s escape response provides insight on how a simple nervous system can utilize a single neurotransmitter to navigate through its environment and evade predators.

B. Results

1. *ser-2* mutants are resistant to exogenous tyramine.

C. elegans immobilizes on plates containing exogenous tyramine in a dose dependent manner (Figure 3-1A, 3-S1, Pirri et al., 2009). To determine whether effects of exogenous tyramine are mediated by GPCRs that are activated by tyramine, we examined locomotion of *ser-2 (pk1357* and *ok2103)*, *tyra-2(tm1815)* and *tyra-3(ok325)* deletion mutants on agar plates containing exogenous tyramine. Wild-type, *tyra-2,* and *tyra-3* mutant animals completely immobilized on 30 mM tyramine within 5 minutes (Figure 3-1, 3-S2A, and Movie 3-1). However 42% of *ser-2* mutant animals sustained movement on plates containing exogenous tyramine (Figure 3-1, 3-S1, and Movie 3-2). Sensitivity to exogenous tyramine is restored back to wild-type levels in *ser-2* mutants containing a *ser-2* genomic transgene (Figure 3-1B-C, and 3-S2B). This suggests that exogenous tyramine mediates its paralytic effects through the hyperactivation of endogenous tyramine signaling pathways.

Head movements and body movements are controlled independently by distinct groups of muscles and motor neurons (White et al., 1986; Alkema et al., 2005). We have previously shown that activation a tyramine-gated chloride channel, LGC-55, inhibits head movements and forward locomotion (Pirri et al., 2009). On exogenous tyramine *lgc-55* mutants body movements are inhibited but head movements continue. Exogenous tyramine initially induced reversals and

inhibited head movements in *ser-2* mutants similar to wild-type, but after 5 minutes *ser-2* mutants resumed forward locomotion and head movements (Figure 3-1C). To dissect the effect exogenous tyramine on head and body movements, we analyzed head movements in an *unc-3* mutant background. *unc-3* encodes a transcription factor required for ventral nerve cord development (Prasad et al., 1998). *unc-3* mutants display few body movements but head movements are unaffected. Like in *unc-3* mutants, head movements of *ser-2 unc-3* double mutants are inhibited on exogenous tyramine. However, approximately 35% of ser-2 mutants do reinitiate head movement after prolonged exposure on exogenous tyramine. *lgc-55;unc-3* mutants displayed sustained head movements on exogenous tyramine (Figure 3-1D). This indicates that exogenous tyramine induces immobilization of head movements mainly through hyper-activation of ionotropic tyramine receptor LGC-55, and immobilization of body movements through the hyper-activation of the metabotropic tyramine receptor, SER-2.

2. SER-2 acts through the $G\alpha_o$ signaling pathway.

To identify additional genes involved in tyramine signaling, we performed a genetic screen for mutants that are resistant to the immobilizing effects exogenous tyramine on body movements. Three isolates from this screen, *zf47*, *zf97* and *zf98,* continued movement on plates containing 30 mM tyramine.

Genetic mapping, complementation tests and sequence analysis showed that *zf47* was an allele of *goa-1.* *goa-1* encodes the *C. elegans* orthologue of the neural G protein-alpha subunit of the $G\alpha_{i/o}$ class. *zf97* and *zf98* were alleles of *dgk-1*, which encodes the *C. elegans* orthologue of the vertebrate brain diacylglycerol kinase theta (Houssa et al., 1997; Nurrish et al., 1999) and likely is a downstream effector of GOA-1/ $G\alpha_{i/o}$. Previously characterized null mutants for *goa-1* and *dgk-1* were resistant to the paralytic effect of tyramine on both head and body movements (Figure 3-1B). Unlike *goa-1* and *dgk-1* mutants, which exhibit hyperactive locomotion and egg laying behavior, *ser-2* mutants did not have obvious behavioral defects. GOA-1/$G\alpha_{i/o}$ is expressed throughout the nervous system and is thought to negatively regulate synaptic transmission through the inhibition of EGL-30, the *C. elegans* orthologue $G\alpha_q$ (Lackner et al., 1999; Miller et al., 1999). We found that *egl-30*/$G\alpha_q$ gain-of-function mutants and mutants for *eat-16,* which encodes an RGS protein that inhibits EGL-30 (Hajdu-Cronin et al., 1999), are resistant to exogenous tyramine (Figure 3-1B). Therefore, mutations that reduce GOA-1/ $G\alpha_{i/o}$ signaling or increase EGL-30/$G\alpha_q$ signaling confer resistance to exogenous tyramine. Our observations indicate that SER-2 signals through GOA-1/ $G\alpha_{i/o}$ to modulate locomotion.

3. *ser-2* is expressed in GABAergic neurons.

Where does SER-2 act to confer resistance to exogenous tyramine? A *ser-2* transgene which includes a 2 kb promoter and the genomic sequence restored sensitivity of *ser-2* mutants to exogenous tyramine indicating that it is expressed in cells that modulate locomotion. We found that *pser-2*::mCherry reporter (11 kb promoter with the first intron) was expressed in head muscles, as well as neurons in the head and ventral cord (Figure 3-2A). Whereas the lgc-55 reporter is expressed in neck muscles (third and fourth row of muscle cells), the *ser-2* reporter is expressed in head muscles (first and second row of muscle cells) (Figure 3-S3). *ser-2* mutants did suppress head movements in response to touch, indicating that only LGC-55 is required for tyramine induced head relaxation. The *ser-2* reporter is not expressed in command interneurons that control locomotion, as expression did not overlap with *glr-1*::GFP and *lgc-55*::GFP reporters (data not shown). *ser-2* reporter expression was observed in 13 cells in the ventral cord. The ventral cord is composed of cholinergic and GABAergic motor neurons that innervate body wall muscles and control locomotion. Acetylcholine (ACh) is the major excitatory neurotransmitter, and GABA is the major inhibitory neurotransmitter of the neuromuscular junction in *C. elegans*. Coexpression analysis with GFP reporters that specifically label cholinergic or GABAergic neurons showed that *pser-2*::mCherry were highly expressed in a subset GABAergic motor neurons (Figure 3-2B-D). GABAergic ventral nerve cord neurons are subdivided into 13 VD motor neurons that

synapse onto the ventral body wall muscles, and 6 DD motor neurons that synapse onto the dorsal body wall muscles. The cells that highly express the *ser-2* reporter do not co-label with a *pflp-13*::GFP reporter (data not shown), which is expressed in the DD motor neurons (Kim and Li, 2004). This indicates SER-2 is specifically expressed in the GABAergic VD motor neurons.

Since GABAergic motor neurons are required for normal locomotion, we tested if SER-2 acts in these cells to mediate the inhibitory effects of tyramine on movement. Expression of *ser-2* cDNA in GABAergic neurons (*punc-47::*SER-2) restored sensitivity of *ser-2* mutants to exogenous tyramine similar to the wild-type (Figure 3-3A). To determine if GABA signaling affects tyramine sensitivity GABA deficient mutants for were tested on exogenous tyramine. We found that *unc-25* mutants, which lack glutamate decarboxylase required for GABA synthesis (Jin et al., 1999), were hypersensitive to the immobilizing effects of exogenous tyramine (Figure 3-3A). This indicates that reduced GABA signaling increases the sensitivity to exogenous tyramine. GABA deficiency did suppress the resistance phenotype of *ser-2* mutants, as *unc-25;ser-2* double mutants were equally sensitive to tyramine as *unc-25* single mutants (Figure 3A). These epistasis experiments show that SER-2 acts upstream or in parallel to GABAergic signaling. Our data are consistent with the hypothesis that SER-2 acts in GABAergic neurons to control locomotion.

4. SER-2 inhibits GABA release.

To determine if SER-2 can modulate neurotransmitter release in from ventral cord motor neurons, we analyzed mutants for their sensitivity to the acetylcholinesterase inhibitor aldicarb. Aldicarb increases ACh concentrations at the neuromuscular junction, causing muscle contraction and eventual paralysis (Nonet et al., 1998). Mutants with impaired ACh release are resistant to aldicarb-induced paralysis (Nguyen et al., 1995). *egl-30*/Gα_q mutants are resistant to aldicarb, whereas *goa-1* mutants are hypersensitive to aldicarb-induced paralysis indicating that EGL-30/Gα_q stimulates and GOA-1/G$a_{i/o}$ inhibits ACh release from motor neurons. Since body wall muscles also receive inhibitory GABA inputs, hypersensitivity to aldicarb can also be caused by a decrease in GABA release at the NMJ (Loria et al. 2004, Jiang et al., 2005, Vashlishan 2008). The time course of paralysis of *ser-2* mutants induced by aldicarb was similar to the wild-type (Figure 3-3B). This may be due to the restricted expression of *ser-2* in a subset of GABAergic neurons. We therefore generated transgenic lines that over expressed *ser-2* in all cholinergic (*pacr-2*::SER-2) or GABAergic (*punc-47*::SER-2) motor neurons and analyzed the rate of aldicarb induced paralysis. The time course of paralysis of transgenic animals that express SER-2 in cholinergic or GABAergic VNC motor neurons was similar to the wild-type (Figure 3-3B). Since there might be insufficient endogenous tyramine signaling to modulate neurotransmitter release under regular assay conditions, we examined paralysis on plates that contained both aldicarb and tyramine. On plates that contained

both aldicarb and 30 mM tyramine, animals that over expressed *ser-2* in cholinergic neurons (p*acr-2*::SER-2) were more resistant to the paralytic effects of aldicarb than the wild-type. Conversely, animals that over expressed *ser-2* in all GABAergic neurons (p*unc-47*::SER-2) were hypersensitive to paralysis (Figure 3-3C) on plates containing aldicarb and tyramine. These data are consistent with the hypothesis that SER-2 couples to the GOA-1/$G\alpha_{i/o}$ pathway to inhibit neurotransmitter release.

5. Tyramine-mediated reduction in GABA synaptic release requires SER-2.

The GABAergic VD motor neurons that express *ser-2* make synaptic contacts onto ventral musculature. Therefore, to directly evaluate whether tyramine modulates synaptic release of GABA from motor neurons, we measured the frequency of endogenous inhibitory post-synaptic currents (IPSCs) in whole-cell recordings from ventral body wall muscle cells. To isolate GABA currents, recording were made from ventral muscles of *unc-29;acr-16* double mutants that lack excitatory neurotransmission at the NMJ (Francis and Maricq, 2006; Touroutine et al., 2005). In these animals, we observed high levels of endogenous IPSC activity (~13 events/s) that gradually declined over the time course of the recording period (~10 minutes) (Figure 3-4A). This basal level of inhibitory activity is consistent with previous reports that have used other, non-genetic approaches to isolate IPSCs. After an initial period of recording basal

activity (~ 60 s) we switched to a bath solution containing tyramine. Within 30 s of tyramine exposure we noted a rapid decrease in the rate of IPSCs to approximately 66% of the rate prior to tyramine exposure (Figure 3-4A and C). This reduction was not reversible within the time course of our recordings. These results suggest that tyramine can modulate GABA-mediated inhibitory transmission at the NMJ, potentially acting through a pathway with high tyramine affinity. To test whether the reduction in IPSC frequency involved SER-2, we examined the effects of tyramine exposure in recordings from *unc-29;acr-16;ser-2* triple mutants (Figure 3-4B). We found that the basal IPSC frequency was not changed significantly by deletion of *ser-2*; however, the tyramine-mediated reduction in GABA release was significantly attenuated in these animals (17% reduction, versus 34% in animals wt for the *ser-2* locus) (Figure 3-4D-E), suggesting the tyramine effects on inhibitory transmission are predominantly mediated by SER-2. It should be noted that the residual (SER-2 independent) effects of tyramine we observed in part reflect a decline in the activity of the preparation over time as we noted a decrease in IPSC frequency in untreated animals over the same time course. The amplitude of endogenous GABA IPSCs were not significantly different in +/+ animals and *ser-2* mutants (+/+: 29.5 ± 1.4 pA, *ser-2*: 31.9 ± 3.9 pA), indicating that clustering and function of postsynaptic GABA receptors are normal in *ser-2* mutants (Figure 3-4F). Similarly, the amplitude of GABA IPSCs was not significantly affected by tyramine exposure for either strain (+/+: 26.9 ± 1.2 pA, *ser-2*: 30.7 ± 4.4 pA).

6. Asymmetric activation or inhibition of GABAergic motor neurons induces bending.

C. elegans moves on its side by propagating a sinusoidal wave of muscle contractions and relaxations along the length of its body. The sinusoidal wave is propagated by GABA mediated relaxations and acetylcholine mediated contractions of body wall muscles. GABAergic motor neurons receive synaptic inputs from VA/VB and DA/DB cholinergic motor neurons, and form synapses on body wall muscles (Figure 3-5A) (McIntire, et al., 1993). This arrangement suggests GABA mediated inhibition of body wall muscles occurs contralateral to acetylcholine mediated contractions, allowing for serial flexures of a sinusoidal wave. How VD and DD motor neurons could mediate navigation and directionality of the wave is unknown, therefore we laser ablated the VD and DD motor neurons subsets separately. Following laser ablation of the VD neurons, animals moved with a ventral bias. Conversely, animals with ablated DD neurons moved with a dorsal bias (Figure 3-5B-C, and Movies 3-3 and 3-4). Laser ablated animals still propagated a wave along the anterior-posterior axis, but with deeper dorsal or ventral flexures. The ablation of the GABAergic neurons suggests that insufficient relaxation of the body wall muscles results in a directional bias in locomotion. DD ablated animals crawled in tighter circles than VD ablated animals. It is not clear if this is due to a difference of quantity or strength of synapses between subsets of the D motor neurons, or the number of neurons ablated in each animal. *unc-25* animals that lack GABA signaling in

both VD and DD motor neurons made shallow body bends, but showed no direction bias in their locomotion pattern (Figure 3-5C). Could SER-2 play a role in navigation of forward locomotion by inhibiting GABA release along the ventral body wall muscles? To test this, we also tracked *ser-2* mutants to evaluate their navigational direction and saw that there was no difference from wild-type (Figure 3-5C).

Our laser ablation studies indicate that asymmetric relaxation of ventral or dorsal muscle bending can lead to a navigational bias for the animal. To determine if acute asymmetric activation or inhibition of GABA signaling could also lead to dorsal or ventral bending we used optogenetics. We expressed channelrhodopsin-2 (ChR2) and halorhodopsin (NpHR) in six DD motor neurons using the *flp-13* promoter. Using the Colbert worm tracking system (Leifer, 2011), which allows for restricted temporal and spatial exposure to UV light, we exposed the ventral nerve cord to periods of light while recording turning behavior. Our transgenic animals behaved as remote control worms upon blue and green light exposure. Blue light activation of channelrhodopsin in DD motor neurons activates GABA release on the dorsal body wall muscles, leading to a relaxation of the dorsal side of the worm, resulting in a ventral turn. In contrast, when the animal was exposed to green light, halorhodopsin inhibits GABA release on the dorsal body wall muscles, and subsequently results in a dorsal turn (Figure 3-6A and Movie 3-5). To quantify our observations of our remote control worm with multiple blue and green light exposures we calculated a

bending index. We found that animals expressing channelrhodopsin and halorhodopsin have a dorsal bending bias when exposed to green light, and a ventral bending bias when exposed to blue light (Figure 3-6B). A bending index of zero indicates no directional bias. These effects were not seen when the transgene was not present, or retinal was not fed to the animals prior to the experiment. Our results show that not only can a chronic disruption of GABAergic signaling lead to a navigational defect in *C. elegans*, but acute activation and inhibition of GABA release can also lead to directional changes of locomotion.

7. *ser-2* is required for the execution of omega turns.

Could SER-2 play a role in *C. elegans* turning behavior? We have shown that tyramine plays a crucial role in the coordination of backing response and the suppression of head oscillations in the escape response through the activation of a novel tyramine gated chloride channel, *lgc-55* (Pirri et al., 2009). Reversals are usually coupled to an omega turn, which allows the animal to reinitiate forward locomotion approximately 180° from the stimulus leading to an escape (Croll, 1975; Gray et al. 2005). After a reversal, the omega turn is initiated by a steep ventral bend of the head, and typically makes contact with the body anterior to the vulva, sliding along the ventral side of the body, before reinitiating forward locomotion. We found that the likelihood that an animal initiates an omega turn

in response to anterior touch correlates with the length of the reversal (Figure 3-7A). These results are consistent with data from spontaneous reversals (Gray et al., 2005), where omega turns tend to occur 60% of the time when a reversal is longer than three body bends (Figure 3-7A).

Since tyramine inhibits GABA release on the ventral side, and SER-2 is expressed in neurons that innervate the ventral body wall muscle, we decided to investigate the role SER-2 plays in omega turns. Like the wild-type, upon anterior touch, *ser-2* mutants suppressed head oscillations and reversed directions with body bend lengths similar to wild-type animals (Figure 3-S4). Furthermore, *ser-2* mutants initiated an omega turn at the same frequency as the wild-type (Figure3-7A) by making a steep ventral head bend and changing direction by greater than 90°. However, once *ser-2* mutants have initiated the omega turn they contract less tight during the turn. Whereas most wild-type animal's head touch the body anterior to the vulva 85% of the time, *ser-2* mutant animals fail fully close the omega turn and touch the head to the body at a lower frequency of 27% (Figure 3-7B-C, Movies 3-6 and 3-7). To further analyze the omega turn defect, the angle of closure (omega angle) was measured from the deepest most contracted region of the body to the closest or touching points in the head and tail (Figure 3-7B and D). Wild-type worms typically closed their omega turns, while *ser-2* mutants often conducted an open omega turn, averaging an omega angle of 24°. Our genomic *ser-2* rescue lines regained the ability to close the omega turn (Figure 3-7C-D).

Since anterior touch with an eyebrow hair has some inherent variability, we also induced reversals by blue light. When exposed to blue light, *pmec-4*::ChR2 worms conduct backward runs similar to runs stimulated by touch (Nagel et al., 2005, Leifer et al. 2011). We analyzed omega turns of *pmec-4*::ChR2 transgenic animals in both wild-type and *ser-2* mutant backgrounds and found that *ser-2* mutants have a lower frequency of closing omega turns and a higher omega turning angle than the wild-type, showing a similar defect in omega turns as with reversals induced by touch (Figure 3-7C-D).

We also conducted touch assays with DD and VD ablated animals. The wild-type and mock ablated animals executed closed omega turns in response to gentle anterior touch with typical nose to tail touch. However, animals in which the DD neurons were ablated initiated omega turns, but could not turn ventrally deep enough to execute a closed omega. Conversely, animals with VD ablated neurons were not deficient for closing omega turns and were prone to hypercontract the ventral turn, leading a nose and tail crossover while the head and body were in contact during the turn (Figure 3-S5). As a result of a shallow omega turn, the escape angle, a change in direction in response to touch, was changed in *ser-2* mutants. Wild-type worms averaged an escape angle of 179°. *ser-2* mutants made a more shallow escape angle, changing their direction from the point of stimulus by approximately 150° (Figure 3-7E-F). SER-2 may enable the animal to escape efficiently from a stimulus, by causing a complete omega turn, allowing the animal to turn around and head in the opposite direction. Our

results support a model of the *C. elegans* escape response (Figure 3-8), where gentle anterior touch induces tyramine release from the RIM neurons, leading to a suppression of head oscillations and reversal by synaptic activation of LGC-55, followed by an omega turn mediated by the asymmetric inhibition of GABA by the extrasynaptic activation of SER-2.

C. Discussion

1. SER-2 modulates neural circuit output in *C. elegans.*

We identified an endogenous function for SER-2, a tyraminergic G protein-coupled receptor. Previous *in vitro* analysis of SER-2 in COS-7 cells demonstrated that SER-2 can bind tyramine. Upon tyramine application, cAMP levels in the cell decrease, suggesting that tyramine may act as the natural ligand, and that SER-2 is most likely an inhibitory GPCR (Rex et al., 2002). In this study, our genetic screen for mutants resistant to the paralytic effects of exogenous tyramine unveiled a role for the $G\alpha_o$ signaling pathway in *C. elegans* locomotion. Our candidate gene approach showed that *ser-2* mutants were quite resistant to exogenous tyramine, while mutants of the other two known tyramine activated GPCRs, *tyra-2* and *tyra-3* displayed wild-type-like or hypersensitive phenotypes. Furthermore, from our detailed expression analysis and epistasis analysis experiments for *ser-2*, we discovered that *ser-2* asymmetrically inhibits GABA in the ventral nerve cord.

The $G\alpha_{i/o}$ (GOA-1) pathway in *C. elegans* has been extensively studied as it modulates many aspects of locomotion and egg laying behavior. This inhibitory pathway is present in all 302 neurons, and is believed to dampen neurotransmitter release by inhibiting the EGL-30 ($G_{\alpha q}$) pathway (Miller et al., 1999). Mutants of *goa-1* have hyperactive locomotion rates, deep body bends, and constitutively lay eggs (Ségalat et al., 1995; Mendel et al., 1995). However, many strains with mutations in different GPCRs do not have as obvious behavioral defects, demonstrating that the fine manipulation of biogenic amine behavioral control is at the receptor level, and not the downstream signaling components. Biogenic amine signaling works through many receptor types, allowing for highly regulated, cell-specific control of behavior.

Tyramine has been shown to act as a genuine neurotransmitter in the nematode through the ligand-gated ion channel, LGC-55. From our genetic and behavioral analysis, we have uncovered an added level of complexity to the tyraminergic circuit, connecting tyramine release to the extrasynaptic activation of a G protein-coupled receptor. Interestingly, expression of *lgc-55* and *ser-2* do not overlap, with the exception of the SDQ neuron (Pirri et al., 2005; Tsalik et al., 2003). Behavioral defects in mutants of *lgc-55* and *ser-2* are also different. *lgc-55* mutants move their head on exogenous tyramine, fail to suppress head oscillations in response to anterior touch, and have shorter reversals, while *ser-2* mutants can move their body on exogenous tyramine and suppress head oscillations. Although the suppression of head oscillations in *ser*-2 mutants is

similar to wild-type, reinitiation of head oscillations may commence before forward locomotion is reinitiated (unpublished observation), which suggests a role for *ser-2* in head muscles. LGC-55 is expressed in the neck muscles, AVB, RMD, and SMD neurons ; cells and tissues that are post-synaptic to the tyraminergic RIM neurons. SER-2 expression in the ventral nerve cord is extrasynaptic to the RIM, suggesting humoral activation of a GPCR by tyramine. Other biogenic amines have been shown to act in a similar manner, for example dopamine activated GPCRs in *C. elegans* are also extrasynaptic to dopaminergic neurons (Chase et al., 2004), indicating a conserved genetic strategy for fine modulation of motor output.

2. Tyramine orchestrates a multi-stepped escape response.

The *C. elegans* escape response is a series of locomotory behaviors. Upon anterior touch, the animal stops moving forward, initiates backward locomotion while suppressing head oscillations, and then either chooses to reinitiate forward locomotion, or perform an omega turn in order to continue forward locomotion in the opposite direction (Figure 3-8A). The dual level of tyraminergic signaling control, using the fast-acting chloride channel and a slow-acting metabotrophic GPCR, together coordinate this complex behavior. Tyramine is released by the RIM neurons after mechanical stimulation, activating the fast acting inhibitory chloride channel, LGC-55, the AVB cease forward

locomotion in the neck muscles to suppress head oscillations (Pirri et al., 2009). Subsequently, after a reversal of three or more body bends, the animal initiates an omega turn with a deep ventral bend of the head. SER-2 is then activated in the ventral GABAergic motor neurons (VDs) where GABA is inhibited to allow full contraction of the ventral body wall muscles (Figure 3-8B), enabling the worm to fully fold and slide down the length of the body and continue forward locomotion and head oscillations. We have shown that this asymmetrical inhibition of GABA leads to a closed and efficient omega turn where the nematode can completely change directions.

Tyramine is a known behavioral modulator in invertebrates with demonstrated roles at the neuromuscular junction (Kutsukake et al., 2000) and the Malpighian tube (Blumenthal et al., 2003) of *Drosophila*. In mammals, application of tyramine and other trace can cause a decrease in GABAergic inhibition in rat brain slices (Berretta et al., 2005). While not much is known about the role for trace amines, other biogenic amines are known modulators of escape behavior. For example, serotonin can act as an excitatory and inhibitory neurotransmitter in the swimming escape response of the gastropod *Tritonia* (McClellan et al., 1994) as well as a modulator of the lateral giant escape command neurons of crayfish (Glanzman et al., 1983; Teshiba et al., 2001). Asymmetry is important for escape responses to activate one set of muscles to quickly move away from the perceived threat. In goldfish, the C-start, which is characterized by a unilateral bending away from the stimulus, is critical for the

fish's survival (Zottoli et al., 1977). An animal's ability to quickly contract and relax a set of muscles on one side of its body is a conserved mechanism for a quick reaction to a predator. Our study of SER-2 demonstrates this conserved behavior, and illustrates a molecular mechanism of asymmetrical GABA inhibition, which allows for a consistently efficient ventral bend that is important for an effective escape response.

D. Materials and Methods

1. Strains

The wild-type strain used in assays was Bristol N2. All worm cultures were grown at room temperature (22°C) on nematode growth media (NGM) agar plates with OP50 *E. coli* as a food source (Brenner, 1974). G-protein coupled receptor and signaling component mutants used in this study are as follows: *ser-2(pk1357), ser-2(ok2103), lgc-55(tm2913), tyra-2(tm1815), tyra-3(ok325), goa-1(sa734), dgk-1(sa748), eat-16 (sa609), gpb-2 (sa603), egl-30(tg26)*.

Transgenic strains were microinjected into the germ line of *lin-15(n765ts*) with pL15EK and integrated by x-ray. A *pser-2*::SER-2::GFP rescue construct was made by cloning 10.2 kb of genomic sequence including 2.2 kb upstream of the first translational start site into the pPD95.70 vector. The genomic rescue constructs used for exogenous tyramine and omega turn assays were injected

between 10-20 ng/µl. A *pser-2*::mCherry mini-gene reporter was constructed by inserting an 11.8kb sequence that included three start sites, first intron, and part of exon 2 into the pDM1247 mCherry vector. The GABAergic and cholinergic cell-specific rescue lines were cloned using *ser-2* cDNA behind the *unc-47* (1.2 kb) and *acr-2* (3.4 kb) promoters, respectively (Eastman et al., 1999; Hallam et al., 2000).

A *pmec-4*::ChR2 plasmid (Nagel et al., 2005) was injected at 80 ng/µl. The integrated strain was crossed into two *ser-2* mutant allele backgrounds. *pflp*-13::ChR2::YFP; *pflp-13*::NpHR::CFP was cloned by inserting a 2kb promoter from *pflp-13*::GFP (Kim and Li, 2004) into ChR2 and NpHR vectors (Nagel et al., 2005; Zhang et al., 2007). Strains carrying channelrhodopsin or halorhodopsin transgenes were cultured on NGM agar plates containing OP50 *E. coli* supplemented with 1.3 mM all-trans retinal for one generation. L4 animals were staged to retinal plates 24 hours before behavioral assays.

ser-2 ventral nerve cord expression analysis was performed using *pser-2*::mCherry(*zfIs8*), *punc-47*::GFP(*osIs12*) and *punc-17*::GFP(*vsIs48*). Head muscle analysis was done using *prom1ser-2*::GFP(*otIs107*) and *plgc-55*::mCherry(*zfIs4*). Images were taken using confocal microscopy (Zeiss and Pascal imaging software) and formatted using ImageJ software.

2. Behavioral assays

Drug assays were conducted using young adult animals grown at room temperature (22°C) 24 hours post-L4. Exogenous tyramine assays were done on agar plates containing 30 mM tyramine hydrochloride (Sigma) and 2 mM acetic acid. Approximately 10 animals were transferred to assay plates and scored for locomotion every minute for a 20 minute period. Animals were scored as immobilized if there was no sustained forward or backward locomotion in a 5 second interval. Aldicarb drug assays were performed using NGM agar plates supplemented with 0.5 mM aldicarb (Sigma) with or without 30 mM tyramine. A relatively high concentration of tyramine (30 mM) was used in plates containing aldicarb because aldicarb assays are conducted using NGM agar instead of agar which is used in exogenous tyramine assays. Animals do not paralyze on plates with 30 mM tyramine dissolved in NGM (data not shown). Animals were scored as paralyzed when they did not move when prodded with a platinum wire.

Optogenetic blue and green light induced bending assays were performed with *pflp-13*::ChR2;*pflp-13*::NpHR transgenic animals in a *lite-1* mutant background. Bending behavior movies, worm track traces and kymographs were generated using the Colbert worm tracking system as previously described (Leifer et al., 2011). This system allowed for restricted illumination of the ventral nerve cord. For bending bias quantification assays, young adult animals were transferred to NGM plates without food for 45 minutes. A ring of 4M fructose was

used to prevent animals from leaving the plate. Starvation induced long forward runs necessary for observing ventral or dorsal bending. The full body of the animal was exposed to blue or green light, using GFP and RFP filters at 20 x and 40 x respectively for 3 seconds. A dorsal or ventral bend was determined to be a turn of 45 degrees or more. The bending index was calculated as the fraction of dorsally bending worms minus the fraction of ventrally bending worms. A positive fraction indicates a dorsal bias, a negative fraction indicated a ventral bias, and a zero value represents no directional bias or no response to light exposures.

Omega turns were analyzed on NGM agar plates two days post pouring to control for assay plate humidity. Assay plates (60 mm diameter) were seeded with 40 µl OP50 *E. coli* and grown overnight at 37°C to produce a thin bacterial lawn. Young adult worms were transferred to an omega assay plate and allowed to acclimate for at least 10 minutes. Omega turns were then induced by gentle anterior touch while recording using a firewire camera and Astro IIDC software. For *pmec-4*::ChR2 induced omega turns, blue light from a GFP filter was turned on at 100x magnification for 5 seconds to induce a reversal. Video was reviewed, still images were exported, and angles were measured using Image J software. An omega turn was classified as a deep turn over 90° from reversal direction, resulting after a reversal of 3 or more body bends. An omega angle was measured by using the deepest part of the bend as the apex with vectors extending to the closest points along the body. Angles larger than 60° were not

scored as omega turns. The escape angle was measured as the difference between the reversal direction and the direction of reinitiation of forward locomotion.

3. Laser Ablations

Animals were mounted on agar pads and anesthetized with 20 mM sodium azide. Laser ablations were done using standard methods (Bargmann et al., 2005). DD and VD motor neurons were identified in *pflp-13*::GFP (NY2037) L2 animals and *pser-2*::GFP (OH2246) L3-L4 animals respectively. One to three days recovery post ablations, locomotion and omega turn assays were conducted on young adult animals. Locomotion patterns of animals that exhibited coordinated long runs were recorded at 7.5 fps. Video analysis was done using MATLAB and the MATLAB Image Acquisition Toolbox (Ramot et al., 2008). To determine directionality for each locomotion trace, the slope of instantaneous direction over time was measured for individual 360 degree turning events. Laser ablation of motor neurons was confirmed by lack of GFP expression in the cell body following behavioral experiments in adult animals.

4. Electrophysiology

Adult *C. elegans* held at drop of bath solution were glued down to the sylgard coated glass coverslip with cyanoacrylate tissue adhesive (Skinstitch Corp.) applied along the dorsal side of the body. A longitudinal incision was made by sharp glass electrode tip in dorsolateral area, intestine and gonad removed, and the cuticle flap along the incision was glued down in order to expose the ventral medial body wall muscles along the ventral nerve cord. Preparation was then washed briefly for ~20 s with a solution of collagenase type IV from Clostridium hystolyticum (Sigma-Aldrich) in extracellular bath solution (at a concentration of 1mg/ml) in order to remove the basement membrane overlying the muscles.

Intracellular pipette solution contained (in mM): 15 K-Gluconate, 125 KCl, 50 HEPES, 0.1 $CaCl_2$, 1 BAPTA-4K, 5 Mg_2ATP, 0.5 NaGTP, 0.5 cAMP, 0.5 cGMP, adjusted by 10 mM sucrose ~ 340 mOsm, pH 7.35 with KOH. Extracellular bath solutions consisted of (in mM): 150 NaCl, 5 KCl, 4 $MgCl_2$, 1 $CaCl_2$, 15 HEPES, 10 glucose, and was adjusted by 10 mM sucrose to ~345 Osm, and pH 7.35 with NaOH.

Whole-cell voltage clamp recordings from *C. elegans* body wall muscle cells (group of ventral medial muscles 9, 11, 13) from +/+ and *ser-2* strains were performed as previously described (Francis et al., 2005) using an EPC-10 amplifier (HEKA). Data acquisition and voltage protocols were controlled by

HEKA Patchmaster software. Patch-clamp electrodes were pulled from borosilicate glass with filament (Sutter Instrument), fire-polished to a resistance of 4-6 MΩ and filled with an internal solution. 1M KCl electrode with agarose bridge served as reference electrode. Leak currents and liquid junction potentials were not compensated, though pipette offset was zeroed immediately before getting a gigaohm seal. The membrane potential was clamped at -60 mV. Data were digitized at 6.67 kHz and low pass filtered at 3.3 kHz. Membrane capacitance and the series resistance (at least 20%, up to 60%) were compensated, and only recordings in which the series resistance was stable throughout the course of the recording were included. Endogenous synaptic activity data were collected in continuous mode (saved as 30 s recording sweeps). Typically, 60-90 s of control endogenous was recorded followed by 90 s bath of tyramine (100 uM) application, and subsequent tyramine wash-out (occasional). *C. elegans* preparation was continuously perfused by extracellular solution with or without tyramine by gravity flow at a perfusion rate 2 ml/min. Cells were excluded from analysis if a leak current > 300 pA was observed. Only recordings with series resistance R_s < 15 MΩ were included to analysis. All electrophysiology experiments were carried out at room temperature.

Data analysis and graphing were performed using Excel (Microsoft), Igor Pro (WaveMetrics Inc.) and GraphPrism (GraphPad Software). Moreover, Mini Analysis software (Synaptosoft Inc.) was used to detect and analyze the endogenous events off-line. Parameters for detection of event were set as

follows: amplitude threshold 12 pA, period to search local minimum 80 ms, time before a peak for baseline 20 ms, period to search a decay time 30 ms, fraction of peak to find a decay time 0.37, period to average a baseline 10 ms, area threshold 10, number of points to average for peak 3. In addition, following automatic detection of endogenous postsynaptic currents, traces were visually inspected, and all events were manually verified and accepted/rejected or recalculated, if necessary. 60 s of continuous data were used in analysis. Segment of 60 s recording prior to tyramine application served as control. Tyramine effect was evaluated in last 60 s of 90 s perfusion i.e. initial 30 s of recording with tyramine in bath solution were eliminated from analysis in order to allow enough time for adequate tyramine perfusion and stabilization effect. Data from each group were averaged, and statistical significance between the strains was determined by two-tailed unpaired Student's t-test. Data are presented as mean ± S.E.M. All chemical were purchased from Sigma-Aldrich.

Figure 3-1

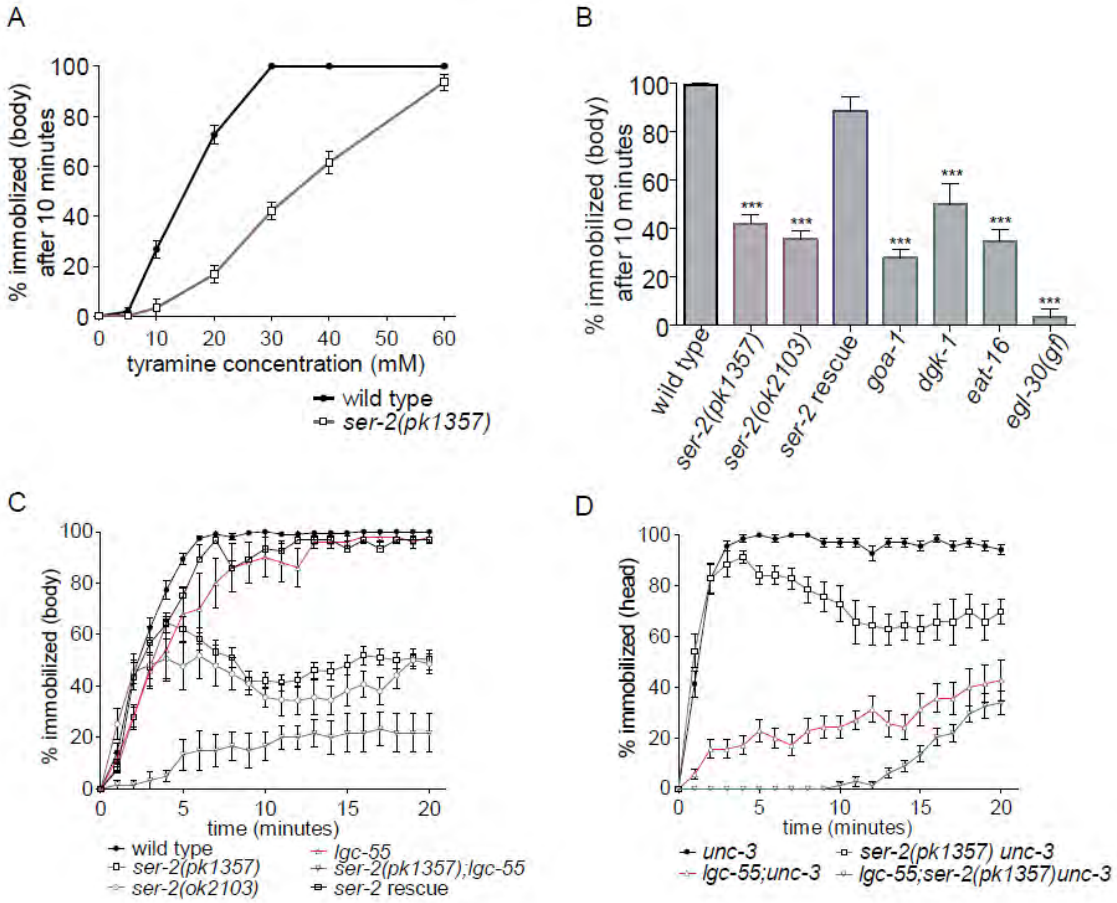
A
% immoblized (body) after 10 minutes
tyramine concentration (mM)
wild type
ser-2(pk1357)
B
% immobilized (body) after 10 minutes
wild type
ser-2(pk1357)
ser-2(ok2103)
ser-2 rescue
goa-1
dgk-1
eat-16
egl-30(gf)
C
% immobilized (body)
time (minutes)
wild type
ser-2(pk1357)
ser-2(ok2103)
lgc-55
ser-2(pk1357);lgc-55
ser-2 rescue
D
% immobilized (head)
time (minutes)
unc-3
lgc-55;unc-3
ser-2(pk1357) unc-3
lgc-55;ser-2(pk1357)unc-3

Figure 3-1

***ser-2* mutants are partially resistant to the paralytic effects of tyramine.**

(A) Dose response curves measuring immobilization induced by varying concentrations of exogenous tyramine. Tyramine induces immobilization in a dose dependent manner. (B) Body immobilization after 10 minutes on 30 mM exogenous tyramine. Each bar represents the mean percentage of animals immobilized ± SEM for at least 4 trials, totaling a minimum of 40 animals. *ser-2* mutants and GOA-1 pathway G-protein signaling mutants are similarly resistant to immobilization by exogenous tyramine. (C,D) Quantification of sustained body (C) or head (D) movements on 30 mM tyramine plates. Each data point represents the mean percentage of animals immobilized ± standard error of the mean (SEM) for at least 6 trials, totaling a minimum of 60 animals. *ser-2* mutants are partially resistant to body immobilization, and *lgc-55* mutants are partially resistant to head immobilization. *lgc-55;ser-2* double mutants are resistant to both body and head immobilization. Statistical significance to wild-type; ***p< 0.0001, two-tailed Student's t test.

Figure 3-2

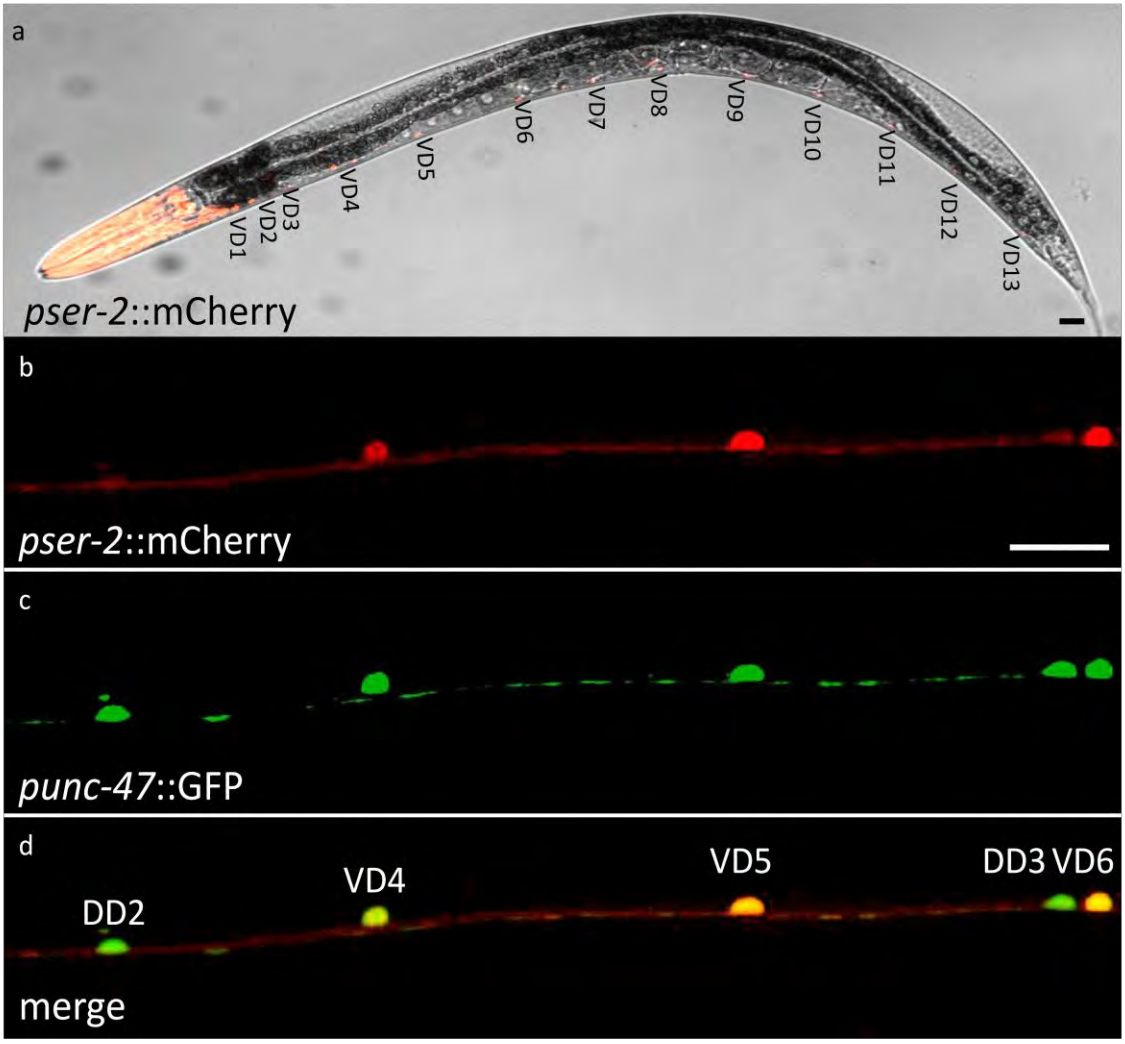

***ser-2* is expressed in VD motor neurons.**

(A) Adult animal showing expression of *pser-2*::mCherry(*zfIs8*) in head muscles, head neurons, and the ventral nerve cord. (B-D) Higher magnification of the ventral nerve cord. (B) *pser-2*::mCherry expression in a subset of ventral nerve cord neurons. (C) *punc-47*::GFP expression in all GABAergic neurons. (d) Strong coexpression the VD subset of GABAergic neurons. Weak to no coexpression in DD neurons. Scale bar, 20 μm.

Figure 3-3

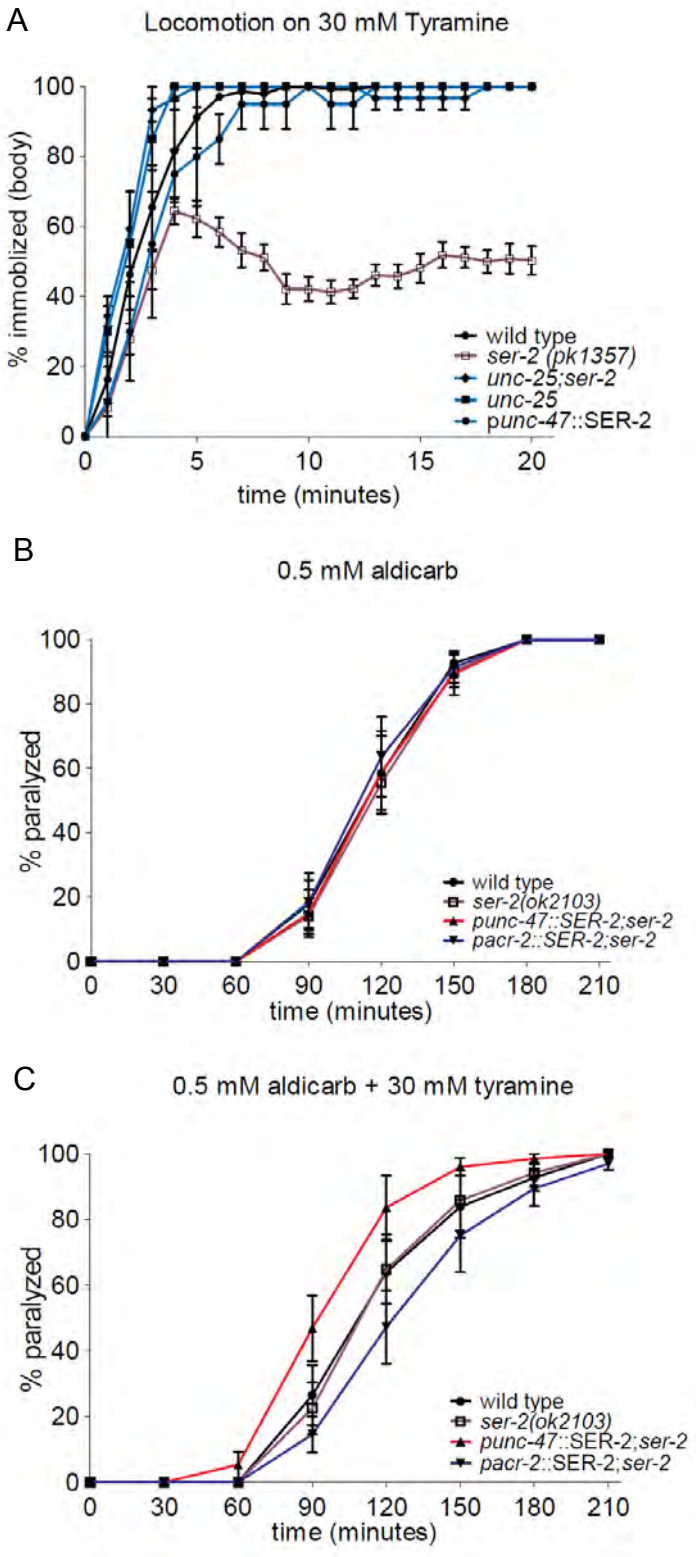
A
Locomotion on 30 mM Tyramine
% immoblized (body)
time (minutes)
wild type
ser-2 (pk1357)
unc-25;ser-2
unc-25
punc-47::SER-2
B
0.5 mM aldicarb
% paralyzed
time (minutes)
wild type
ser-2(ok2103)
punc-47::SER-2;ser-2
pacr-2::SER-2;ser-2
C
0.5 mM aldicarb + 30 mM tyramine
% paralyzed
time (minutes)
wild type
ser-2(ok2103)
punc-47::SER-2;ser-2
pacr-2::SER-2;ser-2

Figure 3-3

SER-2 inhibits GABA release.

(A) Quantification of sustained body movement on 30 mM exogenous tyramine. GABA deficient mutants (*unc-25*) are not resistant to exogenous tyramine, and *unc-25;ser-2* (*pk1357*) double mutants show a suppression of the tyramine resistant phenotype of *ser-2* mutants. Cell-specific rescue of SER-2 in all GABAergic neurons (*punc-47*::SER-2) also rescues the *ser-2* mutant phenotype. (B) Time course of paralysis on 0.5 mM aldicarb supplemented NGM plates. All strains paralyze at the same rate. (C) Time course of paralysis on 0.5 mM aldicarb and 30 mM tyramine supplemented NGM plates. Cell-specific expression of SER-2 in motor neuron subsets shifts paralysis curves displaying an inhibition of GABA and acetylcholine.

Figure3-4

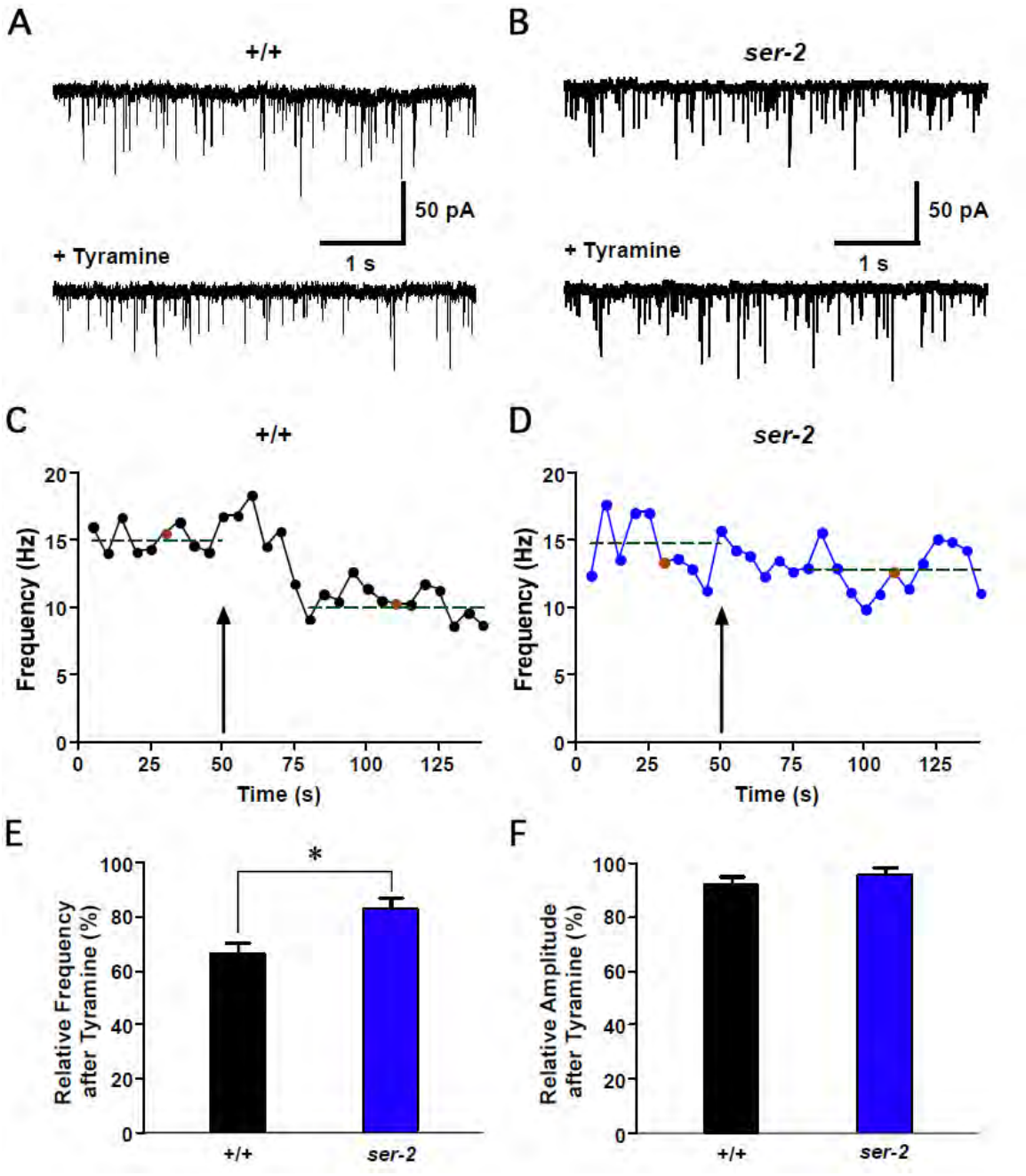
A
+/+
50 pA
1 s
+ Tyramine
B
ser-2
50 pA
1 s
+ Tyramine
C
+/+
Frequency (Hz)
Time (s)
D
ser-2
Frequency (Hz)
Time (s)
E
Relative Frequency after Tyramine (%)
*
+/+
ser-2
F
Relative Amplitude after Tyramine (%)
+/+
ser-2

Figure 3-4

Tyramine-mediated reduction in GABA synaptic release requires SER-2.

(A-B)Sample of frequency of endogenous inhibitory post-synaptic currents (IPSCs) in whole-cell recordings from ventral body wall muscle. +/+ is *unc-29;acr-16* double mutants that lack excitatory neurotransmission at the NMJ. *ser-2* is in double mutant background. (C-D)Tyramine application decreased the rate of IPSCs in +/+, but not *ser-2* mutants. Arrow depicts tyramine application time point. (E) Average relative frequency of IPSCs after tyramine application. (F) Relative amplitude of IPSCs after tyramine release. Error bars depict S.E.M. Statistical differences calculated from +/+; *$p < 0.05$, two-tailed Student's t test.

Figure 3-5

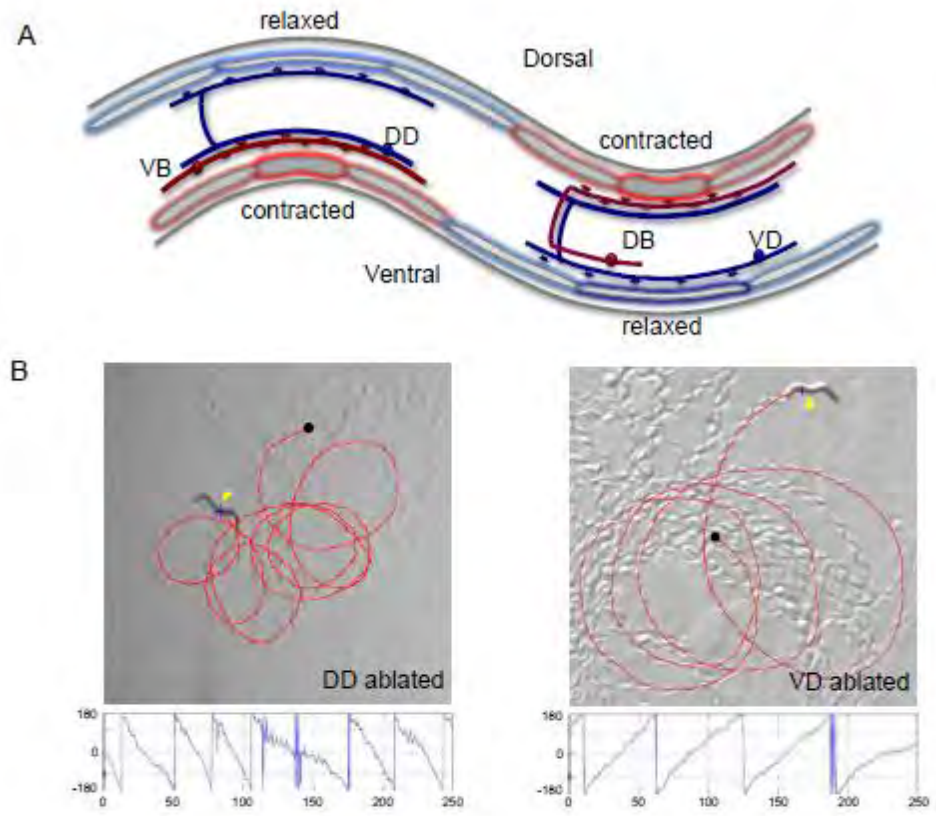

C

strain	direction (°/sec)	(n)
VD ablated	4° ± 1	8
DD ablated	-14° ± 2	13
mock ablated	-1° ± 1	46
wild type	-1° ± 1	43
unc-25(e156)	2° ± 1	57
ser-2 (pk1357)	-1° ± 1	32
ser-2 (ok2103)	-1° ± 1	21

Figure 3-5

VD and DD motor neurons modulate *C. elegans* navigation.

(A) Schematic of D-motor neuron wiring. VD motor neurons receive input from DB cholinergic neurons, and release GABA on ventral bodywall muscles. DD motor neurons receive input from VB motor neurons and release GABA on dorsal bodywall muscles. Figure adapted from wormatlas.org. (B) Chronic disruption of GABA signaling by laser ablation of subsets of GABAergic motor induces navigational biases. DD ablated animals navigate with a dorsal bias while VD ablated animals navigate with a ventral bias. Traces of locomotion and turning angle were generated by worm tracking software. (C) VD and DD ablated animals showed navigational biases. Mock ablated animals, GABA deficient mutants (*unc-25*), and *ser-2* mutants did not show navigational biases. Turning angle was calculated using worm tracking software.

Figure 3-6

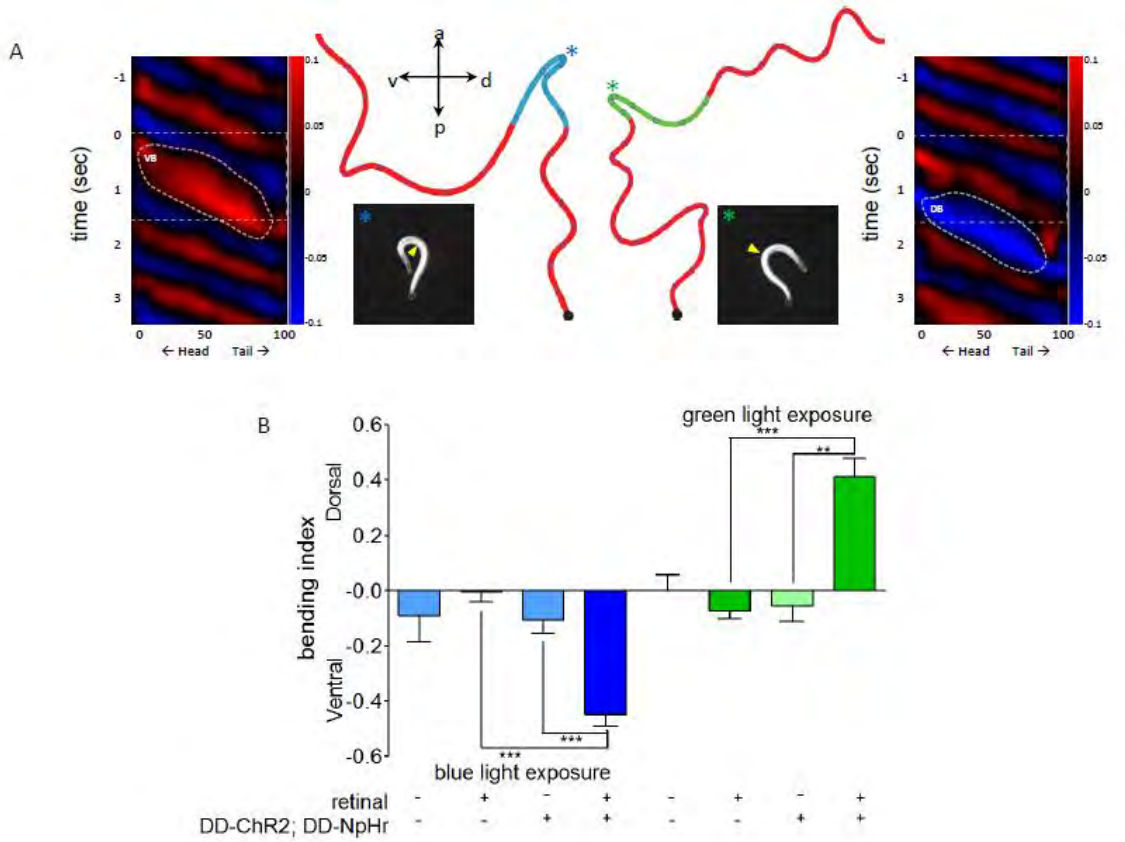

Remote control worm demonstrates navigational changes with acute GABA activation and inhibition.

(a) Acute disruption of GABA signaling using DD expressed channelrhodopsin and halorhodopsin (*pflp-13*::ChR2::YFP;*pflp-13*-NpHr::CFP) affects turning behavior with green and blue light exposure. Activation of GABA release induced by blue light causes a ventral turn, while inhibition of GABA release induced by green light causes a dorsal turn. Worm track traces signify the time course of blue and green light exposure. Kymographs display change in sinusoidal wave amplitude before, during, and after light exposure. Still images were taken at * location on worm track. Yellow triangle depicts vulva. (c) Quantification of bending behavior with green and blue light exposure. Bending bias was calculated as fraction of dorsal turns – fraction of ventral turns after blue or green light exposure. Controls were done without retinal feeding and without transgene. Statistical significance to controls; **p<0.001 and ***p< 0.0001, two-tailed Student's t test.

Figure 3-7

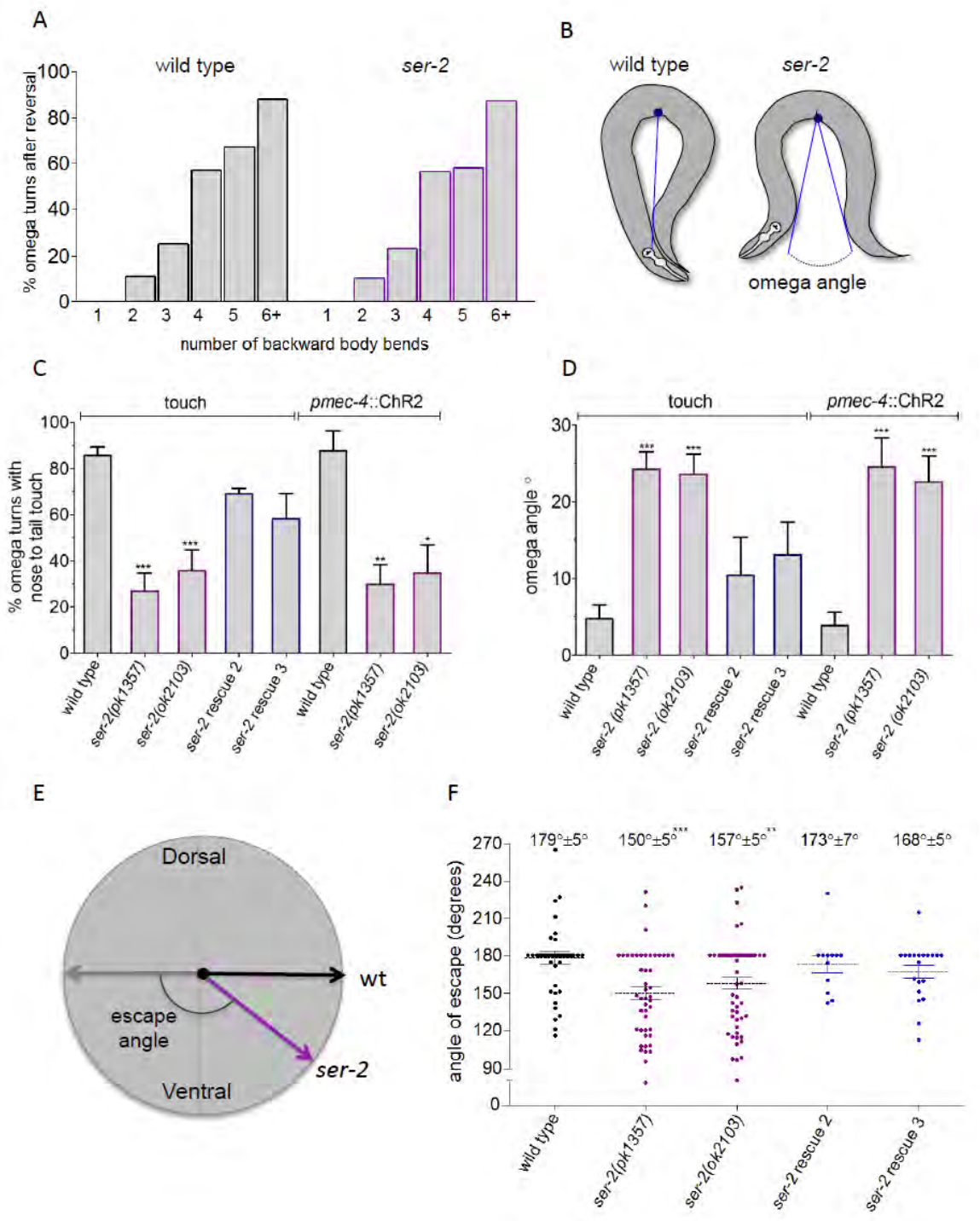
A
wild type
ser-2
% omega turns after reversal
number of backward body bends
B
wild type
ser-2
omega angle
C
touch
pmec-4::ChR2
% omega turns with nose to tail touch
wild type
ser-2(pk1357)
ser-2(ok2103)
ser-2 rescue 2
ser-2 rescue 3
D
touch
pmec-4::ChR2
omega angle °
E
Dorsal
wt
escape angle
ser-2
Ventral
F
179°±5°
150°±5°
157°±5°
173°±7°
168°±5°
angle of escape (degrees)

Figure 3-7

***ser-2* mutants make defective omega turns and escape less efficiently.**

(A) Percent of reversal lengths that conclude with an omega turn. Wild-type and *ser-2* mutants both initiate omega turns at the same rate. (B) Omega angle measured from deepest ventral bend to closest or touching points anterior and posterior of the animal. Images were traced from exported video frames to represent real animals at the most ventrally contracted state of the escape response. (C) Percent of omega turns which touch nose to tail, resulting in a closed omega turn. *ser-2* mutants touch nose to tail less frequently than wild-type in omega turns induced by both touch and UV light in a *pmec-4*::ChR2 background. Genomic rescue lines rescue mutant turning phenotype. (D) *ser-2* mutants make a wider omega turn than wild-type. Genomic rescue lines make turns similar to wild-type. E) Escape angles were measured from the direction of the reversal (induced by gentle anterior touch) to the direction of reinitiation of forward locomotion. (F) Wild-type animals escape in the opposite direction from the touch stimulus, where *ser-2* mutants make a shallower escape angle. Error bars depict SEM. Statistical differences calculated from wild-type; *$p < 0.05$, **$p < 0.01$, ***$p < 0.001$, two-tailed Student's t test.

Figure 3-8

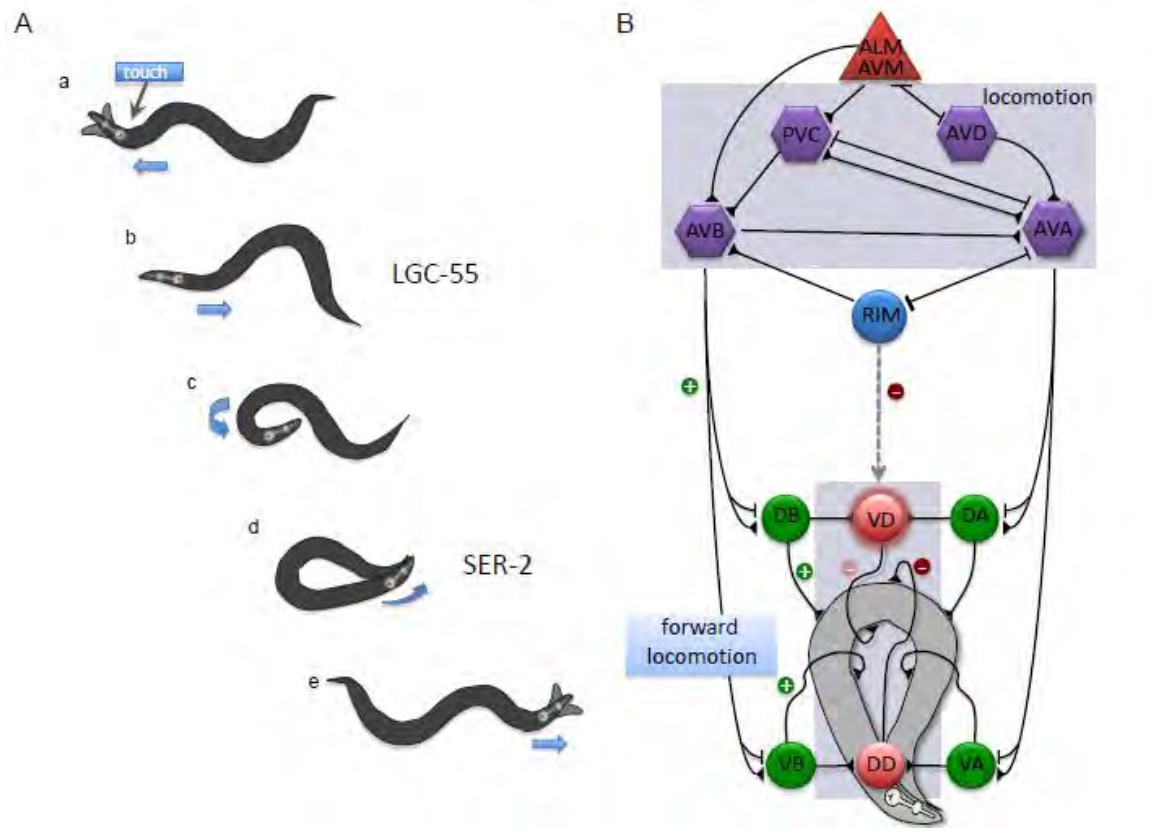

Model: Tyramine modulates the *C. elegans* escape response during an omega turn.

(A) Silhouettes of *C. elegans* during an escape response. Still images were extracted from a movie of an animal escaping a touch stimulus. (B) *C. elegans* sinusoidal locomotion is propagated by alternatively contracting and relaxing opposing ventral and dorsal body wall muscles of the animal using cholinergic and GABAergic motor neurons. Not all motor neurons are represented. Upon tyramine release from the RIM, and omega turn is induced, activating SER-2 in the VD motor neurons, which decreases GABA release on the ventral side, allowing for a fully contracted, closed omega turn.

Figure 3-S1

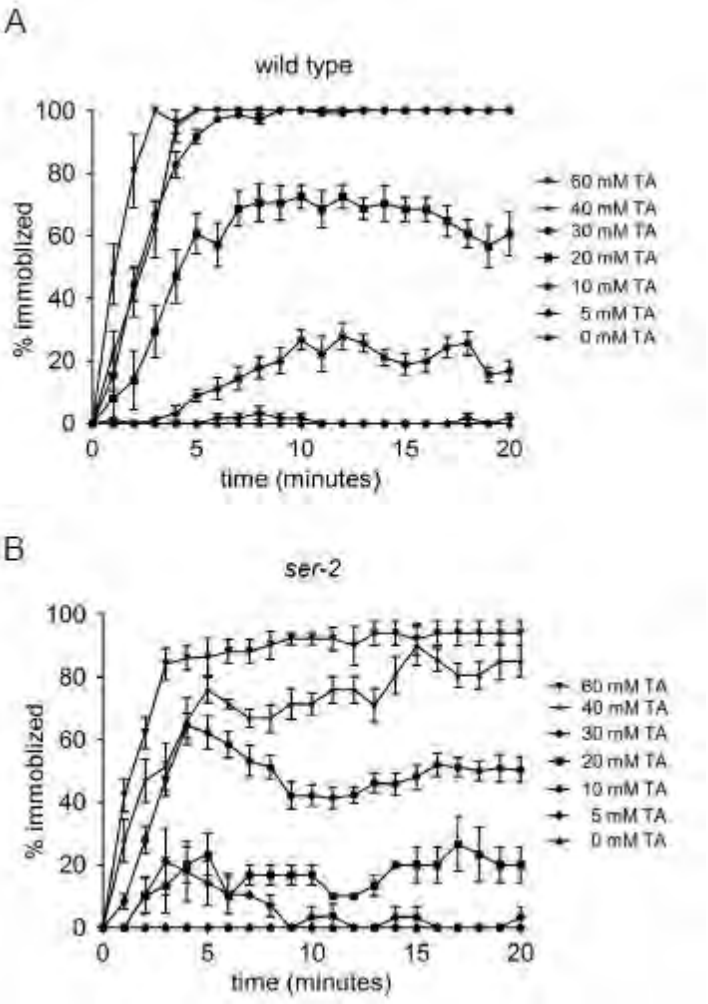

Exogenous tyramine body immobilization is dose dependent.

(A) Wild-type immobilizes completely within 5 minutes on 30 mM tyramine. (B) *ser-2* mutants are resistant to body immobilization compared to wild-type, but become immobilized by 60 mM tyramine.

Figure 3-S2

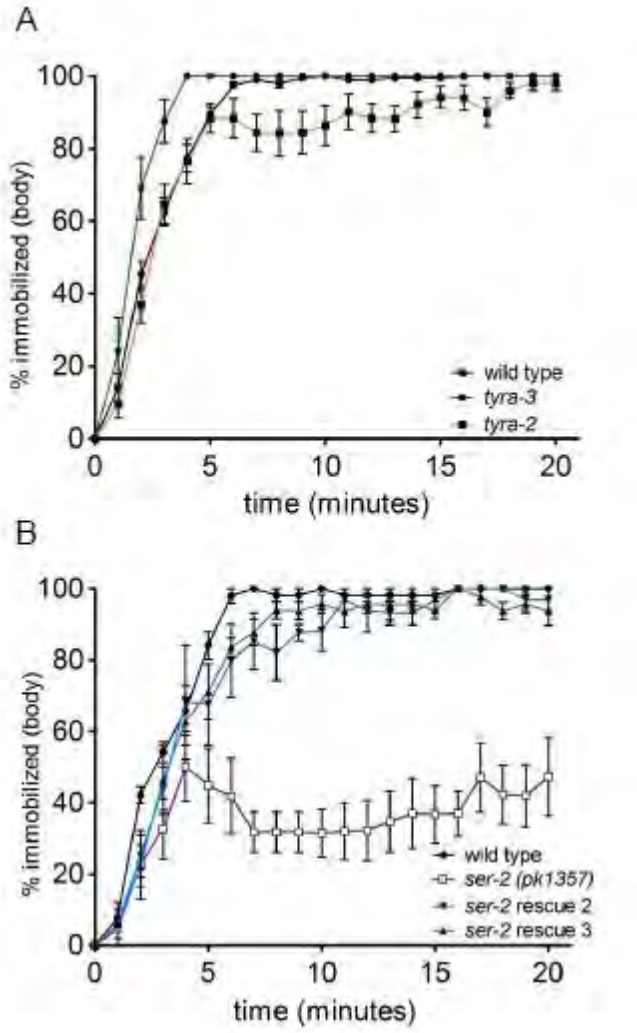

Body immobilization on 30 mM exogenous tyramine.

(A) *tyra-2* and *tyra-3* mutants are not resistant to paralysis. (B) Two additional SER-2 rescue strains (10 ng/µl injection) also rescue the body immobilization resistance phenotype of *ser-2* mutants.

Figure 3-S3

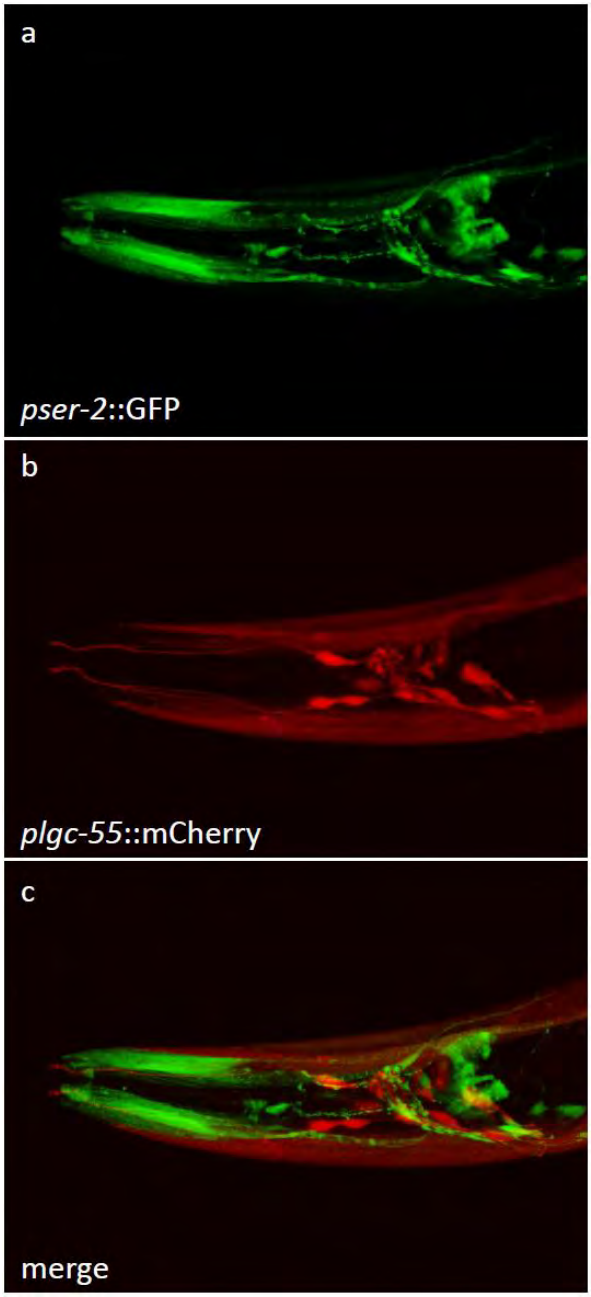

Coexpression analysis of *ser-2* and *lgc-55.*

Coexpression of (A) *prom1ser-2*::GFP and (B) *plgc-55*::mCherry. (C) Head muscle expression of *prom1ser-2*::GFP does not overlap with neck muscle expression of *plcg-55*::mCherry.

Figure 3-S4

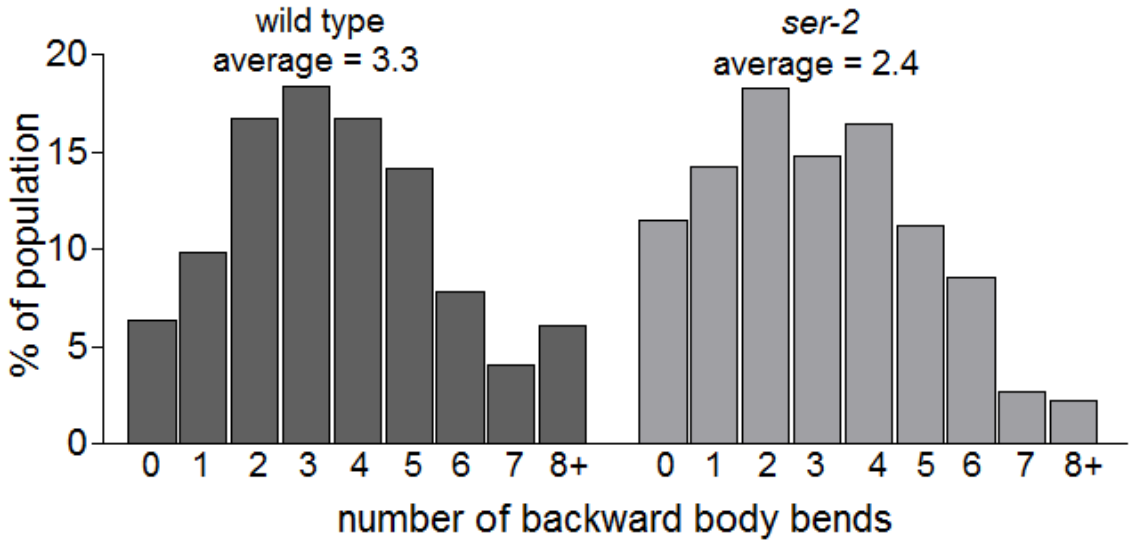

Reversal length after gentle anterior touch.

Wild-type and *ser-2* mutants have similar reversal lengths after a gentle anterior touch. n ≥ 250 animals per genotype.

Figure 3-S5

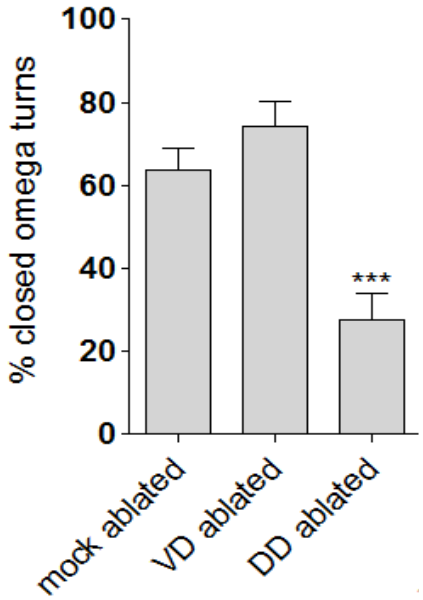

DD GABAergic neurons modulate closed omega turns.

DD ablated animals fail to close omega turns compared to wild-type. VD ablated animals show a slight increase in closure percentage compared to wild-type. Statistical differences calculated from wild-type; ***$p < 0.0001$, two-tailed Student's t test.

Movie 3-1

Immobilized wild-type animal on 30 mM exogenous tyramine.

Young adult animals were placed on exogenous 30 mM exogenous tyramine plates. Movie depicts animal after 7 minutes on drug plate. Head and neck are relaxed and straight, while body and head are immobilized.

Movie 3-2

Resistant *ser-2* mutant animal on 30 mM exogenous tyramine.

Young adult animals were placed on exogenous 30 mM exogenous tyramine plates. Movie depicts animal after 7 minutes on drug plate. Animal is able to move in a sinusoidal wave, albeit slower than on a plate without drugs.

Movie 3-3

VD ablated animal.

After VD motor neuron ablations during the L2 larval stage, the animal progresses into an adult. Movie depicts ventral biased navigation. Vulva is oriented toward the inside of the concentric worm track circles (ventral facing in). Movie is shown at 5x speed.

Movie 3-4

DD ablated animal.

After DD motor neuron ablations during the L2 larval stage, the animal progresses into an adult. Movie depicts dorsal biased navigation. Vulva is oriented toward the outside of the concentric worm track circles (dorsal side facing in). Movie is shown at 5x speed.

Movie 3-5

Acute activation and inhibition of DD motor neurons using light-gated proteins.

Animal expressing integrated *pflp-13*::ChR2;*pflp-13*::NpHR transgene is suspended in dextran solution. Upon blue light activation of channelrhodopsin in the DD motor neurons, the dorsal muscles relax, and a deep ventral bend is executed. In the same animal, upon green light exposure, halorhodopsin inhibits GABA release on the dorsal side, inducing a dorsal contraction. Light exposure is restricted to the ventral nerve cord by using the Colbert system, thus by eliminating activation and inhibition of head neurons expressing *pflp-13*::ChR2;*pflp-13*::NpHR.

Movie 3-6

Wild-type omega turn after gentle anterior touch.

Adult animal is on an NGM plate with a thin lawn of *E. coli* (OP50). Upon gentle anterior touch with a thin hair, the animal reverses, suppresses head oscillations, and executes a deep ventral turn, touching nose to body, and sliding down the length of the worm.

Movie 3-7

***ser-2* omega turn after gentle anterior touch.**

Adult animal is on an NGM plate with a thin lawn of *E. coli* (OP50). Upon gentle anterior touch with a thin hair, the animal reverses, suppressed head oscillations, and begins to execute a deep ventral turn, but fails to touch nose to body before reinitiating forward locomotion.

CHAPTER IV

A Novel Approach to Study Instantaneous Velocity During the *C. elegans* Escape Response

This chapter is comprised of preliminary findings using a worm tracking system to carefully examine velocity changes during the escape response. The experiments were carried out by me, with critical help from Andrew Leifer, who wrote the velocity analysis software. I composed the following text and figures with editorial and content feedback from Mark Alkema and Christopher Clark.

A. INTRODUCTION

As the nematode moves through its environment, navigation is modulated by different states of locomotion. The frequency of the sinusoidal wave of movement can accelerate or decelerate, come to a halt, reverse, increase or decrease the body bending amplitude, or even leave its typical two-dimensional rhythm using head lifts off the agar plate. With the recent invention of worm tracking, behavioral analysis has been conducted with a greater level of detail, with the potential for high throughput assays. Here, we have developed an assay using a worm tracker to analyze the detailed changes in velocity during the *C. elegans* escape response.

Velocity of the nematode changes based on many environmental factors including viscosity of substrate, presence or absence of food, and temperature. By acclimating to external cues, changing locomotion rates increases the animal's ability to survive. Mechanical stimuli also can change the velocity of the animal. It has been shown that posterior touch causes acceleration in the forward direction, nose and anterior touch cause a reversal and acceleration in the backward direction (Chalfie et al., 1985). The mechanism for sensing mechanical stimuli is well defined from the mechanosensory circuit down to the touch receptors and signal transduction pathways (Chalfie et al., 1985; Chalfie and Au, 1989; Goodman et al., 2002; Goodman and Schwarz, 2003) . However, it is not well understood how changes in velocity of the sinusoidal wave occur.

Worm tracking allows for the production of high resolution video by using a motorized stage and software to keep the animal in frame. The movies can then be used for behavioral analysis, either with additional programs, or by eye. Previous studies have investigated egg laying and various aspects of locomotion behavior (Hardaker et al., 2001; Baek et al., 2002; Huang et al., 2006). Analysis has included using channelrhodopsin to stimulate neurons and mutant analysis to elucidate signaling pathways (Huang et al., 2006; Leifer et al., 2011; Stirman et al., 2011). These amazing technological advances in *C. elegans* research tools have increased our ability to further our understanding of fine modulation of motor output.

Biogenic amines modulate many aspects of locomotion behavior in *C. elegans*. Serotonin, dopamine, and octopamine act to relay the information on the availability of food to adjust to different states of locomotion such as the basal slowing response, enhanced slowing response, and area restricted search (Sawin et al., 2000; Hills et al., 2004). Dopamine can also control locomotion based on previous experiences (Sanyal et al., 2004). In addition, tyramine has been shown to play a key role in modulating escape response locomotion (Alkema et al., 2005; Pirri et al., 2009).

The *C. elegans* escape response has been well defined from behavior to circuitry to receptors. In each step of the escape response, there are several key aspects of locomotory behavior. Upon gentle anterior touch, forward locomotion

ceases, followed by a reversal and suppression of foraging head oscillations. After a long reversal, a high angled turn or omega turn is often executed by the animal to change direction, as forward locomotion is reinitiated (Chalfie et al., 1985; Alkema et al., 2005; Chapter 3). It has been shown that tyramine modulates reversal behavior, the suppression of head oscillations after anterior touch, and omega turns (Alkema et al., 2005; Pirri et al., 2009;Chapter 3). How other biogenic amines may modulate similar aspects of escape response locomotion behavior has not been investigated. Here we examine the velocity of the escape response, and how biogenic amines may modulate this evolutionarily important behavior.

B. RESULTS

1. Wild-type animals increase velocity during the escape response.

In order to assess the instantaneous velocity during an escape response, we developed an assay using machine vision tracking and algorithmic analysis. For analysis, a single young adult was transferred from a growth plate to an NGM plate with a thin, new lawn of bacteria. The animal was allowed to recover from the touch stimulus during transfer, and acclimate to the new plate for 10 minutes. Using the worm tracker described by the Schafer Lab (Worm Tracker 2.0) (Huang et al., 2006), a high resolution movie was made. For the first minute, the basal velocity of the animal was recorded, followed by a brief vibration of the

plate, followed by two additional minutes of recording to monitor the escape velocity (Figure 4-1). The recordings were then analyzed using a MATLAB based program to extract the instantaneous velocity from each frame of the movie. This approach allowed for detailed instantaneous velocity analysis compared to previous reports which tracked average velocities.

When wild-type animals are stimulated with vibrations, a reversal ensues the majority of the time, and accelerated forward locomotion in the remaining trials (Chiba and Rankin, 1990). We saw a similar trend during our experiment (data not shown), and chose to quantify only the trials in which a reversal was induced after the vibration stimulus. To quantify different parameters for each tracking, a program was used to outline and virtually divide the animal into 100 segments, each of which would be used to extract location changes, and body bending details. From this, instantaneous velocity could be calculated and analyzed. The velocity was normalized to the length of the worm; hence the speed was presented as wormlengths per second. A representative worm tracking trace displays the complete conglomerate of steps in the escape response, from basal rate, stimulus, reversal, and reinitiation of forward locomotion (Figure 4-2A-B, Movie 4-1). As the trace crosses the x-axis with a velocity of zero, a change of direction occurs. Also shown in the kymograph, a change of direction is visualized as a change of slope in the red and blue bands. Wild-type animals average a basal forward velocity of approximately 0.4 wormlengths/second on a thin bacterial lawn (Figure 4-4F). After a vibration

pulse, a reversal is induced, reaching a maximum velocity of approximately 2 wormlengths/second (Figure 4-2E). Typically, an omega turn occurs, and reinitiation of forward locomotion ensues at an elevated velocity (0.87 wormlengths/second) (Figure 4-2F) compared to the basal rate. By detailed data extraction from a multi-stepped behavior, we can begin to decipher each phase, examining how the animal executes the escape response.

2. Spontaneous and induced omega turns are conducted at different velocities.

C. elegans locomotion across an agar plate is characterized by long forward runs with intermittent reversals, some of which result in an omega turn. It has been shown that longer reversals, both spontaneous and induced, can result in an omega turn (Gray et al, 2005; Chapter 3). Here, we ask the question: are these omega turns the same? Is the animal behaving the same way before, during, and after the deep turn? To answer these questions, both instantaneous velocities during spontaneous and induced omega turns were compared (Figure 4-2). Unlike an induced omega turn, the reversal velocity directly preceding the omega turn was not increased from the basal velocity rate (Figure 4-2E). Upon reinitiation of forward locomotion after the spontaneous reversal, the velocity rate was similar to the basal level, and not accelerated as it was in the induced reversal experiment (Figure 4-2F). These data show that the escape response is

a distinct behavioral sequence, different from a spontaneous reversal and omega turn.

3. Touch induced escape recapitulates the vibration induced velocity increases

Since direct touch of the nematode can induce different behavioral responses depending on location of the stimulus (Chalfie et al., 1985), and a vibration stimulus affects the whole animal, we sought to determine if the type of stimulus affected the escape response. To determine if there is a difference in behavior dependent on the type of mechanical induced escape response, we conducted a similar experiment. Due to the worm tracking apparatus, a touch induced reversal could not be tracked using machine-based vision, and thus not be analyzed with the same precision as the vibration reversal paradigm. Therefore, a low-tech assessment of velocity was conducted upon touch induced escape responses.

Similar to the machine based paradigm, the animals were transferred to NGM plates with thin, newly seeded lawns of bacteria and allowed to acclimate for 10 minutes. To analyze the basal rate of locomotion, body bends were counted over a 30 second interval. Subsequently, a thin hair was used to gently touch the anterior region of the animal, to induce a reversal. After forward locomotion was reinitiated, body bends were counted over the following 30

seconds. In each trial, the rate of locomotion increased for each animal (Figure 4-3A). The average basal velocity was 10 body bends in 30 seconds, and the velocity increased to an average of 18 body bends in 30 seconds (Figure 4-3B). Even at this low level of resolution, the increase in velocity after an induced escape response can be visualized. These experiments lead us to believe that the same circuitry is being utilized in the well-defined touch circuit, as well as in our vibration escape paradigm.

4. Biogenic amines modulate escape velocity

To determine which signaling molecules modulate the velocity changes, and the decay in velocity back to baseline, we did a mutant analysis of animals deficient in each of the four biogenic amines: dopamine, serotonin, octopamine, and tyramine. Biogenic amine mutants, as well as a mutant of the dopamine transporter (*dat-1*) were tested alongside the wild-type to investigate velocity differences in each stage of the escape response. Select traces are shown for each biogenic amine mutant (*tdc-1, tbh-1, cat-2, tph-1,* and *dat-1*) in the vibration induced escape response paradigm (Figure 4-4A-E). Basal velocity before induction of a reversal was not significantly different for any of the biogenic amine mutants, although there was a noted decrease in the velocity of *tdc-1* mutants (Figure 4-4F). After stimulation, the reversal velocity was scored as the highest rate of instantaneous velocity in the reverse direction. Serotonin deficient

mutants (*tph-1*) displayed a significant decrease in reversal velocity, albeit was still an accelerated rate compared to basal forward locomotion (Figure 4-4G). Since the escape response induces an increase in velocity following stimulation, the velocity was assessed upon reinitiation of forward locomotion. We saw that dopamine deficient mutants (*cat-2*) were significantly faster during this initial phase, and serotonin deficient mutants (*tph-1*) were slower compared to the wild-type (Figure 4-4H). Furthermore, the decay rate of velocity was calculated to determine if biogenic amines modulate the return to basal locomotion (Table 4-1). *tdc-1* and *cat-2* mutants showed a significant increase in decay rate for instantaneous velocity, indicating that tyramine and dopamine may be modulating the state of elevated velocity during the escape response.

C. Methods and Materials

1. Strains and growing conditions

All strains were maintained on NGM agar plates supplemented with *E. coli* (strain OP50) as a food source and grown at room temperature (22°C). The strains used were wild-type (N2 bristol), *tdc-1*(*n3420*), *cat-2*(*tm2261*), *tbh-1*(*n3247*), *tph-1*(*n4622*), and *dat-1*(*ok157*).

2. Escape response behavioral experiments

Freshly prepared NGM agar plates (24-48 hours old) were seeded with 40 µl *E. coli* (OP50) and grown overnight at 37°C. A single young adult animal (24 hours post L4) was gently placed on a plate, and allowed to acclimate for 10 minutes undisturbed. The plate was then turned up-side down on the worm tracker stage. High contrast between background and the animal, as well as a 30 frames/second recording rate were necessary for a quality experiment. A one minute movie was recorded to determine the basal velocity. To induce an escape response, a vibration was applied to the exterior of the plate for one second with an electric toothbrush (Sonicare). An additional 90 seconds were recorded. For each genotype, n≥12. Spontaneous omega turns were analyzed by recording long periods of unstimulated locomotion on the worm tracker, and subsequent review of movies to identify spontaneous turning behavior.

3. Worm tracking data extraction and analysis

Each movie recorded with the worm tracker was converted from bright field into a reverse image (white worm on black background) and changed to size using VirtualDub software. In each movie, the worm was skeletonized and segmented for analysis using software written by Andrew Leifer (Leifer et al., 2011). A MATLAB file was generated for analysis, which could then be used to extract instantaneous velocity for each frame of the recording. The matrix of velocity points was exported to Excel (Microsoft) where values were plotted,

maximum velocities were extracted, and decay rates were calculated. Basal rates were determined as the average of a 2 binned interval (60 data points) prior to stimulus, ignoring negative values. The decay rate was taken as the slope from the maximum velocity to 15 seconds post maximum. Maximum values were extracted from the matrix during each behavioral step of the escape response.

D. Discussion

Our novel approach to precisely define the velocity of an escape response is the first attempt to use a worm tracker for an extended analysis of locomotion behavior. Here, we have shown that the escape response consists of changes in velocity that are not observed during non-stimulated turning behavior, and that a state of accelerated velocity is extended post omega turn. The ability to evaluate a behavior with great detail may aid in detecting more subtle phenotypes that may have previously been over-looked. Biogenic amine signaling is known to affect locomotion on many different levels, therefore it was hypothesized that one or more of the four amines may modulate velocity during the escape response.

Upon initial observations, there are differences amongst biogenic amine mutants in the instantaneous velocity of the escape response. Serotonin mutants (*tph-1*) have a defect in maximizing the reversal velocity and during the reinitiation of forward locomotion. This defect could be further analyzed using

serotonin receptor mutants, including *mod-1*, which has been reported to be expressed in the ventral nerve cord (Ranganathan et al., 2000). *mod-1* mutants have been reported to have grossly normal behavior. By utilizing a worm tracker to analyze behavior in more detail, the role for this serotonin-gated chloride channel may be elucidated. Since *tph-1* mutants are slightly egg-laying defective, these experiments should be repeated using L4 larva to rule out velocity deficiencies based on mechanical restrictions due to an accumulation of eggs in the uterus.

Interestingly, tyramine mutants show a difference in the decay of velocity after the escape response. Tyramine has already been determined to be a key regulator in the initial stages of the escape response during the reversal, suppression of head oscillations, and the omega turn (Alkema et al., 2005; Pirri et al., 2009; Chapter 3). Now, with a fourth role in elevating velocity for an extended period of time post escape, the importance of tyramine in this behavioral pattern has been re-established. Two of the four tyramine receptors, LGC-55 and SER-2 (Pirri et al., 2009; Rex et al., 2002), have been shown to modulate the escape response, but the roles (if any) of TYRA-2 and TYRA-3 (Rex et al., 2005; Wragg et al., 2007) in modulating escape behavior have yet to be uncovered. *tyra-2* and *tyra-3* mutants reverse, suppress head oscillations, and perform normal omega turns in response to anterior touch (data not shown), yet velocity during and after the escape response has not been assessed.

Previous studies may not have been able to detect the subtleties that a machine-based tracker can now analyze.

Dopamine has been described as the “attention” molecule. In our instantaneous velocity escape paradigm, *cat-2* mutants fail to maintain an elevated speed post omega turn. This may demonstrate a disconnect between the rapid reversal and rapid forward movement away from the stimulus. Dopamine activated GPCRs are expressed in the ventral nerve cord (Chase et al., 2004), indicating a possible site of action in modulating velocity changes. Additional experiments could shed light on how dopamine signals in the animal to aid the escape, by being at a heightened state of attention after an encounter with a predator. Interestingly, the converse role of excess dopamine at the synapse in *dat-1* mutants does not show the opposing phenotype, with a longer lasting acceleration in velocity. Similarly, *dat-1* mutants do not show behavioral phenotypes in basal slowing response assays or area restricted search assays, indicating that the presence of dopamine signaling is critical for the animal’s behavior, but the effects of a surplus is unknown.

Our preliminary findings provide a unique behavioral paradigm to investigate locomotion changes during the escape response. The outlook for future experiments is promising, since differences were observed in three of the four biogenic amine mutants. Upon further analysis of receptor mutants and utilization of additional technologies such as neuronal subset specific

channelrhodopsin, the complete circuit and signal transduction pathways of the *C. elegans* escape response may be uncovered.

Figure 4-1

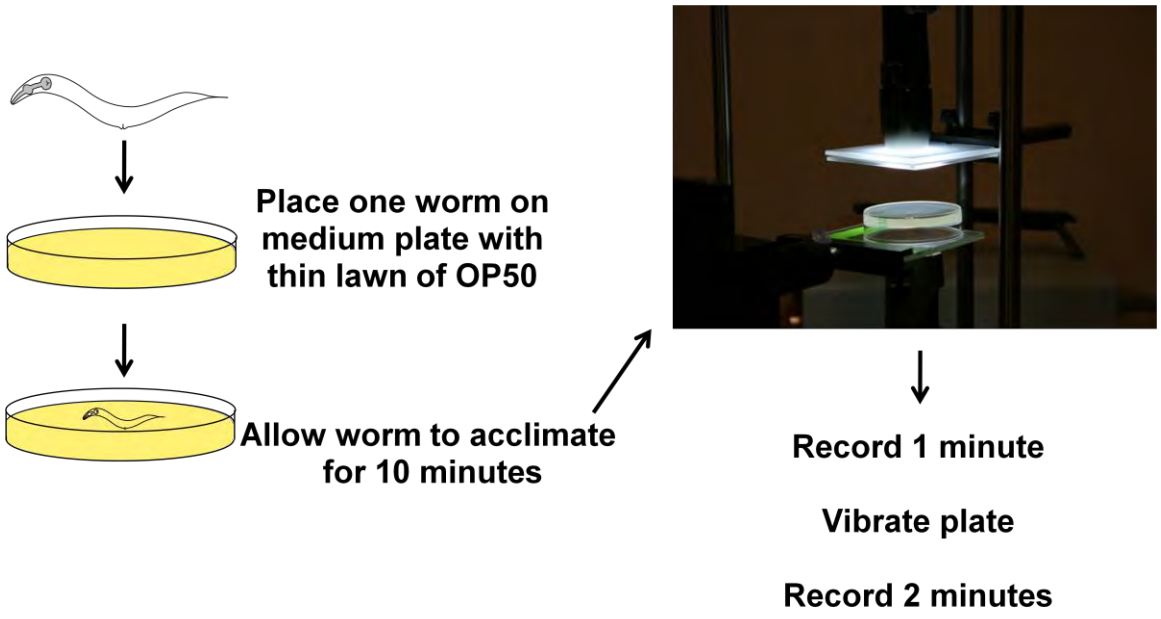

Worm tracking experimental procedure

A single animal was transferred to a plate seeded with a thin lawn of bacteria. After transfer, ten minutes were allowed for the animal to acclimate to the new plate. The plate was placed face down on the worm tracker. One minute of video was recorded, and then the plate was stimulated with a 1 second pulse vibration. Two more minutes of video was recorded as the worm velocity decayed to baseline.

Figure 4-2

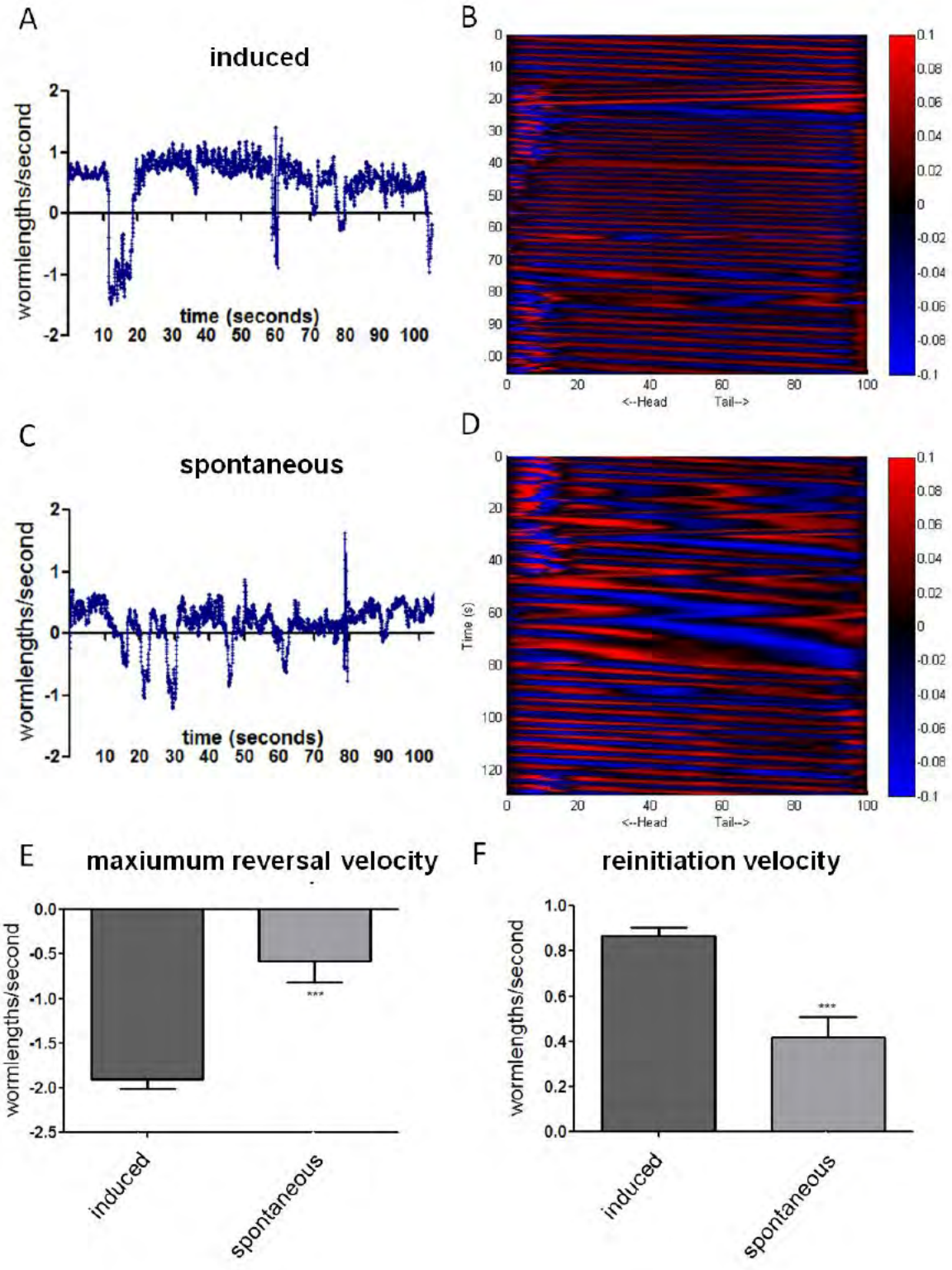
A
induced
wormlengths/second
time (seconds)
B
<--Head
Tail-->
C
spontaneous
wormlengths/second
time (seconds)
D
Time (s)
<--Head
Tail-->
E
maxiumum reversal velocity
wormlengths/second
induced
spontaneous
***
F
reinitiation velocity
wormlengths/second
induced
spontaneous
***

Figure 4-2

Analysis of wild-type instantaneous velocity during spontaneous and escape response behavior.

(A) Wild-type time course of instantaneous velocity during an escape response experiment. Arrow depicts vibration. Positive values represent forward locomotion, and negative values represent backward locomotion. (B) Kymograph of escape response experiment. Color depicts body bending depth, thickness of bands depict velocity. Change of slope of bands indicates a direction change. (C) Time course of spontaneous locomotion. * indicates initiation of reversal ending in an omega turn. (D) Kymograph of spontaneous locomotion. (E) Wild-type animals reverse at a faster velocity during an escape response versus a spontaneous reversal. (F) Velocity of forward locomotion immediately following an omega turn. An escape response has an elevated velocity. Statistical difference compared using Student's two-tailed t test; ***p value < 0.001.

Figure 4-3

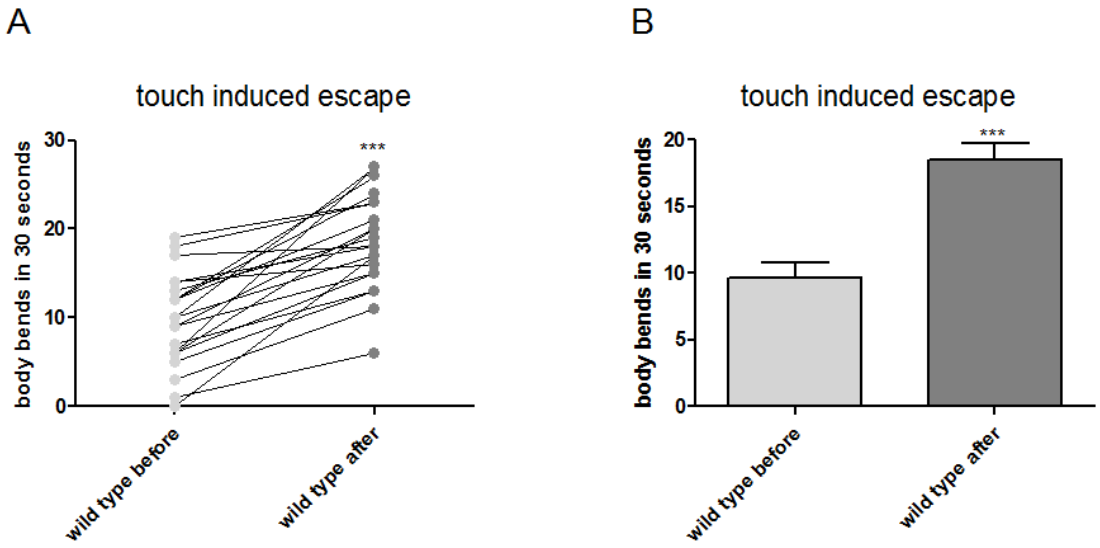

Touch induced escape responses result in an increase in velocity.

(A) Paired observations of basal and post-omega velocities after touch induced reversals. (B) Average basal and post-omega velocities. Velocity increases after a gentle anterior touch induced escape response. Statistical difference compared using Student's two-tailed paired t test; ***p value < 0.001.

Figure 4-4

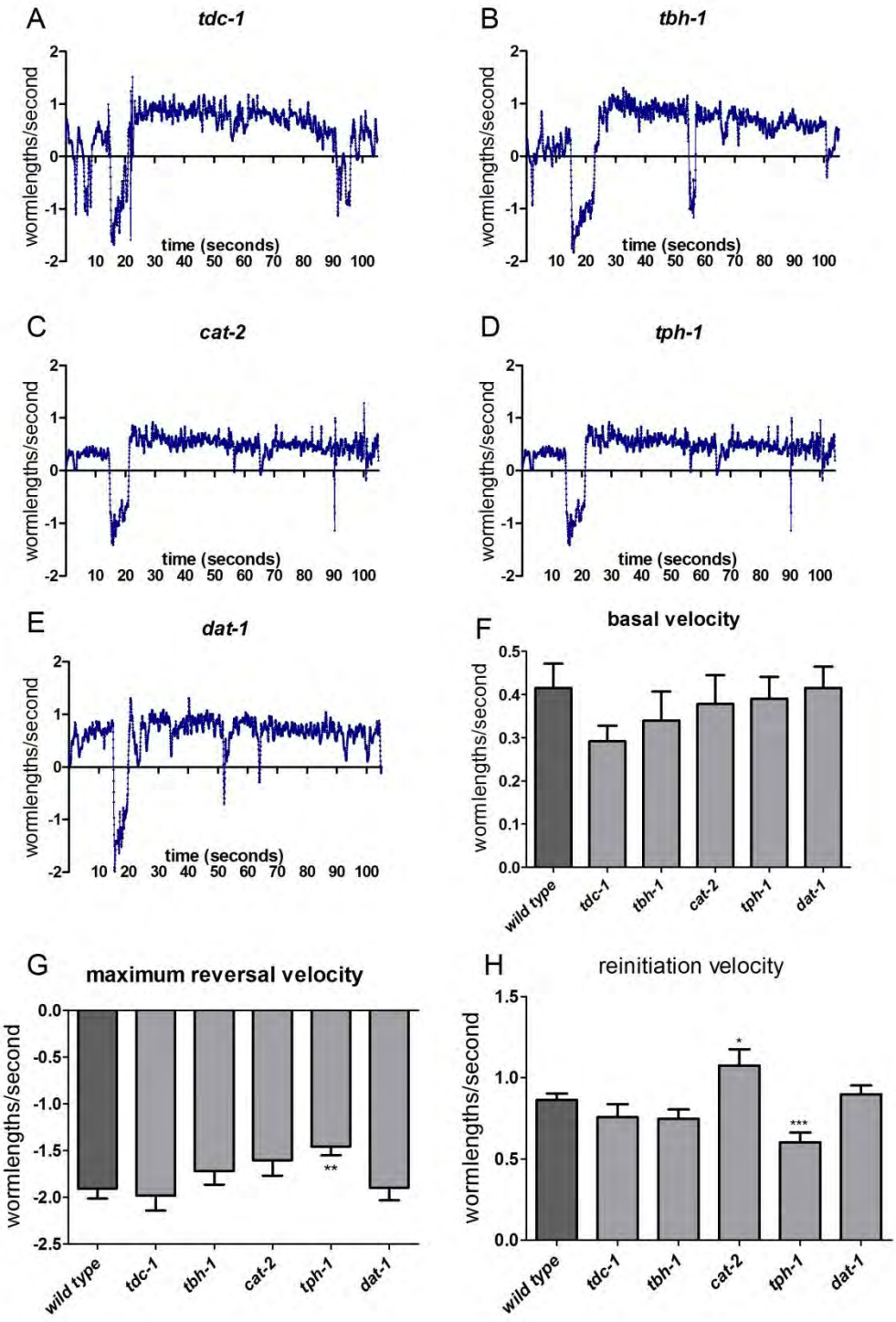
A
tdc-1
B
tbh-1
C
cat-2
D
tph-1
E
dat-1
wormlengths/second
time (seconds)
10 20 30 40 50 60 70 80 90 100
F
basal velocity
wormlengths/second
wild type
tdc-1
tbh-1
cat-2
tph-1
dat-1
G
maximum reversal velocity
wormlengths/second
**
H
reinitiation velocity
wormlengths/second
*
***

Figure 4-4

Biogenic amine signaling modulates velocity during an escape response.

(A-E) Representative instantaneous velocity traces of biogenic amine mutants during vibration induced escape response. (F) Basal velocities of biogenic amine mutants were not significantly different from wild-type. (G) Maximum reversal velocity during the escape response. *tph-1* mutants reversed at a slower rate. (H) Maximum forward reinitiation velocity after omega turn during the escape response. *cat-2* mutants reinitiated at an increased velocity compared to wild-type, and *tph-1* mutants reinitiated at a slower rate compared to wild-type. Statistical difference compared to wild-type; Student's t test *$p<0.05$, **$p<0.005$, ***$p<0.001$.

Table 4-1

strain	slope of decay	SEM	p value
wild-type	-0.0041	±0.001	-------
tdc-1	-0.0132	±0.005	*
tbh-1	-0.0060	±0.005	n.s.
cat-2	-0.0124	±0.003	**
tph-1	-0.0007	±0.001	n.s.
dat-1	-0.0040	±0.005	n.s.

Decay of velocity after reinitiation of forward locomotion

Instantaneous velocity decreased back to basal levels over time after reversal and omega turn during the escape response. Slope of decay was determined by linear regression over a 15 second time interval. Average slope of decay was calculated and SEM was determined. Statistical difference was compared to wild-type; Student's two-tailed t test, *p< 0.05, **p<0.005.

Movie 4-1

***C. elegans* escape response during a vibrational stimulus.**

Wild-type animal locomotion behavior is recorded to analyze basal instantaneous velocity. At 15 seconds, a vibration pulse is applied to the plate, inducing an escape response. Reversal and reinitiation velocity is subsequently analyzed post escape. Movie has been converted from bright field to format necessary for velocity analysis.

CHAPTER V

Final Thoughts

A. General Discussion

This thesis has aimed to investigate how the *C. elegans* escape response is modulated by tyramine. To uncover the mechanisms that control this multi-stepped behavior, detailed analysis and quantifications were done to describe the neuronal circuitry and elucidate the key molecular players.

In Chapter II, we sought to find new tyraminergic signaling pathways through forward and reverse genetic screens. Similar strategies have long been used to produce new mutations with a desired phenotype. By isolating a library of exogenous tyramine resistant mutants, we have determined that tyramine signaling is used in the animal's locomotory behavior. Specifically, the most interesting mutants that were isolated were alleles of *lgc-55*, a tyramine-gated chloride channel. Subsequently, Jennifer Pirri fully analyzed the behavior of these mutants and conducted electrophysiology to characterize the channel (Pirri et al., 2009). This discovery has led to the establishment of tyramine as a

genuine neurotransmitter in *C. elegans*, as it is expressed directly post-synaptic to the RIM tyraminergic neurons.

Since G protein signaling component mutants were also isolated from the EMS screen, this led to the majority of my dissertation research on the tyraminergic receptor, SER-2. As *lgc-55* mutants were shown to be resistant to exogenous tyramine for head movements (Pirri et al.,2009; Chapter 3), *ser-2* mutants were resistant to body paralysis on 30 mM tyramine drug plates. By carefully analyzing the first five minutes of the exogenous tyramine assay, we saw that these two receptors were playing very distinct roles in the kinetics of immobilization of the animal. *lgc-55* mutants were slower to immobilize body movements than wild-type, and *ser-2* mutants initially began to immobilize in the first few minutes, but recovered and remained mobile for the remainder of the 20 minute assay. This may be a visualization of the effects of a fast-acting chloride channel, versus a slow-acting metabotropic receptor.

In addition to evaluating the kinetics of tyramine receptors in pharmacological assays, a behavioral impact of *ser-2* was uncovered. Previous work had yet to determine a physiological role for the receptor and reported an overall normal locomotion phenotype, but here we have shed light on an essential function for this receptor in the correct navigation of the animal during the escape response. What led to this discovery was the unique expression pattern seen in the ventral nerve cord. Expression patterns of *ser-2* have already

been published, showing differential expression based on three variable promoters of the receptor (Tsalik, 2003). One promoter (*prom1*) was reported as having robust expression in the head muscles, head neurons, and the ventral nerve cord. Since our pharmacological data supported a role for SER-2 in locomotion, the first neurons we sought to identify were those of the ventral nerve cord. Not only did we find that *ser-2* expression was GABAergic, but it was strikingly restricted to a subset of GABA neurons that innervate the ventral musculature. This led us to ask the question: what behaviors in the animal have a ventral bias? I began to investigate the *C. elegans* omega turn, which is almost always executed as a deep ventral bend.

In Chapter III, I provide data showing that a behavioral role for SER-2 is to inhibit GABA release on the ventral body wall muscles to allow the nematode to effectively contract into a complete omega turn. Here, we show by electrophysiology, done my Michael Francis, that SER-2 activation by tyramine inhibits GABA release. This is the first recording in *C.elegans* that shows the effect of a GPCR in modulating neurotransmitter release events. Other biogenic amine receptors have also been shown to modulate locomotion such as the dopaminergic GPCRs, DOP-1 and DOP-3 in the basal slowing response (Chase et al., 2004), and the serotonin-gated chloride channel, MOD-1, in the enhanced slowing response (Ranganathan et al., 2000; Sawin et al., 2000). By showing that SER-2 modulates navigation by asymmetric expression in VD neurons, we

began to further investigate how the VD and DD GABAergic motor neurons control locomotion.

The approach to study VD and DD roles in navigation incorporated two methods: chronic disruption by laser ablation of each subset of GABAergic neurons, and acute activation and inhibition of the DD subset using light activated proteins. This multi-faceted investigation determined that activation and inhibition of ventral or dorsal GABA neurons, resulting in differential release of GABA, changed navigation behavior. Interestingly, ablated and light induced changes of GABA release led to an animal that could still propagate a sinusoidal wave of movement, unlike changes in cholinergic neurotransmission. Because of this remainder of normal locomotion with changes in directionality, we have effectively made the first “remote controlled worm”, opening new avenues into studying how activation and inhibition of control and motor neurons can guide an animal to a desired location.

After the activation of LGC-55 and SER-2 to execute the escape, how does locomotion recommence? Chapter IV yields a new assay to evaluate instantaneous velocity during the escape response. Previous experiments have analyzed the frequency of spontaneous omega turns of wild-type and signaling mutants using a worm tracker (Huang et al., 2006). Our approach uses machine vision tracking of single worms to do a detailed analysis of behavior from pre-stimulus, through the escape, and after the omega turn. As we have diagramed

the different phases of the escape response (Figure 1-1), we now can describe the characteristics of the final step, as reinitiation of forward locomotion involves an elevated velocity. Although it is not surprising that an animal would "flee" from a stimulus (or a predator in the wild), we have begun to investigate when these changes in velocity occur and which biogenic amines are responsible for the effects. Our preliminary results indicate that tyramine and dopamine signaling are modulating the velocity after the induced omega turn, showing that tyramine and dopamine deficient mutants do not maintain an elevated rate of velocity compared to wild-type.

In invertebrates, octopamine has been well studied and determined to play a role in escape responses of the giant squid, crayfish and cockroach (Glanzman and Krasne, 1983; Reale et al., 1986; Goldstein and Camhi, 1999; Araki and Nagayama, 2005; Araki et al., 2005). Now, with the characterization of two tyramine receptors and their roles in the *C. elegans* escape response, we have established tyramine as a key player in the survival mechanism of the nematode. By enabling the nematode to translate a mechanical sensory stimulus into a predicted reversal, suppression of head oscillations, tight omega bend to turn around, and an increase in speed upon reinitiation of forward locomotion, tyramine holds the key to a smooth get-away (Figure 5-1). May this be from the constricting rings of nematophagous fungi, or from another predator, this compilation of locomotory output has been conserved across nematode species (Sean Maguire and Mark Alkema, personal communication).

B. Future Directions

To further our understanding of tyramine signaling in *C. elegans*, additional characterization of isolated mutants from our EMS screen could be done. As most of the mapping of exogenous tyramine mutants was done using SNP mapping techniques (Davis et al., 2005), which may have interfered with correctly identifying homozygous mutants, classical mapping techniques are advised. Many of the isolated mutants displayed a more subtle phenotype, which may indicate that these mutants are partial losses of function in signaling genes, or more interestingly, they may not be disrupting a ubiquitous signaling pathway but are tyramine signaling specific.

The Alkema lab has now behaviorally characterized two tyramine receptor mutants, but two are left: *tyra-2* and *tyra-3*. By further dissecting the expression pattern, we may be able to predict possible behaviors that these tyraminergic GPCRs modulate. *tyra-3* mutants are hypersensitive to exogenous tyramine (Figure 2-3), indicating a potential role in modulation of locomotion. Initial observations show typical overall locomotion and a normal escape response, but a detailed analysis of the instantaneous velocity of these mutants has yet to be done.

Now that we have characterized the escape response as a multi-stepped process (Figure 1-1), we can further investigate each phase of the behavior.

LGC-55 modulates the reversal and suppression of head oscillations, and SER-2 works to execute an efficient omega turn. What are the signaling pathways that initiate omega turns, since *ser-2* mutants are still able to initiate a ventral bend? Previous research has reported that the RIV motor neurons are required to initiate spontaneous omegas (Gray et al., 2005). We have yet to investigate if SER-2 plays a role in instantaneous omega turns. Through laser ablation and channelrhodopsin experiments, we will be able to determine if the same circuitry and receptors that are required to execute the escape response are also used in spontaneous reversals and turning behavior.

There still remain questions as to the mechanism of extrasynaptic activation of SER-2. Our model hypothesizes release of tyramine from the RIM neurons in the nerve ring upon activation through the mechanosensory circuit. After tyramine is released in the head region, how does the molecule reach the receptors located down the length of the nematode's body? LSD binding assays have determined that SER-2 has the highest affinity for tyramine, compared to other biogenic amines in *C. elegans,* with a pKi of 7.10±0.1. There is an approximate 30-fold increase in affinity over octopamine when comparing the K_i in a competition experiment between endogenous signaling molecules (Rex et al., 2004). This indicates that tyramine may act as the endogenous ligand, but also shows that other biogenic amines may have the ability to activate SER-2 at high enough concentrations. Similar specificity has been noted for the DOP-2 G protein-coupled receptor in competition experiments with dopamine (Suo et al.,

2003). If our model is correct, then tyramine would be released from the RIM neurons and diffuse throughout the body of the nematode, along the ventral nerve cord, binding to SER-2 at theoretically low concentrations.

Tyramine diffusion throughout the body would rely on several key elements. First, tyramine in concentrations high enough to activate the SER-2 receptors would depend on its lack of degradation. In mammals, biogenic amines are typically broken down by monoamine oxidases. Currently, there are no known monoamine oxidases in *C. elegans*, indicating that tyramine may be a long lasting signaling molecule in the nematode. Second, biogenic amines can also be transported back into neurons. Although there is a known dopamine transporter in *C. elegans* that is expressed in all dopaminergic neurons (Jayanthi et al., 1998; Nass et al., 2002), tyramine does not have a known transporter, suggesting that once tyramine is released, extrasynaptic flow is possible. Lastly, in order for tyramine to modulate neurons in the distal region of the animal, the pseudocoelom must be an environment capable of diffusion. This cavity contains fluid that bathes all systems and tissues in the animal (Bird and Bird, 1991). The pseudocoelomic system has been hypothesized to be the mechanism of nutrient and small molecule transport. Small bacteria, GFP, india ink, and other foreign materials have been tested for their ability to move through the body cavity and be endocytosed by the coelomocytes (Fares and Greenwald, 2001; Zhang et al., 2001; Fares and Grant, 2002), indicating the possibility for tyramine to be transported as well. Additionally, injection of fluorescently labeled antibodies into

the pseudocoelom displays a graded diffusion throughout the body, reaching all areas from nose to tail (Gottschalk and Schafer, 2006), demonstrating that although the RIM is in the head, there is a system in place which could transport a small molecule like tyramine along the VNC.

To test if tyramine is acting extrasynaptically by diffusion through the pseudocoelom, we could examine a variety of checkpoints. First, since the coelomocytes indiscriminately endocytose cavity fluid to survey for the presence of viruses and bacteria, we could isolate coelomocytic cells and conduct HPLC to detect intracellular tyramine. The presence of tyramine in coelomocytes would indicate that tyramine has breached the confines of synaptic localization. Secondly, the pseudocoelom could be disturbed by disruption of the excretory system. It has been shown that ablation of excretory cells or CAN neurons, or mutations in *egl-15* (FGF-like receptor tyrosine kinase) and *clr-1* (receptor tyrosine phosphatase) lead to a clear phenotype in the worm, indicative of fluid homeostasis interference (Huang and Stern, 2004). If our model of precise timing of tyramine diffusion and activation of SER-2 during the escape response is correct, then fluid dynamics changes may affect omega turning behavior. Lastly, to test if extrasynaptic activation of SER-2 in the VNC is required for omega turning behavior, we could conduct promoter bashing experiments, or use a restricted promoter previously defined (Tsalik et al., 2003) to determine if an animal only mutant for SER-2 in the VNC makes loose omega turns similar to a completely null animal (Chapter 3). Our data, combined with these additional

analyses would further support the hypothesis that tyramine release from the RIM neurons in the anterior region could extrasynaptically modulate behavior through a GPCR located along the body of the nematode.

Although the RIMs are the only neuronal source of tyramine, *tdc-1* is also expressed in the UV1 cells that wrap around the vulva (Sherwood and Sternberg, 2003; Alkema et al., 2005). The UV1 cells are neuroendocrine cells that express stretch receptors (Jose et al., 2007), which may be induced to secrete molecules as an egg passes through during egg laying episodes. This mechanism and circuitry of the egg laying neurons and muscles could enable a feedback loop in the egg laying circuit (Zhang et al., 2010). Tyramine could potentially be released upon activation of the stretch receptors, providing a signal to the HSN (hermaphrodite specific neuron) which is essential for egg laying. LGC-55 is expressed in the HSN, and has been shown to modulate egg laying behavior in the presence of exogenous tyramine (Pirri et al., 2009). In addition to egg laying, there is the possibility that the contraction of an omega turn could also stimulate release of tyramine from the UV1 cells, and the tyramine released from the RIM post mechanical stimulation is unnecessary. To test this hypothesis, omega turn assays could be performed using L4 stage animals instead of adults. The UV1 cells do not develop until late stage L4, allowing for a simple determination if these cells are necessary for the execution of a closed omega turn. Additionally, laser ablation experiments could also be conducted to confirm these results. If

the absence of the UV1 cells does not affect omega turning behavior, then our current model will remain supported (Figure 3-8).

In Chapter IV, I have begun to investigate the final phase of the escape response: the initiation of forward locomotion. Initial observations indicate that our machine vision based assay will be able to extract subtle, but significant differences in instantaneous velocity. Further experiments should be conducted to test if vibration induced escape responses are using the same circuitry as touch induced escape responses. Calcium imaging of neurons in live, freely moving animals will enable us to compare the activated neurons upon different stimulations. Additionally, since we have identified tyramine and dopamine signaling as possible modulators of velocity after the escape response, the next step would be to identify which tyramine and dopamine receptors are important for velocity behavior. After receptor mutant analysis, expression patterns of receptors may lead us to investigate the circuit, where we will be able to answer the question: how does a worm accelerate and decelerate?

My doctoral work has broadened the role of the biogenic amine tyramine as an important neuromodulator in *C. elegans* behavior. Upon characterizing the signaling pathway of a tyramine activated GPCR, I have shed light on how trace amines may act to modulate neuronal function in invertebrates as well as higher organisms. By fully analyzing the multi-faceted escape response, subtle behavioral features can be illuminated from molecular signaling pathways to

neuronal circuits, revealing the complete cascade of biogenic amine signaling in nematode navigational behavior.

Figure 5-1

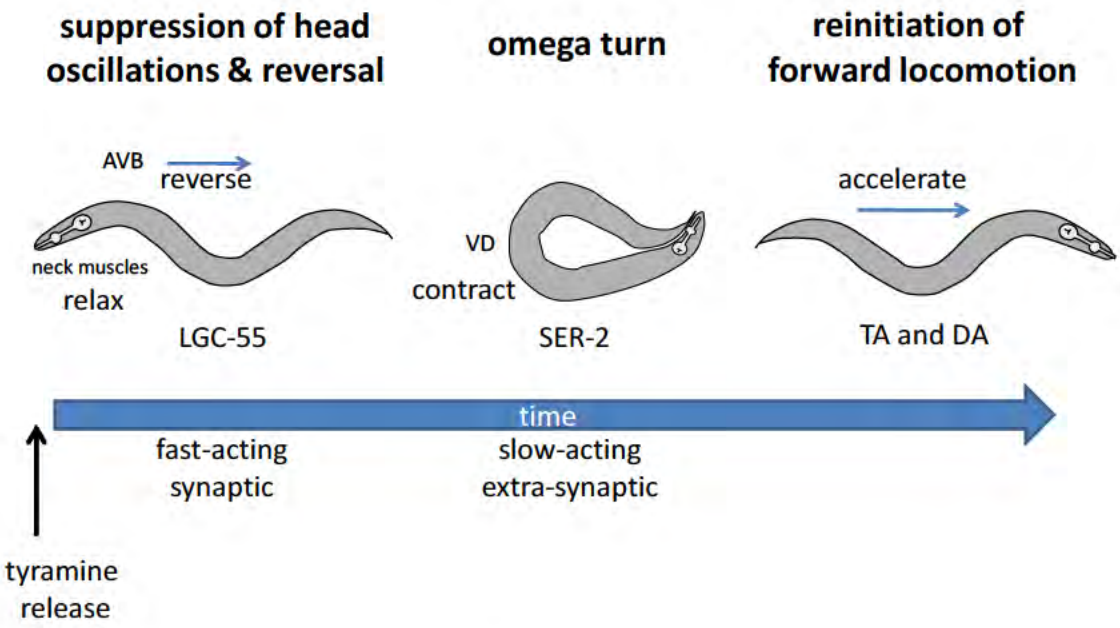

Tyramine temporally modulates the escape response.

After tyramine is released from the RIM neurons in the nerve ring, LGC-55 synaptically relaxes neck muscles, resulting in suppression of head oscillations, and inhibits the AVB forward command neuron, enabling a long reversal. Tyramine subsequently diffuses through the body and extra-synaptically activates SER-2, inhibiting release of GABA from the VD motor neurons, leading to a full contraction of the ventral muscles during the execution of an omega turn. Upon reinitiation of forward locomotion, tyramine and dopamine modulate the acceleration of velocity as the animal escapes.

BIBLIOGRAPHY

Alfonso, A., Grundahl, K., Duerr, J.S., Han, H.-P., and Rand, J.B. (1993). The *Caenorhabditis elegans unc-17* gene: a putative vesicular acetylcholine transporter. Science *261*, 617–619.

Alkema, M.J., Hunter-Ensor, M., Ringstad, N., and Horvitz, H.R. (2005). Tyramine Functions independently of octopamine in the Caenorhabditis elegans nervous system. Neuron *46*, 247-260.

Baek, J.H., Cosman, P., Feng, Z., Silver, J., and Schafer, W.R. (2002). Using machine vision to analyze and classify Caenorhabditis elegans behavioral phenotypes quantitatively. J Neurosci Methods *118*, 9-21.

Bany, I.A., Dong, M.Q., and Koelle, M.R. (2003). Genetic and cellular basis for acetylcholine inhibition of *Caenorhabditis elegans* egg-laying behavior. J. Neurosci. *23*, 8060–8069.

Bargmann, C.I., and Avery, L. (1995). Laser killing of cells in Caenorhabditis elegans. Methods Cell Biol *48*, 225-250.

Barron, G. L. (1977): The Nematode-Destroying Fungi. Topics in Mycobiology No. 1; Canadian Biological Publications; Guelph, Ont./Canada.

Bate, M., and Broadie, K. (1995). Wiring by fly: the neuromuscular system of the Drosophila embryo. Neuron *15*, 513–525.

Bendesky, A., Tsunozaki, M., Rockman, M.V., Kruglyak, L., and Bargmann, C.I. (2011). Catecholamine receptor polymorphisms affect decision-making in C. elegans. Nature *472*, 313-318.

Berretta, N., Giustizieri, M., Bernardi, G., and Mercuri, N.B. (2005). Trace amines reduce GABA(B) receptor-mediated presynaptic inhibition at GABAergic synapses of the rat substantia nigra pars compacta. Brain Res *1062*, 175-178.

Bird A.F. and Bird J. 1991. The structure of nematodes. Academic Press, California.

Blenau, W., Balfanz, S., and Baumann, A. (2000). Amtyr1: characterization of a gene from honeybee (Apis mellifera) brain encoding a functional tyramine receptor. J Neurochem *74*, 900-908.

Blumenthal, E.M. (2003). Regulation of chloride permeability by endogenously produced tyramine in the Drosophila Malpighian tubule. Am J Physiol Cell Physiol *284*, C718-728.

Borowsky, B., Adham, N., Jones, K.A., Raddatz, R., Artymyshyn, R., Ogozalek, K.L., Durkin, M.M., Lakhlani, P.P., Bonini, J.A., Pathirana, S.*, et al.* (2001). Trace amines: identification of a family of mammalian G protein-coupled receptors. Proc Natl Acad Sci U S A *98*, 8966-8971.

Boswell, M., Morgan, P., and Sedensky, M. (1990). Interaction of GABA and volatile anesthetics in the nematode Caenorhabditis elegans. The FASEB Journal *4*, 2506-2510.

Boulton, A.A., and Majer, J.R. (1971). The mass spectrometric identification of the isomers of tyramine: identification of para-tyramine in rat brain. Can J Biochem *49*, 993-998.

Boulton, A.A., and Baker, G.B. (1975). The subcellular distribution of beta-phenylethylamine, p-tyramine and tryptamine in rat brain. J Neurochem *25*, 477-481.

Branchek, T.A., and Blackburn, T.P. (2003). Trace amine receptors as targets for novel therapeutics: legend, myth and fact. Curr Opin Pharmacol *3*, 90-97.

Brandeis, R., Brandys, Y., and Yehuda, S. (1989). The use of the Morris Water Maze in the study of memory and learning. Int J Neurosci *48*, 29-69.

Brenner, S. (1974). The genetics of Caenorhabditis elegans. Genetics *77*, 71-94.

Brown, T.G. (1911). The intrinsic factors in the act of progression in the mammal. Proc. R. Soc. Lond. B. Biol. Sci. *84*, 308-319.

Brown, C.S., and Bryant, S.G. (1988). Monoamine oxidase inhibitors: safety and efficacy issues. Drug Intell Clin Pharm *22*, 232-235.

Bunzow, J.R., Sonders, M.S., Arttamangkul, S., Harrison, L.M., Zhang, G., Quigley, D.I., Darland, T., Suchland, K.L., Pasumamula, S., Kennedy, J.L.*, et al.* (2001). Amphetamine, 3,4-methylenedioxymethamphetamine, lysergic acid diethylamide, and metabolites of the catecholamine neurotransmitters are agonists of a rat trace amine receptor. Mol Pharmacol *60*, 1181-1188.

Burchett, S.A., and Hicks, T.P. (2006). The mysterious trace amines: protean neuromodulators of synaptic transmission in mammalian brain. Prog Neurobiol *79*, 223-246.

Castrejon, F., and Rojas, J.C. (2010). Behavioral Responses of Larvae and Adults of Estigmene acrea (Lepidoptera: Arctiidae) to Light of Different Wavelengths. Florida Entomologist *93*, 505-509.

Chalfie, M., Sulston, J.E., White, J.G., Southgate, E., Thomson, J.N., and Brenner, S. (1985). The neural circuit for touch sensitivity in Caenorhabditis elegans. J Neurosci *5*, 956-964.

Chalfie, M., and Au, M. (1989). Genetic control of differentiation of the Caenorhabditis elegans touch receptor neurons. Science *243*, 1027-1033.

Chalfie M. and White J. (1988). The nervous system. In *The nematode* C. elegans (ed. W.B. Wood), pp. 337–391. Cold Spring Harbor Laboratory Press, Cold Spring Harbor, New York.

Chase, D.L., Pepper, J.S., and Koelle, M.R. (2004). Mechanism of extrasynaptic dopamine signaling in Caenorhabditis elegans. Nat Neurosci *7*, 1096-1103.

Chelur, D.S., Ernstrom, G.G., Goodman, M.B., Yao, C.A., Chen, L., R, O.H., and Chalfie, M. (2002). The mechanosensory protein MEC-6 is a subunit of the C. elegans touch-cell degenerin channel. Nature *420*, 669-673.

Chiba, C.M., and Rankin, C.H. (1990). A developmental analysis of spontaneous and reflexive reversals in the nematode Caenorhabditis elegans. J Neurobiol *21*, 543-554.

Clark, B.J., and Taube, J.S. (2009). Deficits in landmark navigation and path integration after lesions of the interpeduncular nucleus. Behav Neurosci *123*, 490-503.

Croll, N.A. (1975). Components and patterns in the behaviour of the nematode Caenorhabditis elegans. Journal of Zoology *176*, 159-176.

Croll, N.A., and Smith, J.M. (1978). Integrated behaviour in the feeding phase of Caenorhabditis elegans (Nematoda). Journal of Zoology *184*, 507-517.

D'Andrea G, Granella F, Leone M, Perini F, Farruggio A, Bussone G. (2006), Abnormal platelet trace amine profiles in migraine with and without aura. Cephalalgia *8,* 968-72.

D'Andrea, G., Nordera, G., Perini, F., Allais, G., and Granella, F. (2007). Biochemistry of neuromodulation in primary headaches: focus on anomalies of tyrosine metabolism. Neurological Sciences *28*, S94-S96.

Davie, C.A. (2008). A review of Parkinson's disease. British Medical Bulletin *86*, 109-127.

Davis, B.A., and Boulton, A.A. (1994). The trace amines and their acidic metabolites in depression--an overview. Prog Neuropsychopharmacol Biol Psychiatry *18*, 17-45.

Davis, M.W., Hammarlund, M., Harrach, T., Hullett, P., Olsen, S., and Jorgensen, E.M. (2005). Rapid single nucleotide polymorphism mapping in C. elegans. BMC Genomics *6*, 118.

del Castillo, J., de Mello, W.C., and Morales, T. (1963). The physiological role of acetylcholine in the neuromuscular system of *Ascaris lumbricoides*. Arch. Int. Physiol. Biochim. *71*, 741–757.

Dittman, J.S., and Kaplan, J.M. (2008). Behavioral impact of neurotransmitter-activated G-protein-coupled receptors: muscarinic and GABAB receptors regulate Caenorhabditis elegans locomotion. J Neurosci *28*, 7104-7112.

Dixon, S.J., and Roy, P.J. (2005). Muscle arm development in Caenorhabditis elegans. Development *132*, 3079-3092.

Duerr, J.S., Frisby, D.L., Gaskin, J., Duke, A., Asermely, K., Huddleston, D., Eiden, L.E., and Rand, J.B. (1999). The cat-1 gene of Caenorhabditis elegans encodes a vesicular monoamine transporter required for specific monoamine-dependent behaviors. J Neurosci *19*, 72-84.

Dusenbery, D.B. (1980). Appetitive response of the nematode Caenorhabditis-elegans to oxygen. Journal of Comparative Physiology *136*, 333-336.

Eastman, C., Horvitz, H.R., and Jin, Y. (1999). Coordinated transcriptional regulation of the unc-25 glutamic acid decarboxylase and the unc-47 GABA vesicular transporter by the Caenorhabditis elegans UNC-30 homeodomain protein. J Neurosci *19*, 6225-6234.

Edwards, D.H., Heitler, W.J., and Krasne, F.B. (1999). Fifty years of a command neuron: the neurobiology of escape behavior in the crayfish. Trends Neurosci *22*, 153-161.

Etienne, A.S., and Jeffery, K.J. (2004). Path integration in mammals. Hippocampus *14*, 180-192.

Fares, H., and Grant, B. (2002). Deciphering endocytosis in Caenorhabditis elegans. Traffic *3*, 11-19.

Fares, H., and Greenwald, I. (2001). Genetic analysis of endocytosis in Caenorhabditis elegans: coelomocyte uptake defective mutants. Genetics *159*, 133-145.

Fetcho, J.R. (1992). The spinal motor system in early vertebrates and some of its evolutionary changes. Brain Behav Evol *40*, 82-97.

Francis, M.M., and Maricq, A.V. (2006). Electrophysiological analysis of neuronal and muscle function in C. elegans. Methods Mol Biol *351*, 175-192.

Gardiner, J.M., and Atema, J. (2010). The function of bilateral odor arrival time differences in olfactory orientation of sharks. Curr Biol *20*, 1187-1191.

Gerson, E.A., and Kelsey, R.G. (1997). Attraction and direct mortality of pandora moths, Coloradia pandora (Lepidoptera: Saturniidae), by nocturnal fire. Forest Ecology and Management *98*, 71-75.

Glanzman, D.L., and Krasne, F.B. (1983). Serotonin and octopamine have opposite modulatory effects on the crayfish's lateral giant escape reaction. J Neurosci *3*, 2263-2269.

Goodman, M.B., Ernstrom, G.G., Chelur, D.S., O'Hagan, R., Yao, C.A., and Chalfie, M. (2002). MEC-2 regulates C. elegans DEG/ENaC channels needed for mechanosensation. Nature *415*, 1039-1042.

Goodman, M.B., and Schwarz, E.M. (2003). Transducing touch in Caenorhabditis elegans. Annu Rev Physiol *65*, 429-452.

Gottschalk, A., and Schafer, W.R. (2006). Visualization of integral and peripheral cell surface proteins in live Caenorhabditis elegans. J Neurosci Methods *154*, 68-79.

Gray, J.M., Hill, J.J., and Bargmann, C.I. (2005). A circuit for navigation in Caenorhabditis elegans. Proc Natl Acad Sci U S A *102*, 3184-3191.

Gray, J.M., Karow, D.S., Lu, H., Chang, A.J., Chang, J.S., Ellis, R.E., Marletta, M.A., and Bargmann, C.I. (2004). Oxygen sensation and social feeding mediated by a C. elegans guanylate cyclase homologue. Nature *430*, 317-322.

Grillner, S. (2003). The motor infrastructure: from ion channels to neuronal networks. Nature reviews Neuroscience *4*, 573-586.

Grillner, S., Wallen, P., Saitoh, K., Kozlov, A., and Robertson, B. (2008). Neural bases of goal-directed locomotion in vertebrates--an overview. Brain Res Rev *57*, 2-12.

Guastella, J., Johnson, C.D., and Stretton, A.O. W. (1991). GABA-immunoreactive neurons in the nematode *Ascaris*. J. Comp. Neurol. 584–597.

Hajdu-Cronin, Y.M., Chen, W.J., Patikoglou, G., Koelle, M.R., and Sternberg, P.W. (1999). Antagonism between G(o)alpha and G(q)alpha in Caenorhabditis elegans: the RGS protein EAT-16 is necessary for G(o)alpha signaling and regulates G(q)alpha activity. Genes Dev *13*, 1780-1793.

Hamdan, F.F., Ungrin, M.D., Abramovitz, M., Ribeiro, P. (1999). Characterization of a novel serotonin receptor from *Caenorhabditis elegans*: cloning and expression of two splice variants. J. Neurochem. *72*, 1372–1383.

Hallam, S., Singer, E., Waring, D., and Jin, Y. (2000). The C. elegans NeuroD homolog cnd-1 functions in multiple aspects of motor neuron fate specification. Development *127*, 4239-4252.

Hardaker, L.A., Singer, E., Kerr, R., Zhou, G., and Schafer, W.R. (2001). Serotonin modulates locomotory behavior and coordinates egg-laying and movement in Caenorhabditis elegans. J Neurobiol *49*, 303-313.

Hart, A.C., Sims, S., and Kaplan, J.M. (1995). Synaptic code for sensory modalities revealed by C. elegans GLR-1 glutamate receptor. Nature *378*, 82-85.

Hart, A.C., Kass, J., Shapiro, J.E., and Kaplan, J.M. (1999). Distinct signaling pathways mediate touch and osmosensory responses in a polymodal sensory neuron. J Neurosci *19*, 1952-1958.

Hedgecock, E.M., and Russell, R.L. (1975). Normal and mutant thermotaxis in the nematode Caenorhabditis elegans. Proc Natl Acad Sci U S A *72*, 4061-4065.

Hills, T., Brockie, P.J., and Maricq, A.V. (2004). Dopamine and glutamate control area-restricted search behavior in Caenorhabditis elegans. J Neurosci *24*, 1217-1225.

Hobson, R.J., Geng, J., Gray, A.D., Komuniecki, R.W. (2003). SER-7b, a constitutively active Galphas coupled 5-HT7-like receptor expressed in the *Caenorhabditis elegans* M4 pharyngeal motorneuron. J. Neurochem. *87*, 22–29.

Horvitz, H.R., Chalfie, M., Trent, C., Sulston, J.E., and Evans, P.D. (1982). Serotonin and octopamine in the nematode Caenorhabditis elegans. Science *216*, 1012-1014.

Houssa, B., Schaap, D., van der Wal, J., Goto, K., Kondo, H., Yamakawa, A., Shibata, M., Takenawa, T., and van Blitterswijk, W.J. (1997). Cloning of a novel human diacylglycerol kinase (DGKtheta) containing three cysteine-rich domains, a proline-rich region, and a pleckstrin homology domain with an overlapping Ras-associating domain. J Biol Chem *272*, 10422-10428.

Huang, K.M., Cosman, P., and Schafer, W.R. (2006). Machine vision based detection of omega bends and reversals in C. elegans. J Neurosci Methods *158*, 323-336.

Huang, P., and Stern, M.J. (2004). FGF signaling functions in the hypodermis to regulate fluid balance in C. elegans. Development *131*, 2595-2604.

Iino, Y., and Yoshida, K. (2009). Parallel use of two behavioral mechanisms for chemotaxis in Caenorhabditis elegans. J Neurosci *29*, 5370-5380.

Jansen, S.C., van Dusseldorp, M., Bottema, K.C., and Dubois, A.E.J. (2003). Intolerance to dietary biogenic amines: a review. Annals of allergy, asthma & immunology : official publication of the American College of Allergy, Asthma, & Immunology *91*, 233-241.

Jarrard, L.E.,(1989). On the use of ibotenic acid to lesion selectively different components of the hippocampal formation. J Neurosci Methods *29,* 251–259.

Jayanthi, L.D., Apparsundaram, S., Malone, M.D., Ward, E., Miller, D.M., Eppler, M., and Blakely, R.D. (1998). The Caenorhabditis elegans gene T23G5.5

encodes an antidepressant- and cocaine-sensitive dopamine transporter. Mol Pharmacol *54*, 601-609.

Jiang, G., Zhuang, L., Miyauchi, S., Miyake, K., Fei, Y.J., and Ganapathy, V. (2005). A Na+/Cl- -coupled GABA transporter, GAT-1, from Caenorhabditis elegans: structural and functional features, specific expression in GABA-ergic neurons, and involvement in muscle function. J Biol Chem *280*, 2065-2077.

Jin, Y., Jorgensen, E., Hartwieg, E., and Horvitz, H.R. (1999). The *Caenorhabditis elegans* gene *unc-25* encodes glutamic acid decarboxylase and is required for synaptic transmission but not synaptic development. J. Neurosci. *19*, 539–548.

Johnsen, P.B. and J.H. Teeter (1985) Behavioral responses of the bonnethead (*Sphyrna tiburo*) to controlled olfactory stimulation. Marine Behavior and Physiology *11*, 283-291.

Johnson, C.D., and Stretton, A.O. (1987). GABA-immunoreactivity in inhibitory motor neurons of the nematode *Ascaris*. J. Neurosci. *7*, 223–235.

Jose, A.M., Bany, I.A., Chase, D.L., and Koelle, M.R. (2007). A specific subset of transient receptor potential vanilloid-type channel subunits in Caenorhabditis elegans endocrine cells function as mixed heteromers to promote neurotransmitter release. Genetics *175*, 93-105.

Kim, K., and Li, C. (2004). Expression and regulation of an FMRFamide-related neuropeptide gene family in Caenorhabditis elegans. The Journal of Comparative Neurology *475*, 540-550.

Kimchi, T., Etienne, A.S., and Terkel, J. (2004). A subterranean mammal uses the magnetic compass for path integration. Proc Natl Acad Sci U S A *101*, 1105-1109.

Korn, H., and Faber, D.S. (1996). Escape behavior - brainstem and spinal cord circuitry and function. Curr Opin Neurobiol *6*, 826-832.

Korn, H., Triller, A., and Faber, D.S. (1978). Structural correlates of recurrent collateral interneurons producing both electrical and chemical inhibitions of the Mauthner cell. Proc R Soc Lond B Biol Sci *202*, 533-538.

Krasne, F.B. (1969). Excitation and habituation of the crayfish escape reflex: the depolarizing response in lateral giant fibres of the isolated abdomen. J Exp Biol *50*, 29-46.

Kusaga, A., Yamashita, Y., Koeda, T., Hiratani, M., Kaneko, M., Yamada, S., and Matsuishi, T. (2002). Increased urine phenylethylamine after methylphenidate treatment in children with ADHD. Ann Neurol *52*, 372-374.

Kutsukake, M., Komatsu, A., Yamamoto, D., and Ishiwa-Chigusa, S. (2000). A tyramine receptor gene mutation causes a defective olfactory behavior in Drosophila melanogaster. Gene *245*, 31-42.

Lackner, M.R., Nurrish, S.J., and Kaplan, J.M. (1999). Facilitation of synaptic transmission by EGL-30 Gqalpha and EGL-8 PLCbeta: DAG binding to UNC-13 is required to stimulate acetylcholine release. Neuron *24*, 335-346.

Leifer, A.M., Fang-Yen, C., Gershow, M., Alkema, M.J., and Samuel, A.D. (2011). Optogenetic manipulation of neural activity in freely moving Caenorhabditis elegans. Nat Methods *8*, 147-152.

Li, C., Nelson, L.S., Kim, K., Nathoo, A., and Hart, A.C. (1999). Neuropeptide gene families in the nematode *Caenorhabditis elegans*. Ann. N. Y. Acad. Sci. *897*, 239–52.

Li, C. and Kim, K. Neuropeptides (2008), *WormBook*, ed. The *C. elegans* Research Community, WormBook, doi/10.1895/wormbook.1.142.1, http://www.wormbook.org.

Lindemann, L., Meyer, C.A., Jeanneau, K., Bradaia, A., Ozmen, L., Bluethmann, H., Bettler, B., Wettstein, J.G., Borroni, E., Moreau, J.-L., *et al.* (2008). Trace Amine-Associated Receptor 1 Modulates Dopaminergic Activity. Journal of Pharmacology and Experimental Therapeutics *324*, 948-956.

Maricq, A.V., Peckol, E., Driscoll, M., and Bargmann, C.I. (1995). Mechanosensory signalling in C. elegans mediated by the GLR-1 glutamate receptor. Nature *378*, 78-81.

McCabe, B.J. (1986). Dietary tyramine and other pressor amines in MAOI regimens: a review. J Am Diet Assoc *86*, 1059-1064.

McClellan, A.D., Brown, G.D., and Getting, P.A. (1994). Modulation of swimming in Tritonia: excitatory and inhibitory effects of serotonin. J Comp Physiol A *174*, 257-266.

McDonald, P.W., Hardie, S.L., Jessen, T.N., Carvelli, L., Matthies, D.S., and Blakely, R.D. (2007). Vigorous motor activity in Caenorhabditis elegans requires

efficient clearance of dopamine mediated by synaptic localization of the dopamine transporter DAT-1. J Neurosci *27*, 14216-14227.

Mellem, J.E., Brockie, P.J., Zheng, Y., Madsen, D.M., and Maricq, A.V. (2002). Decoding of polymodal sensory stimuli by postsynaptic glutamate receptors in C. elegans. Neuron *36*, 933-944.

McIntire, S.L., Jorgensen, E., Kaplan, J. and Horvitz, H.R. (1993). The GABAergic nervous system of *Caenorhabditis elegans.* Nature *364*, 337-341.

McIntire, S.L., Reimer, R.J., Schuske, K., Edwards, R.H., and Jorgensen, E.M. (1997). Identification and characterization of the vesicular GABA transporter. Nature *389*, 870–876.

Mellanby, H. (1955). The identification and estimation of acetylcholine in three parasitic nematodes (*Ascaris lumbricoides, Litomosoides carinii*, and the microfilariae of *Dirofilaria repens*). Parasitology *45*, 287–294.

Mendel, J.E., Korswagen, H.C., Liu, K.S., Hajdu-Cronin, Y.M., Simon, M.I., Plasterk, R.H., and Sternberg, P.W. (1995). Participation of the protein Go in multiple aspects of behavior in C. elegans. Science *267*, 1652-1655.

Miller, K.G., Emerson, M.D., and Rand, J.B. (1999). Go[alpha] and Diacylglycerol Kinase Negatively Regulate the Gq[alpha] Pathway in C. elegans. Neuron *24*, 323-333.

Morris, R. G. M. (1981). Spatial Localization Does Not Require the Presence of Local Cues. Learning and Motivation, *12*, 239-260.

Morris, R.G., Garrud, P., Rawlins, J.N., and O'Keefe, J. (1982). Place navigation impaired in rats with hippocampal lesions. Nature *297*, 681-683.

Nagel, G., Brauner, M., Liewald, J.F., Adeishvili, N., Bamberg, E., and Gottschalk, A. (2005). Light activation of channelrhodopsin-2 in excitable cells of Caenorhabditis elegans triggers rapid behavioral responses. Curr Biol *15*, 2279-2284.

Nakazawa, K., McHugh, T.J., Wilson, M.A., and Tonegawa, S. (2004). NMDA receptors, place cells and hippocampal spatial memory. Nat Rev Neurosci *5*, 361-372.

Nass, R., Hall, D.H., Miller, D.M., 3rd, and Blakely, R.D. (2002). Neurotoxin-induced degeneration of dopamine neurons in Caenorhabditis elegans. Proc Natl Acad Sci U S A *99*, 3264-3269.

Nathanson, J.A. (1979). Octopamine receptors, adenosine 3',5'-monophosphate, and neural control of firefly flashing. Science *203*, 65-68.

Nathoo, A.N., Moeller, R.A., Westlund, B.A., and Hart, A.C. (2001). Identification of neuropeptide-like protein gene families in Caenorhabditiselegans and other species. Proc Natl Acad Sci U S A *98*, 14000-14005.

Nguyen, M., Alfonso, A., Johnson, C.D., and Rand, J.B. (1995). Caenorhabditis elegans mutants resistant to inhibitors of acetylcholinesterase. Genetics *140*, 527-535.

Niacaris, T., and Avery, L. (2003). Serotonin regulates repolarization of the C. elegans pharyngeal muscle. J Exp Biol *206*, 223-231.

Nurrish, S., Segalat, L., and Kaplan, J.M. (1999). Serotonin inhibition of synaptic transmission: Galpha(0) decreases the abundance of UNC-13 at release sites. Neuron *24*, 231-242.

O'Hagan, R., Chalfie, M., and Goodman, M.B. (2005). The MEC-4 DEG/ENaC channel of Caenorhabditis elegans touch receptor neurons transduces mechanical signals. Nat Neurosci *8*, 43-50.

Ohta, H., Utsumi, T., and Ozoe, Y. (2003). B96Bom encodes a Bombyx mori tyramine receptor negatively coupled to adenylate cyclase. Insect Mol Biol *12*, 217-223.

O'Keefe, J., and Dostrovsky, J. (1971). The hippocampus as a spatial map. Preliminary evidence from unit activity in the freely-moving rat. Brain Res *34*, 171-175.

O'Keefe, J, and Nadel, L. (1978). The hippocampus as a cognitive map. Clarendon, Oxford.

Olde, B., and McCombie, W.R. (1997). Molecular cloning and functional expression of a serotonin receptor from *Caenorhabditis elegans*. J. Mol. Neurosci. *8*, 53–62.

Pierce-Shimomura, J.T., Morse, T.M., and Lockery, S.R. (1999). The fundamental role of pirouettes in Caenorhabditis elegans chemotaxis. J Neurosci *19*, 9557-9569.

Pirri, J.K., McPherson, A.D., Donnelly, J.L., Francis, M.M., and Alkema, M.J. (2009). A tyramine-gated chloride channel coordinates distinct motor programs of a Caenorhabditis elegans escape response. Neuron *62*, 526-538.

Plowman, G.D., Sudarsanam, S., Bingham, J., Whyte, D., and Hunter, T. (1999). The protein kinases of Caenorhabditis elegans: A model for signal transduction in multicellular organisms. Proceedings of the National Academy of Sciences *96*, 13603-13610.

Prasad, B.C., Ye, B., Zackhary, R., Schrader, K., Seydoux, G., and Reed, R.R. (1998). unc-3, a gene required for axonal guidance in Caenorhabditis elegans, encodes a member of the O/E family of transcription factors. Development *125*, 1561-1568.

Ramot, D., Johnson, B.E., Berry, T.L., Jr., Carnell, L., and Goodman, M.B. (2008). The Parallel Worm Tracker: a platform for measuring average speed and drug-induced paralysis in nematodes. PLoS One *3*, e2208.

Ranganathan, R., Cannon, S.C., and Horvitz, H.R. (2000). MOD-1 is a serotonin-gated chloride channel that modulates locomotory behaviour in C.[thinsp]elegans. Nature *408*, 470-475.

Rex, E., and Komuniecki, R.W. (2002). Characterization of a tyramine receptor from Caenorhabditis elegans. J Neurochem *82*, 1352-1359.

Rex, E., Molitor, S.C., Hapiak, V., Xiao, H., Henderson, M., and Komuniecki, R. (2004). Tyramine receptor (SER-2) isoforms are involved in the regulation of pharyngeal pumping and foraging behavior in Caenorhabditis elegans. J Neurochem *91*, 1104-1115.

Rex, E., Hapiak, V., Hobson, R., Smith, K., Xiao, H., and Komuniecki, R. (2005). TYRA-2 (F01E11.5): a Caenorhabditis elegans tyramine receptor expressed in the MC and NSM pharyngeal neurons. J Neurochem *94*, 181-191.

Revel, F.G., Moreau, J.L., Gainetdinov, R.R., Bradaia, A., Sotnikova, T.D., Mory, R., Durkin, S., Zbinden, K.G., Norcross, R., Meyer, C.A.*, et al.* (2011). TAAR1 activation modulates monoaminergic neurotransmission, preventing

hyperdopaminergic and hypoglutamatergic activity. Proc Natl Acad Sci U S A *108*, 8485-8490.

Richmond, J.E., and Jorgensen, E.M. (1999). One GABA and two acetylcholine receptors function at the C. elegans neuromuscular junction. Nat Neurosci *2*, 791-797.

Ringstad, N., Abe, N., and Horvitz, H.R. (2009). Ligand-Gated Chloride Channels Are Receptors for Biogenic Amines in C. elegans. Science *325*, 96-100.

Rogers, C.M., Franks, C.J., Walker, R.J., Burke, J.F., and Holden-Dye, L. (2001). Regulation of the pharynx of Caenorhabditis elegans by 5-HT, octopamine, and FMRFamide-like neuropeptides. J Neurobiol *49*, 235-244.

Rotte, C., Krach, C., Balfanz, S., Baumann, A., Walz, B., and Blenau, W. (2009). Molecular characterization and localization of the first tyramine receptor of the American cockroach (Periplaneta americana). Neuroscience *162*, 1120-1133.

Sakurai, A., and Katz, P.S. (2003). Spike timing-dependent serotonergic neuromodulation of synaptic strength intrinsic to a central pattern generator circuit. J Neurosci *23*, 10745-10755.

Sandler, M., Ruthven, C.R., Goodwin, B.L., Reynolds, G.P., Rao, V.A., and Coppen, A. (1979). Deficient production of tyramine and octopamine in cases of depression. Nature *278*, 357-358.

Sanyal, S., Wintle, R.F., Kindt, K.S., Nuttley, W.M., Arvan, R., Fitzmaurice, P., Bigras, E., Merz, D.C., Hebert, T.E., van der Kooy, D.*, et al.* (2004). Dopamine modulates the plasticity of mechanosensory responses in Caenorhabditis elegans. Embo J *23*, 473-482.

Saudou, F., Amlaiky, N., Plassat, J.L., Borrelli, E., and Hen, R. (1990). Cloning and characterization of a Drosophila tyramine receptor. Embo J *9*, 3611-3617.

Sawin, E.R., Ranganathan, R., and Horvitz, H.R. (2000). C. elegans locomotory rate is modulated by the environment through a dopaminergic pathway and by experience through a serotonergic pathway. Neuron *26*, 619-631.

Schafer, W.R., and Kenyon, C.J. (1995). A calcium-channel homologue required for adaptation to dopamine and serotonin in Caenorhabditis elegans. Nature *375*, 73-78.

Schuske, K., Beg, A.A., and Jorgensen, E.M. (2004). The GABA nervous system in *C. elegans*. Trends Neurosci. *27*, 407–414.

Schwaerzel, M., Monastirioti, M., Scholz, H., Friggi-Grelin, F., Birman, S., and Heisenberg, M. (2003). Dopamine and octopamine differentiate between aversive and appetitive olfactory memories in Drosophila. J Neurosci *23*, 10495-10502.

Segalat, L., Elkes, D.A., and Kaplan, J.M. (1995). Modulation of serotonin-controlled behaviors by Go in Caenorhabditis elegans. Science *267*, 1648-1651.

Sherwood, D.R., and Sternberg, P.W. (2003). Anchor cell invasion into the vulval epithelium in C. elegans. Dev Cell *5*, 21-31.

Sieburth, D., Ch'ng, Q., Dybbs, M., Tavazoie, M., Kennedy, S., Wang, D., Dupuy, D., Rual, J.F., Hill, D.E., Vidal, M.*, et al.* (2005). Systematic analysis of genes required for synapse structure and function. Nature *436*, 510-517.

Shan, G., Kim, K., Li, C., and Walthall, W.W. (2005). Convergent genetic programs regulate similarities and differences between related motor neuron classes in Caenorhabditis elegans. Dev Biol *280*, 494-503.

Srinivasan, M., Zhang, S., Lehrer, M., and Collett, T. (1996). Honeybee navigation en route to the goal: visual flight control and odometry. J Exp Biol *199*, 237-244.

Srivastava, N., Clark, D.A., and Samuel, A.D. (2009). Temporal analysis of stochastic turning behavior of swimming C. elegans. J Neurophysiol *102*, 1172-1179.

Stirman, J.N., Crane, M.M., Husson, S.J., Wabnig, S., Schultheis, C., Gottschalk, A., and Lu, H. (2011). Real-time multimodal optical control of neurons and muscles in freely behaving Caenorhabditis elegans. Nat Methods *8*, 153-158.

Sulston, J.E. and Horvitz, H.R. 1977. Post-embryonic cell lineages of the nematode *Caenorhabditis elegans*. Dev. Biol. *56***,**110-156.

Sulston, J.E., Schierenberg, E., White, J.G. and Thomson, J.N. 1983. The embryonic cell lineage of the nematode *Caenorhabditis elegans*. Dev. Biol. 100**:** 64-119.

Suo, S., Sasagawa, N., Ishiura, S. (2002). Identification of a dopamine receptor from *Caenorhabditis elegans*. Neurosci. Lett. *319*, 13–16.

Suo, S., Sasagawa, N., and Ishiura, S. (2003). Cloning and characterization of a Caenorhabditis elegans D2-like dopamine receptor. J Neurochem *86*, 869-878.

Suo, S., Sasagawa, N., Ishiura, S. (2003). Cloning and characterization of a Caenorhabditis elegans D2-like dopamine receptor. J. Neurochem. *86*, 869–878.

Suo, S., Culotti, J.G., and Van Tol, H.H. (2009). Dopamine counteracts octopamine signalling in a neural circuit mediating food response in C. elegans. Embo J *28*, 2437-2448.

Sutherland, R.J., Whishaw, I.Q., and Kolb, B. (1983). A behavioural analysis of spatial localization following electrolytic, kainate- or colchicine-induced damage to the hippocampal formation in the rat. Behavioural Brain Research *7*, 133-153.

Suzuki, H., Kerr, R., Bianchi, L., Frokjaer-Jensen, C., Slone, D., Xue, J., Gerstbrein, B., Driscoll, M., and Schafer, W.R. (2003). In vivo imaging of C. elegans mechanosensory neurons demonstrates a specific role for the MEC-4 channel in the process of gentle touch sensation. Neuron *39*, 1005-1017.

Teshiba, T., Shamsian, A., Yashar, B., Yeh, S.R., Edwards, D.H., and Krasne, F.B. (2001). Dual and opposing modulatory effects of serotonin on crayfish lateral giant escape command neurons. J Neurosci *21*, 4523-4529.

Thorn, R. G. & Barron, G. L. (1986): Nematoctonus and the tribe Resupinateae in Ontario, Canada. Mycotaxon 25, 321-453; Guelph (Canada).

Touroutine, D., Fox, R.M., Von Stetina, S.E., Burdina, A., Miller, D.M., 3rd, and Richmond, J.E. (2005). acr-16 encodes an essential subunit of the levamisole-resistant nicotinic receptor at the Caenorhabditis elegans neuromuscular junction. J Biol Chem *280*, 27013-27021.

Tsalik, E.L., Niacaris, T., Wenick, A.S., Pau, K., Avery, L., and Hobert, O. (2003). LIM homeobox gene-dependent expression of biogenic amine receptors in restricted regions of the C. elegans nervous system. Dev Biol *263*, 81-102.

Ward, S. (1973). Chemotaxis by the nematode Caenorhabditis elegans: identification of attractants and analysis of the response by use of mutants. Proc Natl Acad Sci U S A *3,* 817-21.

Ward, S., Thomson, N., White, J.G., and Brenner, S. (1975). Electron microscopical reconstruction of the anterior sensory anatomy of the nematode *Caenorhabditis elegans*. J. Comp. Neurol. *160*, 313–33.

Ware, R.W., Clark, D., Crossland, K., and Russell, R.L. (1975). The nerve ring of the nematode *Caenorhabditis elegans*: sensory input and motor output. J. Comp. Neurol. *162*, 71–110.

White J.G., Southgate, E., Thomson, J.N. and Brenner, S. (1976). The structure of the ventral nerve cord of *Caenorhabditis elegans*. Philos. Trans. R. Soc. Lond. Series B. Biol. Sci. *275B,* 327-348.

White, J.G., Horvitz, H.R., and Sulston, J.E. (1982). Neurone differentiation in cell lineage mutants of Caenorhabditis elegans. Nature *297*, 584-587.

White, J.G., Southgate, E., Thomson, J.N. and Brenner, S. (1986). The structure of the nervous system of the nematode *Caenorhabditis elegans*. Philosophical Transactions of the Royal Society of London B. Biological Sciences *314*, 1-340.

Wiersma, C.A. (1946). Muscles consisting of a single motor unit after poliomyelitis. Proc Soc Exp Biol Med *61*, 85-89.

Wragg, R.T., Hapiak, V., Miller, S.B., Harris, G.P., Gray, J., Komuniecki, P.R., and Komuniecki, R.W. (2007). Tyramine and octopamine independently inhibit serotonin-stimulated aversive behaviors in Caenorhabditis elegans through two novel amine receptors. J Neurosci *27*, 13402-13412.

Xie, Z., and Miller, G.M. (2007). Trace amine-associated receptor 1 is a modulator of the dopamine transporter. J Pharmacol Exp Ther *321*, 128-136.

Youdim, M.B.H., Carter, S.B., Sandler, M., Hanington, E., and Wilkinson, M. (1971). Conjugation Defect in Tyramine-sensitive Migraine. Nature *230*, 127-128.

Zhang, F., Wang, L.P., Brauner, M., Liewald, J.F., Kay, K., Watzke, N., Wood, P.G., Bamberg, E., Nagel, G., Gottschalk, A.*, et al.* (2007). Multimodal fast optical interrogation of neural circuitry. Nature *446*, 633-639.

Zhang, M., Schafer, W.R., and Breitling, R. (2010). A circuit model of the temporal pattern generator of Caenorhabditis egg-laying behavior. BMC Syst Biol *4*, 81.

Zheng, Y., Brockie, P.J., Mellem, J.E., Madsen, D.M., and Maricq, A.V. (1999). Neuronal control of locomotion in C. elegans is modified by a dominant mutation in the GLR-1 ionotropic glutamate receptor. Neuron *24*, 347-361.

Zhang, Y., Grant, B., and Hirsh, D. (2001). RME-8, a conserved J-domain protein, is required for endocytosis in Caenorhabditis elegans. Mol Biol Cell *12*, 2011-2021.

Zottoli, S.J. (1977). Correlation of the startle reflex and Mauthner cell auditory responses in unrestrained goldfish. J Exp Biol *66*, 243-254.

Zucchi, R., Chiellini, G., Scanlan, T.S., and Grandy, D.K. (2006). Trace amine-associated receptors and their ligands. Br J Pharmacol *149*, 967-978.

Appendix I:

Glossary of Genes

acr-2 Non-alpha type nicotinic acetylcholine receptor

cat-2 Dopamine biosynthetic enzyme, tyrosine hydroxylase

dat-1 Dopamine reuptake transporter

dgk-1 Diacylglycerol kinase theta

eat-16 RGS protein which regulates G protein signaling

eat-4 Vesicular glutamate transporter

egl-30 Heterotrimeric G protein α subunit of the G_q class

flp-13 FMRF-like peptide

goa-1 Heterotrimeric G protein α subunit of the $G_{i/o}$ class

gpb-2 Heterotrimeric G protein β subunit

lgc-55 Tyramine-gated chloride channel

mec-4 Sodium channel required for sensing gentle mechanical stiumuli

ptr-5 Sterol sensing domain protein involved in molting

ser-2 Tyramine activated G protein-coupled receptor

tbh-1 Octopamine biosynthetic enzyme, tyramine β-hydroxylase

tdc-1 Tyramine biosynthetic enzyme, tyrosine decarboxylase

tph-1 Serotonin biosynthetic enzyme, tryptophan hydroxylase

tyra-2 Tyramine activated G protein-coupled receptor

tyra-3 Tyramine activated G protein-coupled receptor

unc-17 Vesicle acetylcholine transporter (VAchT)

unc-25 GABA biosynthetic enzyme, glutamic acid decarboxylase (GAD)

unc-47 GABA vesicular transporter

unc-9 Integral transmembrane channel protein (innexin) component of gap junctions

y116a8c.24 Protein tyrosine kinase